Identification and characterization novel of cystine-loop ligand- gated chloride channels from *Dirofilaria immitis*: pharmacological analysis and novel compound screening

by

Sierra Varley

A thesis submitted to the
School of Graduate and Postdoctoral Studies in partial
fulfillment of the requirements for the degree of

Doctor of Philosophy in Applied Biosciences

Faculty of Science

University of Ontario Institute of Technology (Ontario Tech University)

Oshawa, Ontario, Canada
December 2023

THESIS EXAMINATION INFORMATION
Submitted by: **Sierra Varley**

Doctor of Philosophy in **Applied Biosciences**

Identification and characterization novel of cystine-loop ligand- gated chloride channels from *Dirofilaria immitis*: pharmacological analysis and novel compound screening

An oral defense of this thesis took place on December 5th, 2023, in front of the following examining committee:

Examining Committee:

Chair of Examining Committee	Dr. Dario Bonetta
Research Supervisor	Dr. Sean Forrester
Research Co-supervisor	N/A
Examining Committee Member	Dr. Jean-Paul Desaulniers
Examining Committee Member	Dr. Helene Leblanc
University Examiner	Dr. Paul Yielder
External Examiner	Dr. Richard Martin, Iowa State University

The above committee determined that the thesis is acceptable in form and content and that a satisfactory knowledge of the field covered by the thesis was demonstrated by the candidate during an oral examination. A signed copy of the Certificate of Approval is available from the School of Graduate and Postdoctoral Studies.

ABSTRACT

Dirofilaria immitis, otherwise known as heartworm, is a parasite that infects the hearts of dogs and causes serious health consequences. While preventative treatments are available drug resistance is developing at an alarming rate. Cystine-loop ligand-gated ion channels are important receptors in nematode neurobiology, and as such are promising drug targets. The UNC-49 (GABA-gated chloride channel) and ACC (acetylcholine-gated chloride channel) family of receptors have been characterized as potential drug targets in other nematodes. However, these receptors have yet to be identified or characterized in *D. immitis*. This thesis investigates the cloning and pharmacological characterization of 5 novel receptor subunits from *D. immitis*: UNC-49B and UNC-49C, ACC-1, LGC-46 and LGC-47. Additionally, novel derivatives of the antiparasitic drug levamisole were tested on ACC receptors to determine if any modifications enhanced levamisole action. *D. immitis* UNC-49B assembled as a homomeric channel and exhibited an EC_{50} of 5mM for GABA. UNC-49B also formed a functional channel with UNC-49C, which exhibited a decrease in GABA sensitivity. Additionally, the *D. immitis* UNC-49 receptors were significantly more sensitive to the open channel blocker picrotoxin compared to the same receptors from the sheep parasite *Haemonchus contortus.* Moreover, *D. immitis* UNC-49C, unlike other UNC-49C subunits, did not cause a decrease in picrotoxin sensitivity when assembled with UNC-49B. *D. immitis* ACC-1, LGC-46, and LGC-47 were unable to form functional channels through heterologous expression in *Xenopus laevis* oocytes. Levamisole derivatives were therefore tested on *H. contortus* ACC-2, which identified at least one showing a higher sensitivity compared to levamisole. Overall, this study characterized 2 novel UNC-49 receptors, identified 3 potential members of the ACC family in *D. immitis* and tested 8 novel derivatives of levamisole. This study lays foundation for the identification of more ligand-gated ion channels and will serve as a starting point for future researchers looking at new drug potential targets in *D. immitis.*

Keywords: Pharmacology, GABA, acetylcholine, UNC-49, ACC, *Diofilaria immitis*

AUTHOR'S DECLARATION

I hereby declare that this thesis consists of original work of which I have authored. This is a true copy of the thesis, including any required final revisions, as accepted by my examiners.

I authorize the University of Ontario Institute of Technology (Ontario Tech University) to lend this thesis to other institutions or individuals for the purpose of scholarly research. I further authorize University of Ontario Institute of Technology (Ontario Tech University) to reproduce this thesis by photocopying or by other means, in total or in part, at the request of other institutions or individuals for the purpose of scholarly research. I understand that my thesis will be made electronically available to the public.

The research work in this thesis that was performed in compliance with the regulations of Research Ethics Board/Animal Care Committee under 16312 - Expression of ion channels in *Xenopus* oocytes.

Sierra Varley

STATEMENT OF CONTRIBUTIONS

The work described in section 3.7, and 0 was work done in collaboration with A. Collins (Ontario Tech University) who synthesized all novel molecules. Heterologous expression as well as pharmacological characterization of these receptors was done by myself. The homology models, docking and ligand interactions by UNC-49 receptors was done by myself. The cloning of *Dirofilaria immitis unc-49b* was completed by the Institut national de la recherche agronomique (INRAE) and sent to us for pharmacological characterization.

ACKNOWLEDGEMENTS

There are many people in my life who have gone above and beyond for me in the last few years to make this degree a reality. I would first like to extend my gratitude to my supervisor Dr. Sean Forrester who has been an immense support on my journey here. You have helped me through the ups and downs of graduate school, and I appreciate all the help you have given to me over the last five years. I also would like to thank my committee members Dr. Jean-Paul Desaulniers and Dr. Helene Leblanc for the valuable contributions to this final product, and over my entire graduate experience. I would like to thank Dr. Jean-Paul Desaulniers as well as Dr. Julia Green-Johnson for the access to your thermal cyclers to keep up with all the PCRs we had to run to accomplish this project. Thank you to both Jen and Amy, who have made the last few years awesome. You are both the most amazing people to work with every day. Funding for this project was provided by Zoetis Inc.

To my lovely husband Andrew, your contributions to this endeavor are immeasurable. I would not have been able to accomplish this without your support. From the countless hours spent editing my thesis to the encouragement, and science talks we have had, you've played an integral role in this achievement. I am so grateful for everything you have done to help get me here. To my mother, Ruth, whose love, and support have been the bedrock of my journey. Her financial assistance, unwavering emotional help, and the comforting voice on the other end of the line during my toughest moments have been an invaluable support system. Thank you to my wonderful in-law's Jan and Bill, who have done so much for me over the years while I get through my degree, including welcomed me into their home. I am so grateful to have so much family support, making me feel so loved through this process. It has been invaluable.

To my amazing friends Sereena, Paula, Alyssa, and Jessica, who have seen me through this this entire journey. You and your partners and families have been an amazing support system for me. Thank you for checking in with me and being the most understanding friends that someone could ask for when embarking on a PhD. I am so grateful and lucky to have friends as good as you.

TABLE OF CONTENTS

THESIS EXAMINATION INFORMATION ii
ABSTRACT iii
AUTHOR'S DECLARATION iv
STATEMENT OF CONTRIBUTIONS v
ACKNOWLEDGEMENTS vi
TABLE OF CONTENTS vii
LIST OF TABLES ix
LIST OF FIGURES x
LIST OF ABBREVIATIONS AND SYMBOLS xv
1. Introduction 1
1.1 Nematode phylogeny 1
1.2 *Dirofilaria immitis*: the parasite responsible for heartworm 4
1.2.1 Life cycle and morphology of *Dirofilaria immitis* 5
1.2.2 Clinical signs and diagnostic screening 7
1.2.3 Current treatment options 9
1.2.4 Resistance to current treatment 11
1.3 Cystine-loop superfamily of ligand gated ion channels as drug targets in nematodes 12
1.3.1 Nematode GABA receptors: and comparison to mammalian receptors 17
1.3.2 Nematode inhibitory acetylcholine receptors 23
2. Rationale and Objectives 27
2.1 Rationale 27
2.2 Objectives 28
3. Methods 31
3.1 Identification and cloning of *unc-49c*, *acc-1*, *lgc-46*, *lgc-47* 31
3.2 Sequence analysis and phylogenetic analysis 34
3.3 Homology modelling and docking of ligands 35
3.4 Heterologous expression of channels in *Xenopus laevis* oocytes 36
3.5 Two-electrode voltage clamp electrophysiology 38

3.6 Quantitative-real time PCR analysis of *unc-49b, unc-49c, acc-1, lgc-46* and, *lgc-47* 41
3.7 Levamisole derivative screening....43
4. Results....45
4.1 Bioinformatic analysis of *unc-49b* from *D. immitis* 45
4.2 Cloning of *unc-49c* from *D. immitis*....47
4.3 Cloning of *lgc-46*, *lgc-47* and *acc-1* from *D. immitis* and identification of *acc-2*....50
4.4 Heterologous expression in *Xenopus laevis* oocytes 55
4.4.1 UNC-49 family of receptors 55
4.5 Phylogenetic analysis of ACC, and UNC-49 receptors in nematodes....63
4.6 Homology modelling and ligand docking of GABA in *D. immitis* UNC-49B and UNC-49C 65
4.6.1 *D. immitis* GABA Receptors....65
4.7 Quantitative-real-time PCR analysis....67
4.8 Characterization of *D. immitis* ACC receptors and levamisole derivative screening 69
5. Discussion and Future Directions 73
5.1 Characterization of UNC-49B and UNC-49C from *D. immitis*....73
5.2 Identification of *lgc-46*, *lgc-47* and *acc-1* in *D. immitis*....81
5.3 Levamisole derivative testing on Hco-ACC-2....83
6. Conclusions....84
7. References....86
8. Appendix....97
8.1 Gene and Protein Sequences....97

LIST OF TABLES

Table 1: Clinical symptoms of heartworm in canines (Nelson 2012). 9
Table 2: Gene specific primers used for cloning into expression vectors. 34
Table 3: Receptor combinations investigated, and ligands tested. Receptor names in green indicate receptors from *H. contortus* not cloned as part of this study but utilized for various experiments. 38
Table 4: Primer sets used for qPCR analysis. Genes in bold are control genes. 42

LIST OF FIGURES

Figure 1: Life cycle of *D. immitis* in dogs. 6

Figure 2: The cystine loop ligand gated ion channel superfamily of the nematode *C. elegans* retrieved from Jones and Sattelle (2008). 13

Figure 3: (A) A view of the transmembrane domains that make up each of the five subunits. (B) Arrangement of the proteins around a central pore. The intracellular, extracellular and transmembrane regions have been labelled..... 15

Figure 4: Visualization of the binding loops in the *H. contortus* UNC-49B receptor. The binding of a ligand occurs with loops A, B, C on the primary subunit and loops D, E and F from the complimentary subunit..... 19

Figure 5: Protein alignment of *H. contortus* UNC-49B and UNC-49C with binding loops shown. ■ indicate residues shown to be important to GABA response through mutagenesis by Foster et al. (2018). ▲ indicates residues shown to be influential to GABA response by Accardi and Forrester (2011) through mutational analysis. 19

Figure 6: Structure of (A) Gamma-aminobutyric acid (GABA), and (B) picrotoxin, (C) Imidazole-4-acetic acid (IMA), (D) (R)-(-)− 4-Amino-3-hydroxybutyric acid (R-GABOB), (E) (S)-(+)− 4-Amino-3-hydroxybutyric acid (S-GABOB), and (F) 5-aminovaleric acid (DAVA)..... 40

Figure 7: Structure of (A) levamisole, (B) acetylcholine and (C) novel levamisole derivative compounds created by Collins (2022) used for testing on Hco-ACC-2 receptors. Compounds 8-10 were first preliminarily tested for activation in comparison to levamisole itself. Compound 10 elicited a higher response than levamisole based on electrophysiology results. For further analysis, compounds 11-15 were subsequently synthesized using compound 10 as the backbone, with varying substitutions on the phenyl group attached to the amine nitrogen. 44

Figure 8: Protein sequence alignment of *D. immitis* UNC-49B with *C. elegans* UNC-49B, and *H. contortus* UNC-49B. Asterisks (*) indicate identical amino acids and (:)

represents similar amino acids. The binding loops, and transmembrane domains (TM) are displayed. Orange stars indicate residues where there are variations from the *H. contortus* receptor, which have been shown previously to be important for GABA sensitivity (Accardi and Forrester 2011). 46

Figure 9: (A) Genomic organization of the *unc-49* receptors in *D. immitis* (NCBI Accession: JAKNDB000000000.1). Black indicates exons shared between both UNC-49B and UNC-49C, providing the characteristic identical 5' regions. Blue indicates UNC49-B exons, green indicates UNC49-C exons. Binding loops are labelled, and transmembrane domains are labelled TM1-TM4 (B) Splicing pattern of the *unc-49B* and *unc-49C* genes. Black lines indicate the introns that are spliced out of the gene. 48

Figure 10: Protein sequence alignment of *D. immitis* UNC-49C with *C. elegans* UNC-49C, and *H. contortus* UNC-49C. Asterisks (*) indicate identical amino acids and (:) represents similar amino acids. The binding loops, and transmembrane domains (TM) are displayed. Orange star are above TM2 is where there are variations associated with picrotoxin resistance (Zhang et al. 1995). 49

Figure 11: Protein sequence alignment of *D. immitis* LGC-46 with *C. elegans* LGC-46, and *H. contortus* LGC-46. Asterisks (*) indicate identical amino acids and (:) represents similar amino acids. The binding loops, and transmembrane domains (TM) are displayed. There is no predicted signal peptide sequence for this protein. 51

Figure 12: Protein sequence alignment of *D. immitis* LGC-46 with *C. elegans* LGC-46, and *H. contortus* LGC-47. Asterisks (*) indicate identical amino acids and (:) represents similar amino acids. The binding loops, and transmembrane domains (TM) are displayed. 52

Figure 13: Protein sequence alignment of *D. immitis* ACC-1 with *C. elegans* ACC-1, and *H. contortus* ACC-1. Asterisks (*) indicate identical amino acids and (:) represents similar amino acids. The binding loops, signal peptide sequence, and transmembrane domains (TM) are displayed. 53

Figure 14: Signal protein prediction done by SignalP6.0 (Teufel et al. 2022) of (A) LGC-46, (B) LGC-47 and (C) ACC-1. The red, orange and yellow line correspond to the N-terminal region, the hydrophobic internal region and the C-terminal region of the signal peptide sequence respectively. The dotted green line is the predicted cleavage site for the protein. Both ACC-1 and LGC-47 are predicted to have a signal peptide sequence, while LGC-46 is not predicted to have one. 54

Figure 15: Shown are representative traces of a dose response for the novel (A) Dim-UNC-49B homomer and (B) Dim-UNC-49B/Dim-UNC-49C heteromer. The heteromeric channel is less sensitive to GABA than the homomeric channel. (C) GABA dose response curve of all tested receptor combinations. 57

Figure 16: (A) GABA EC_{50} values for all receptor combinations tested along with the (B) statistical analysis. No significant difference ($p \leq 0.05$) between receptors identified by the same letter. Dim-UNC-49B receptors combinations have significantly higher EC_{50} when compared to Hco-UNC-49B receptors. In addition, Dim-UNC-49C significantly increases the EC_{50}, whereas Hco-UNC-49C significantly decreases it in all receptor combinations tested. 58

Figure 17: Comparison of the response amplitude (using the maximum current achieved from EC_{50} GABA concentration in nA) between (A) Dim- UNC-49B (DB) homomer and Dim-UNC-49B + Dim-UNC-49C (DB + DC) heteromer, and (B), Dim-UNC-49B (DB) homomer and the Dim-UNC-49B + Hco-UNC-49C (DB + HC) heteromer. Batches indicate the receptors were tested on the same day. Different batches represent oocytes from different frogs. Significance ($p \leq 0.05$) was determined through students t-test and displayed as asterisks. n.s indicates no significant difference ($p > 0.05$) between conditions. The Dim-UNC-49B + Dim-UNC-49C heteromeric channel exhibited significantly lower amplitudes in comparison with the homomeric Dim-UNC-49B channels on all days analyzed. The Dim-UNC-49B + Hco-UNC-49C heteromeric channel had significantly higher amplitude than the Dim-UNC-49B homomeric channel on two of the three days analyzed. 59

Figure 18: (A) Representative electrophysiological traces showing the effect maximal picrotoxin concentration (250 μM) on EC50 GABA. Single line represents EC50 GABA application, double line represents EC50 GABA with 250 μM of Picrotoxin. (B) Maximum EC50 GABA inhibition, with statistical analysis done by students t-test. Groups with the same letter are not significantly different ($p > 0.05$) and groups with different letters are significantly different ($p < 0.05$). 61

Figure 19: (A) Picrotoxin inhibition of GABA EC_{50} response for all receptor combinations tested. (B) IC_{50} picrotoxin concentrations calculated EC_{50} concentration of GABA with increasing concentrations of picrotoxin. No significant difference ($p \leq 0.05$) between receptors identified by the same letter. (C) Summary of the IC_{50} data, the hill slope and number of replicates (N). Hco-UNC-49C increased picrotoxin resistance, but Dim-UNC-49C did not have the same effect. Dim_UNC-49 receptors are more sensitive to picrotoxin than Hco_UNC-49 receptors. 62

Figure 20: Phylogram of nematode cystine loop ligand gated ion channels, including those cloned, and currently unpublished, from our lab. The genes highlighted in yellow were cloned in this study. The genes highlighted in green were cloned by my colleague J. Nichols (2023). Legend displays the percent of amino acid variation as a decimal..... 64

Figure 21: (A) Homology model of Dim-UNC-49B with GABA docked. (B) View of the binding pocket with relevant residues exposed. (C) View of the binding pocket with all non-relevant residues and amino acids removed. Residues are displayed and distances are displayed in Angstroms..... 66

Figure 22: Quantitative-real-time PCR analysis of *unc-49c, unc-49c, acc-1 lgc-46, lgc-47* across female, male and L3 larvae displayed grouped as (A) organism and (B) genes. Error bars represent the standard error of the mean. Higher ∆Cq values relates to higher expression. 68

Figure 23: Percent response of Hco-ACC-2 receptors to 500 μM of the following ligands: acetylcholine, levamisole and 3 levamisole derivatives (compounds 8, 9 and 10).

Compound 10 had higher sensitivity to the receptor compared to levamisole. Compound 10 was chosen for further analysis. 70

Figure 24: (A) Representative trace of the percent response in comparison to acetylcholine with 500 μM of all compounds tested (acetylcholine, levamisole, and derivatives 10-15). (B) Percent response of Hco-ACC-2 receptors to 500 μM acetylcholine, levamisole as well as compound 10-15, created by A. Collins (2022). 71

Figure 25: (A) Representative trace of the dose response curve analysis for compound 13. Concentrations of levamisole and acetylcholine used were 500 μM (B) Dose response curve of compound 13 on Hco-ACC-2 receptors. (C) EC_{50} ± standard error for the response of Hco-ACC-2 to acetylcholine and levamisole, and compound 13. Data for EC_{50} acetylcholine and levamisole were obtained from (Habibi et al. 2018). 72

LIST OF ABBREVIATIONS AND SYMBOLS

Abbreviations	Definitions
Å	Angstroms
ACC	Acetylcholine-gated chloride channel
cDNA	Copy DNA
Cel	*C. elegans*
cRNA	Copy RNA
DAVA	5-aminovaleric acid
Dim	*D. immitis*
EC_{50}	50% of the maximum response
GABA	Gamma-Aminobutyric acid
Hco	*H. contortus*
I	Current
IC_{50}	50% maximum inhibitory concentration
IMA	Imidazole-4-acetic acid
L1-L4	Larval stages 1 through 4
LGC	ligand-gated ion channels of the cystine-loop superfamily
nA	Nano Amperes
R-GABOB	(R)-(-)− 4-Amino-3-hydroxybutyric acid
S-GABOB	(S)-(+)− 4-Amino-3-hydroxybutyric acid
TM(n)	Transmembrane domain where n refers to the number of the domain referred to
UNC	Uncoordinated
wgs	Whole genome shotgun

1. Introduction

1.1 Nematode phylogeny

The phylum *Nematoda* displays remarkable diversity. Nematodes account for about 80% to 90% of all the multicellular organisms alive on earth at any moment, particularly in the deep seas (Platt 1994; Kashyap et al. 2022). In fact, nematodes thrive in extreme ecological environments. Their genetic diversity and rapid reproduction cycles provides a means to adapt to many niche environments (Bellec et al. 2018; Baldrighi et al. 2020). Most nematodes are quite small, but can range in size from 80μm (unnamed marine nematodes) (Koppenhöfer 2000) to up to 9m long, such as the whale parasite, *Placenttnema gigantissima* (Gubanov 1951). Nematodes are categorized into two categories based on their behaviour, parasitic and free-living nematodes.

The free-living group play important roles in many ecosystems and pose no significant threat to animal health. They form foundational parts of the food chain by serving as a food source for many organisms such as fish, or insects, forming the foundational part of the food chain. They also assist in regulating the levels of microorganisms in the environment by consuming bacteria and other microscopic life forms (Majdi and Traunspurger 2015) and contribute to nutrient cycling through the decomposition of organic matter (Freckman 1988).

The free-living nematode, *C. elegans*, is widely employed as a model organism for nematode neurology and development. Its use as a model organism was first introduced by Sydney (Brenner 1974), who investigated the genetics of *C. elegans* with the goal of applying this knowledge to the study of nematode biology and anatomy. Since then, many

researchers have linked similarities of the physiological, neuronal, and molecular pathways between *C. elegans* and other nematodes and vertebrate species. *C. elegans* is easily genetically manipulated, has a short life span, is convenient to culture, and has significant prior research into their nervous system which lays the foundation for translational research, including drug discovery (Bürglin et al. 1998). Compared to higher organisms, the transparent body of *C. elegans* provides a convenient model to explore protein localization in the nematode which has allowed for significant mapping of the neurons. Their simple nervous system, composed of only 302 neurons, facilitates the study of neuronal interactions (Brenner 1974) making it a desirable model organism. Many receptor families have been extensively studied in *C. elegans* including the cystine-loop ligand-gated ion channel family (Jones and Sattelle 2008). Clearly, *C. elegans* serves as an important model organism for many researchers, especially for studies related to parasitic nematodes (Bürglin et al. 1998).

Nematodes are subdivided into clades based on the phylogenetic analysis of nematode small subunit rRNA, and has revealed five distinct evolutionary clades (Clades I-V) (Blaxter et al. 1998; Dorris et al. 1999). The clades reveal some free living and parasitic nematodes grouping together from a common ancestor, which highlights multiple origins of parasitism. For example, both *C. elegans* and the sheep parasite *Haemonchus contortus* (described below) belong to clade V, and the canine heartworm *Dirofilaria immitis* (described below) belongs to clade III.

Parasitic nematodes pose a significant threat to animal, human, and plant health, causing severe economic impacts. The key differentiation between them and their free-living relatives is that the parasitic nematodes spend at least one part of their life stage

infecting a host with a range of harmful outcomes. They infect both plants and animals, specifically vertebrates and arthropods (Kiontke and Fitch 2013). Vertebrate parasitic nematodes are suggested to have a minimum of four independent origins of evolution from their free-living cousins (Blaxter et al. 1998). This showcases the versatility and resilience of nematode evolution and their ability to adapt to various ecological niches, which is why they are considered to be one of the most successful and adaptable animal groups (Hailu and Hailu 2020). Multiple origins of parasite evolution also highlight convergent evolution, as nematodes have repeatedly adopted parasitism as a successful means of survival. Furthermore, over time, parasitic nematodes have honed various tactics to elude host immune responses through evolutionary processes (Li et al. 2007). However, this adaptability has also led to the concerning emergence of drug resistance among many parasitic nematodes, posing significant challenges to the effectiveness of current treatment regimens targeting these parasites.

H. contortus, commonly known as the barber pole worm, is a parasitic nematode of ruminants that has been widely studied in the field of drug discovery and resistance due to its worldwide economic impact. It has an exceptional tendency to develop resistance to anthelmintic treatments, and as such, has been a significant focus of research (Kaplan 2004). The information gained from research into *H. contortus* has provided valuable insights into various topics, including mechanisms of anthelmintic resistance, the significance of host-parasite interactions, and nematode neurobiology. The extensive research into *H. contortus* allows it to serve as a model for research into other nematodes ((Gilleard 2013). In 2013, both the genome and a partial transcriptome were published which helped lay the foundation for follow up research into the genetics of drug resistance

and mechanisms for drug action in other nematodes (Laing et al. 2013a). Oftentimes, when used in parallel with *C. elegans* many comparative insights can be generated based on their similarities and differences in areas such as protein sequence, receptor assembly and response as well as drug sensitivity (Gilleard 2013). Due to these reasons, many researchers, including our lab, have done significant work on anthelmintic drug discovery using *H. contortus* as a model for parasitic nematodes.

1.2 *Dirofilaria immitis*: the parasite responsible for heartworm

Dirofilaria immitis, commonly referred to as heartworm due to its localization within the heart, is a filarial parasitic nematode responsible for the infection known as dirofilariasis. Dirofilariasis is a serious and life-threatening cardiovascular infection, occurring most commonly and severely in dogs. Although canines are the primary target for this parasite, infections have been documented in various other animals including; muskrats (Goble 1942), grey fox (Simmons et al. 1980), wolves, coyotes (Erickson 1944), sea lions, seals, walruses (Faust et al. 1941), cats (Mann and Fratta 1953), and humans (Browne et al. 2005). In non-native hosts, infection will not migrate to the heart of the organism and often remains subcutaneous. Subcutaneous infections are less dangerous than cardiovascular infections since there is no way for *D immitis* to reproduce in the skin, making the infected organism the terminal host, and incapable of spreading the parasite to a new host. Humans have been aware of this disease for over a century. The first observation of *D. immitis* comes from an old French Medical Research book, where they discussed the "worms" that were found living in blood of living humans and animals (Blanchard and Laveran 1895). Since then, there has been significant research into the *D. immitis* due to the worldwide economic and health impact associated with canine

heartworm. *D. immitis* is found globally, and according to a recent study investigating the prevalence of heartworm in dogs between 1965 and 2019, the infection rate is highest in Australia (22.68%) followed by Asia (12.07%) and North America (11.60%) (Anvari et al. 2020). Mosquitoes are essential for the propagation of the parasite life cycle and as such impact the spread of the infection significantly. Fittingly, the high rate of infection in Australia is likely due to the *Culex* mosquito, which freely propagates in the humid, populated coastal regions (Shi et al. 2017). Overall, the regions affected by heartworm globally are increasing at an alarming rate, particularly due to increased travel, climate change, the movement of dogs globally, and urbanization as reviewed by (Morchón et al. 2022).

1.2.1 Life cycle and morphology of *Dirofilaria immitis*

The life cycle of *D. immitis* is complex and nuanced, and understanding it is crucial to drug development. The life cycle of heartworm, outlined in Figure 1, is as follows: female worms release the first of five larval stages, called microfilariae (L1), directly into the bloodstream of the infected animal. Mosquitoes then ingest the larvae at the L1 stage, and after approximately 24 hours, the larvae molt into the L2 stage. After this initial molt, it takes three days for the larvae to further molt into the L3 stage. The L3 stage is the infective larval form and will be transmitted to a new host animal when the mosquito feeds. Once inside the new host, the L3 larva molts in the subcutaneous, adipose, or skeletal muscle tissue. The final molt to the L5 stage occurs several weeks later. These immature adults then travel through the bloodstream to the heart's vascular system, where they remain to mature for just over seven weeks. During this time, the males and females' mate, and can live for up to five years in the dog and the cycle repeats. Adult male *D. immitis* can grow

up to 18 cm in length, and females can reach up to 30 cm, causing significant blood flow impairment in the heart.

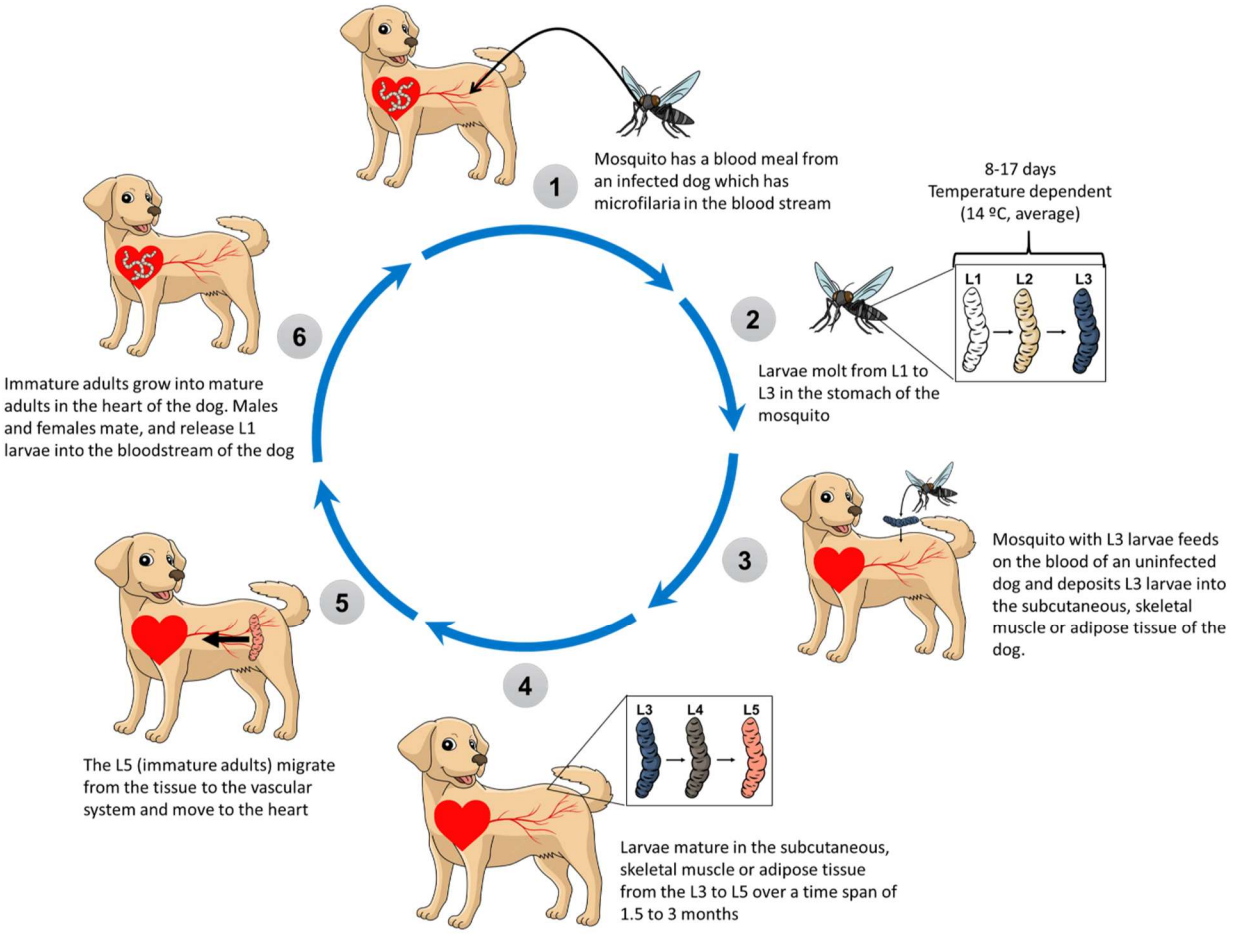

Figure 1: Life cycle of *D. immitis* in dogs.

The transmission of heartworm is completely dependent on the ability of the intermediate host (mosquitoes) to ingest the blood meal with L1 larvae and survive long enough to deliver the infective form to a new host. Therefore, climate and environmental conditions play a vital role in the transmission of heartworm between hosts. Warmer temperatures will naturally accelerate the rate of heartworm larval development. The average daily temperature required for heartworm development is 14 ºC (Ledesma and Harrington 2015). There is a linear relationship between temperature and mosquito

development between 18 and 34 º C (Fortin and Slocombe 1981). As global temperatures continue to increase, both the mosquito geographical coverage and breeding season increase, thereby increasing the amount of time that *D. immitis* can be transmitted. Climate plays a large role in the rate of *D. immitis* transmission due to the role it has on mosquito survival and geographical distribution. Over 60 species of mosquitoes are known to be capable of heartworm transmission, and 22 of them are present in Ontario, Canada (Ludlam et al. 1970; McGill et al. 2019). As stated previously, the large distribution of heartworm in Australia can be directly linked to a high presence of a vector capable of carrying *D. immitis* (Shi et al. 2017; Anvari et al. 2020). Since mosquitoes are ectothermic organisms, their core temperature are therefore highly influenced by the environment. Mosquito populations cannot properly survive or reproduce in environmental conditions that are above 35ºC or below 10ºC, however their optimal developmental range is mostly between 21ºC and 32ºC (Brust 1967; Agyekum et al. 2021). It is reasonable to infer that *D. immitis* transmission is impacted by the environment, especially during the spring and summer months. With global warming on the rise, the generation of "urban heat islands" and improper wastewater management, causes the threat of *D. immitis* infection to increase yearly (Morchón et al. 2012; Anvari et al. 2020). Due to the overall warmer temperatures, the geographical coverage of mosquitoes, and therefore will continue to increase significantly as the climate continues to warm (Genchi et al. 2009; McGill et al. 2019).

1.2.2 Clinical signs and diagnostic screening

Clinical signs from heartworm infection can vary depending on the nematode load in the organism. Some dogs with low heartworm loads may remain asymptomatic, while others may experience lethargy, cough, exercise intolerance and weight loss. In severe

cases, there may be fluid accumulation in the abdomen, lack of blood flow to body organs and even death (American Heartworm Society et al. 2018).

According to guidelines set by the American Heartworm Society, dog owners should undergo annual diagnostic screening for heartworm infection to ensure infection can identified in a timely manner (American Heartworm Society et al. 2018). Heartworm antigen test kits are the gold standard of *D. immitis* detection in dogs and are commonly used in veterinary clinics worldwide (Atkins 2003). Despite the sensitive methods, studies have shown that up to 7% of dogs tested will be antigen negative, even when they are microfilaria positive (Velasquez et al. 2014). For this reason, tandem testing is recommended to pet owners who want to ensure the safety of their canines (Nelson et al. 2005). Another method of diagnostic testing is the modified Knotts test (Knott 1939; Newton and Wright 1956), a widely used method which allows for the detection and quantification of microfilaria in blood. This allows technicians to distinguish *D. immitis* from other non-pathogenic filarial species. This test functions by concentrating a lysed blood cell sample from a dog and then staining it with methylene blue. The sample is then examined under a microscope for morphological properties known to be associated with *D. immitis.* Due to the nature of the heartworm life cycle (Figure 1), the presence of microfilaria in the blood stream cannot indicate the stage of the infection, and further visual investigation is required.

To diagnose the infection visually, radiography or echocardiography can be performed by a veterinary clinic. Radiography (or X-Ray analysis) is a reliable method used to identify severity of the disease and whether any cardio-pulmonary implications may arise due to the blockage of the heart (Barnette et al.). With echocardiography, ultrasounds are used to

create an image of internal structures allowing technicians to see how many adult worms may be in the heart of the dog. Both techniques are useful to determine how treatment will progress. In addition to both these methods, clinical symptoms of dogs (outlined in Table 1) can be assessed to indicate to clinicians the severity of the progression of heartworm infection.

Table 1: Clinical symptoms of heartworm in canines (Nelson 2012).

Class of infection	**Clinical symptoms**
1	Asymptomatic
2	Intolerance to exercise, fever, cough
3	Exhaustion, coughing of blood, difficulty breathing, abdominal distension
4	Everything at class 3 including fainting and collapse from shock

1.2.3 Current treatment options

To effectively combat *D. immitis* infections, it's important to focus on the stages of its life cycle when they are inside the dog's body. This strategy is vital due to the complexities associated with targeting the parasite during its mosquito phase, which include the daunting task of managing mosquito populations. Overall, there are only four classes of anthelminthic to treat parasitic nematode infections; benzodiazepine, macrocyclic lactones, nicotinic acetylcholine receptors agonists and acetonitrile derivatives (Miller et al. 1979; Kaminsky et al. 2008). Currently canine heartworm prevention relies mostly on macrocyclic lactones, which include the common antiparasitic ivermectin. These drugs aim to prevent adult worms from establishing in the heart of the dog. They are taken once a month and kill the heartworm at the L3 or L4 stage before they can infect the heart (Bowman and Mannella 2011). The larvae are usually within this stage for over 2 months so as long as the medication is taken monthly, all L3 and L4 larvae present in the animal

should be killed within the recommended administration time (Kume and Itagaki 1955). These drugs function to kill the parasite by binding to glutamate-gated chloride channels, causing irreversible opening and paralysis of the larvae (Wolstenholme and Rogers 2005). Despite best practices, in some situations such as natural disasters or in the presence of stray dogs, the chance for heartworm preventatives will have passed, and in that case, the adult worms must be killed.

To kill adult infections within the heart, the arsenic based anthelmintic, melarsomine, is used and administered intramuscularly through an injection into the muscle between the L3 and L5 vertebrae (American Heartworm Society et al. 2018). The mechanism of action has not been fully elucidated, but it does bind to sulfhydryl moieties of enzymes such as glutathione reductase and thioredoxin reductase causing inactivation of the enzyme (Robertson et al. 2012). This works to paralyze the adult worms which eventually die. The adults are processed through the hosts immune system that will remove the biological debris. As such, this can cause major complications to the dogs. The heartworms, once dead, will fragment into many pieces, which have the potential to lead to organ failure by obstructing blood flow to the organs (Frank et al. 1997). In addition to drug treatment, there are a few other considerations that pet owners must be aware of to allow proper recovery of dogs infected with adult heartworm. Once diagnosed with adult *D. immitis* infection, dogs need to be on severe exercise restriction to prevent cardiac issues. Due to the shock it can cause to dogs, it is only recommended as a final treatment option. This is why treating the infection at the larval stage is the significantly safer and preferred alternative.

1.2.4 Resistance to current treatment

Although there are current treatment options that exist for *D. immitis* infection, resistance has been shown to be developing at an alarming rate. Phenotypic reports of loss of efficacy of heartworm preventatives first began in 1998 according to (Hampshire 2005), and this rate nearly doubled in both 2001 and 2002. Many researchers attributed the loss of efficacy to a lack of compliance with preventatives, promoting the selection of drug resistant phenotypes (Prichard 2021). In addition to this, resistance has also been shown to occur through genetic diversity, where random genetic polymorphisms may confer the parasites resistance (Bourguinat et al. 2011; Pulaski et al. 2014). A hypothesis regarding the emergence of drug resistance suggests that resistant strains likely already exist, and the use of anthelmintics are contributing to the selection of these resistant strains (Wolstenholme et al. 2015). As discussed previously, current treatment options function by targeting the heartworm at the L3 or L4 life stage, and not the microfilaria. If the treatment is given to infected dogs prior to the development into the L3 and L4 stages or while the adult worms are mating in the heart, the microfilaria are given an opportunity to become resistant to macrocyclic lactones through exposure (Wolstenholme et al. 2015). Additionally, incorrect usage can cause resistance. A meta-analysis performed in Mississippi demonstrated that in 80% of 301 heartworm cases, purchase records showed an inadequate amount of preventatives were used, even though the veterinary clinics self-reported complete compliance (Atkins et al. 2014). Incorrect usage would allow exposure of the macrocyclic lactones at low doses to microfilaria essentially selecting for resistance. Regardless of the mechanism, it is clear that macrocyclic lactone resistance in heartworm

is developing at an alarming rate and new drug targets need to be investigated to prevent widespread distribution of a macrocyclic lactone resistant *D. immitis* strains.

1.3 Cystine-loop superfamily of ligand gated ion channels as drug targets in nematodes

Ion channels are essential in all living cells. They are used to maintain the distribution of ions across the cellular membrane and play roles in feeding, locomotion, mating, and many other neurological processes. Ion channels transport various ions such as calcium, sodium, potassium, and chloride and their structure imparts remarkable selectivity for their intended ion (Roux 2017). One type of ion channel with significant importance to the nematode nervous system, and the target of nematocidal drugs, is cystine loop ligand gated ion channels.

In nematodes, cystine-loop ligand-gated ion channels (LGIC) mediate fast synaptic transmission in the nervous system as well as other areas such as the pharynx and muscles. The members of the cystine-loop family of receptors share many similarities both in structure and function. The entire family of cystine-loop receptors have been identified in *C. elegans* and are commonly used as a model for studying other nematodes (Figure 2). These pentametric ligand-gated ion channels consist of five homologous or heterologous subunits arranged around the central pore. Naturally, these proteins are in their closed state, not allowing the passage of ions through the membrane. Once their ligand enters the binding site, these receptors transform into an open configuration, allowing the flow of specific ions down their gradient into the membrane (Lynagh and Lynch 2012). This will create either a stimulatory response when the cationic channels such as the nicotinic

acetylcholine receptors open or an inhibitory response with the activation of chloride channels such as the gamma-aminobutyric acid (GABA) receptors. In *C. elegans* a class of nichotinic acetylcholine receptors was discovered that are inhibitory in nature and consist of *acc-1*, *acc−2*, *acc−3*, and *acc−4,* as well as *lgc-46*, *lgc−47*, *lgc−48*, and *lgc−49* (Jones and Sattelle 2004; Putrenko et al. 2005). All these receptors are found in *H. contortus* with the absence of *lgc-48* (Laing et al. 2013).

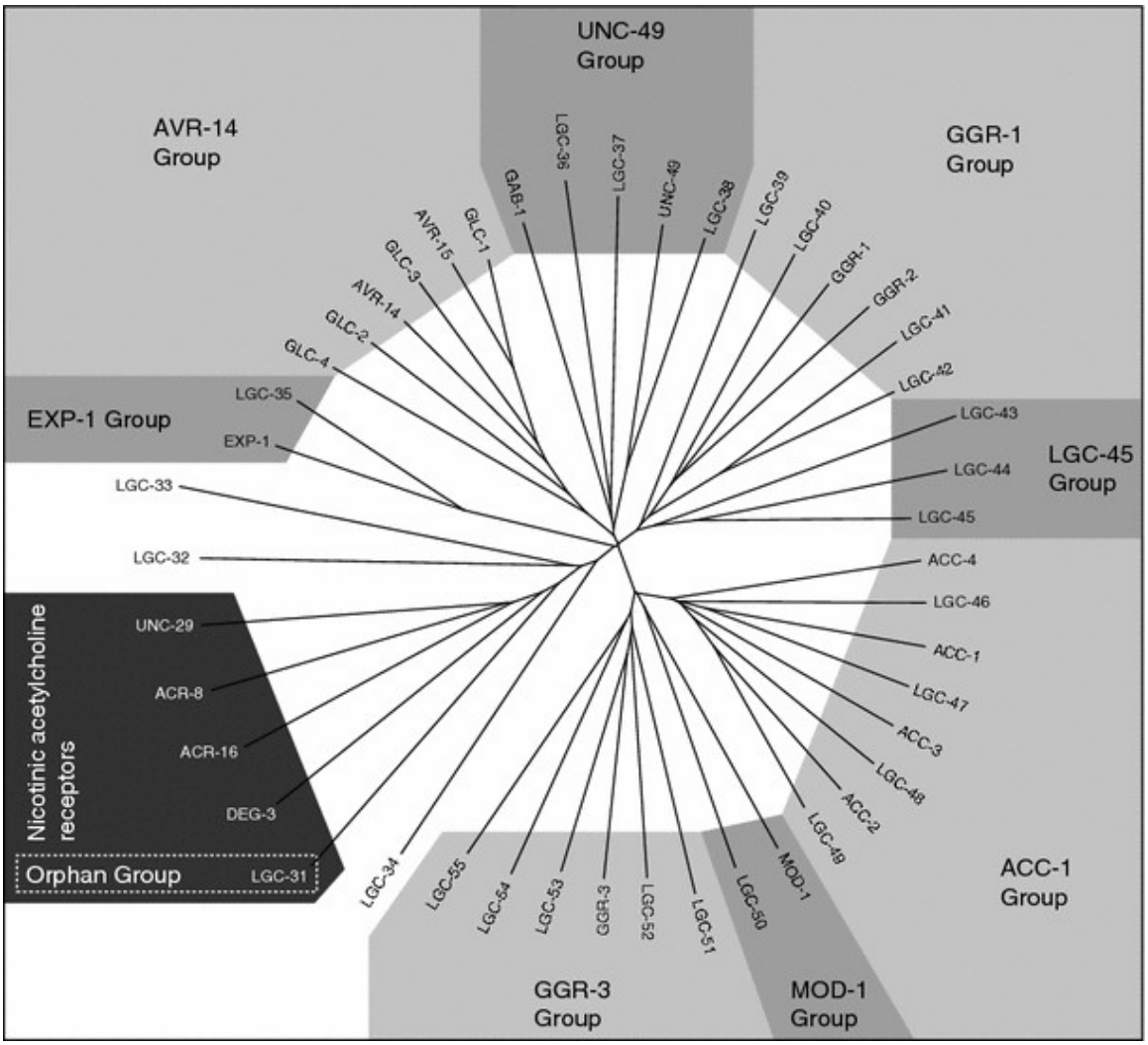

Figure 2: The cystine loop ligand gated ion channel superfamily of the nematode *C. elegans* retrieved from (Jones and Sattelle 2008).

These receptors have been extensively researched both mutationally and through x-ray crystallography. The crystal structure of a pentameric ligand gated ion channel was first

published from a snail (*Lymnaea stagnalis*) in 2001, significantly propelling the field forward (Brejc et al. 2001). This data confirmed predictions in channel structure and ligand binding. They were able to confirm the arrangement of subunits around a pore and provided valuable information into the specific location of the residues that are conserved family wide (Brejc et al. 2001) (Figure 3 A). The receptor structure consists of an extracellular domain, transmembrane domains and a small intracellular region, each their own features. The extracellular portion is the ligand binding domain (Figure 3 A). It contains the characteristic N-terminal extracellular cystine-loop motif of ionotropic neurotransmitters and contains 2 cysteine residues separated by thirteen amino acids. This motif is involved in receptor assembly (Green and Wanamaker 1997) ion permeability, and ligand response (Shen et al. 2003; Grutter et al. 2005). The transmembrane region of the receptor is comprised of 4 transmembrane domains (TM1-TM4) (Figure 3 B), TM2 lines the receptor pore. The amino acids which lines the pore are what determines the ions that are able to pass through the membrane (Roux 2017). TM1, TM3 and TM4 line the hydrophobic side of the receptor. The intracellular loop between TM1 and TM2 has been shown by mutagenesis to be responsible for the ion selectivity of the receptor (Filippova et al. 2000). The loop between TM3 and TM4 has been shown to have various functions such as interaction with other proteins and channel conductance as reviewed by Thompson et al. (2010). In the electric ray (*Torpedo marmorata*) GABA receptors, it has been shown that Protein Kinase A phosphorylates a highly conserved serine residue (Wecker et al. 2001) within the intracellular loop. The phosphorylation can allow for both the short term and long term modulation of the ion channels and can affect the sensitivity of the receptor to

ligands (Levitan 1994). The TM3-TM4 loop is also shown to be involved in anchoring the receptor to the cytoskeleton of the cell, providing stability (Kneussel and Betz 2000).

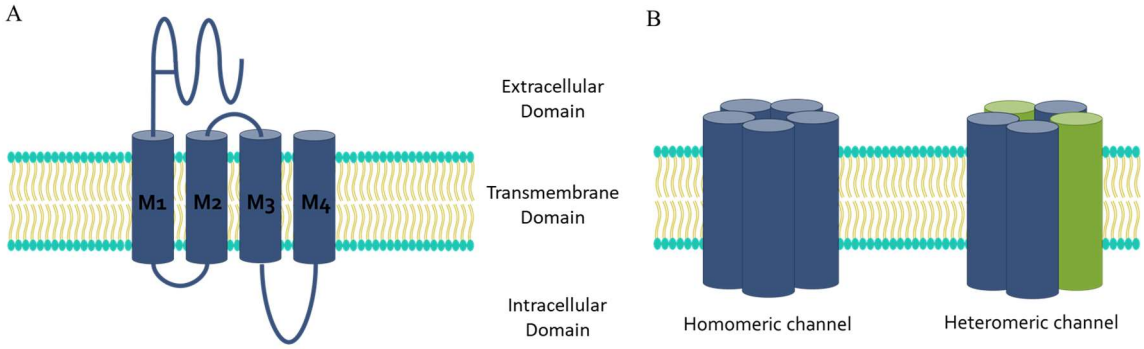

Figure 3: (A) A view of the transmembrane domains that make up each of the five subunits. (B) Arrangement of the proteins around a central pore. The intracellular, extracellular and transmembrane regions have been labelled.

Channel activation usually occurs through the binding of agonist molecules to the interface between two of any 5 adjacent subunits (Sine 2002), if no agonist exists, the channel has a low probability of opening. Upon binding of an agonist, a conformational shape change allows the passage of the correct ions into the cell. This is mediated through the slight rotation of TM1 and TM2, in the counter clockwise direction, which does not change the outer structure significantly (Perozo et al. 1999).

These cystine-loop receptors arrange in various pemtameric stochiometric ratios forming many different receptor subtypes which determine the pharmacological properties of the receptor (Figure 3 B). *C. elegans*, the model nematode, has the largest known family of cystine-loop ligand gated ion channels with 90 identified (Bargmann 1998). For perspective, insects have 20 and humans have 60. Due to this, *C. elegans* have ligand gated ion channels that are not present in vertebrates and are activated by a wide variety of molecules that do not target vertebrate receptors. The structural similarity of these receptors are strongly conserved in nematodes even when sequences are apparently divergent (Dent

2010). Although there is a lack of amino acid similarity in some regions, there are several resides which have proven to be conserved in almost all of these receptors through multiple sequence alignment and have been shown to be essential to channel function (Dent 2006; Dent 2010).

In vertebrates, there are four families of cystine-loop ligand gated ion channels that exist: excitatory (cationic) $5HT_3$ and nicotinic acetylcholine receptors and inhibitory (anionic) GABA and glycine receptors. As mentioned previously, nematodes have a much greater diversity in their families of ligand gated ion channels and have significantly more ligands that can activate these receptors. These include anion channels gated by glutamate (Cully et al. 1994; Wolstenholme and Rogers 2005), serotonin (Ranganathan et al. 2000), tyramine (Ringstad et al. 2009), and acetylcholine (Putrenko et al. 2005b), and cationic GABA receptors (Beg and Jorgensen 2003) and excitatory acetylcholine receptors (Del Castillo et al. 1963). In vertebrates, these receptors are often located in the central nervous system, requiring the passage of the blood brain barrier (BBB) to take effect. Due to the presence of p-glycoproteins which prevent the passage of these drugs through the BBB, this presents a unique opportunity to selectively target a range of nematode ion channels with little off target effects in vertebrates. The ligand binding site is the most important component in the receptor for channel activation. The binding site is located at the interface between adjacent subunits, and each receptor therefore has up to 5 putative binding sites (Figure 3). While this binding pattern is observed in all nematode cystine loop ligand gated ion channels, the amino acids in the binding pocket are variable and influence the type of ligands that bind to the receptors.

1.3.1 Nematode GABA receptors: and comparison to mammalian receptors

The involvement of gamma-aminobutyric acid (GABA) in nematode fast neurotransmission was originally identified in the parasite *Ascaris* where researchers discovered GABA receptors on the parasite somatic muscle where the application of GABA inhibited action potentials. The specific receptors that these neurotransmitters act have not been fully identified (Del Castillo et al. 1964; Holden-Dye et al. 1989). Despite this, researchers have demonstrated that GABA receptors in nematodes are pharmacologically distinct from those in vertebrates (Holden-Dye et al. 1989; Martin et al. 1995). In 1999, the first ionotropic GABA receptor gene *unc-49* was cloned in nematodes from *C. elegans* (Bamber et al. 1999), where the 'unc' stands for the uncoordinated phenotype that occurs with this gene knockout. Bamber and his colleagues identified three genes encoding three distinct subunits: *cel-unc-49a, cel-unc-49b* and *cel-unc-49c.* Only the former two were shown to have functional roles both *in vivo* and *in vitro* (Bamber et al. 1999). This study showed that in nematodes, the 5' end of the gene, which encodes a section of 188 amino acids at the N-terminal portion of the receptors are identical, and due to differential splicing, only the C-terminal ends differ. The identical N terminal portion comprises two of the 3 binding loops shown to be involved in ligand binding. Transcriptome analysis showed that *unc-49a* was likely not involved in the GABA response in *C. elegans.* UNC-49B can form a homomeric channel, or a heteromeric channel with UNC-49C, however UNC-49C cannot form a homomeric channel on its own (Bamber et al. 1999). In *C. elegans,* UNC-49C significantly increases the EC_{50} of GABA, making the channel slightly less sensitive to lower concentrations (Bamber et al. 1999). However, in a similar study done in *H. contortus,* it was shown that UNC-49C increased the

sensitivity of UNC-49B to GABA (Siddiqui et al. 2010). This demonstrates that there are possibly species-specific adaptations which occur in these receptors that modify the sensitivity to various ligands. This research laid the fundamental work for the basis of this project.

Studies demonstrate that in *H. contortus* GABA receptors are localized to the ventral nerve cords, head neurons, motor neurons and inter neurons (Skinner et al. 1998) revealing their importance in neurological function. This makes them appealing targets for pharmacological research. In more recent years, the amino acid residues in UNC-49 GABA binding site has been identified by methods such as site directed mutagenesis (Accardi and Forrester 2011; Yamamoto et al. 2012; Kaji et al. 2015). The binding site in nematode UNC-49 receptors occurs between two B subunits and involves binding loops A, B, and C on the primary subunit and loops D, E and F on the complimentary subunit (Figure 4). The *H. contortus* UNC-49B and UNC-49C have been extensively studied by mutagenesis to determine which residues in the binding pocket are important for ligand binding. As shown in Figure 5, mutagenesis done by both (Accardi and Forrester 2011; Foster et al. 2018) have located several residues important for GABA binding in the binding loops (Figure 4). Specifically, aromatic and polar amino acid residues in these loops have proven to be important and are known to be influential in mammalian GABA receptors. Overall, residues that were mutated in nematode UNC-49C had no effect on the EC_{50} of the heteromeric channel demonstrating that UNC-49C does not directly contribute to the agonist binding site.

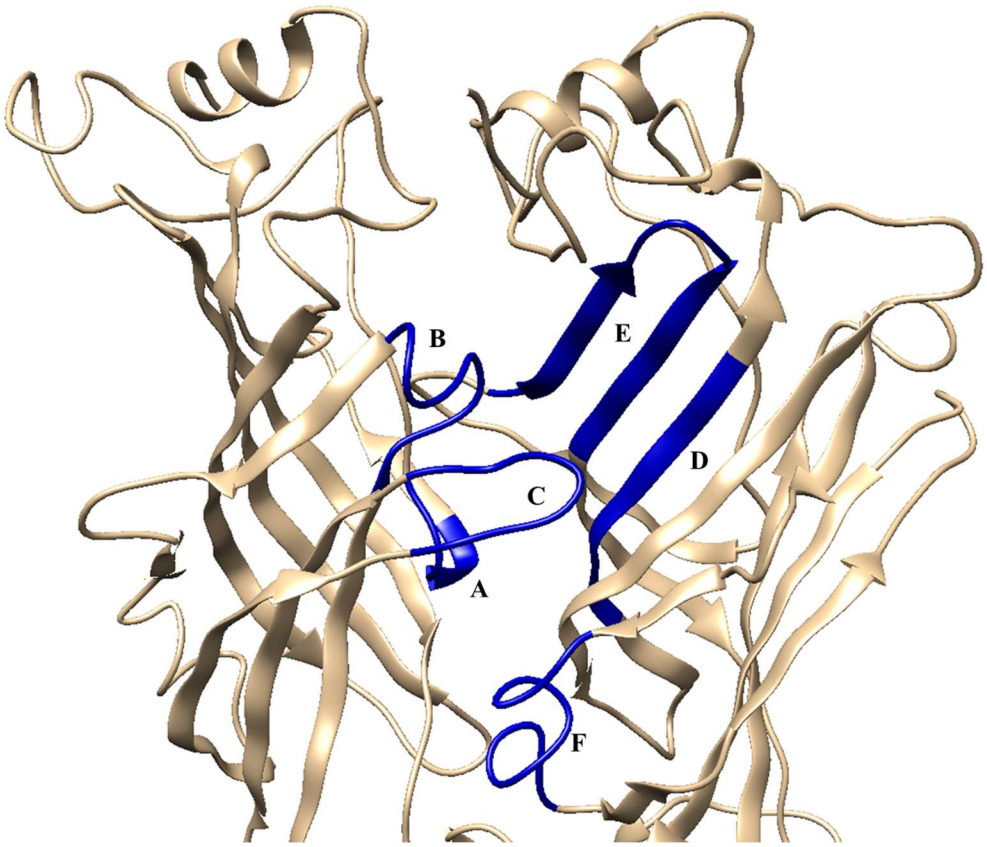

Figure 4: Visualization of the binding loops in the *H. contortus* UNC-49B receptor. The binding of a ligand occurs with loops A, B, C on the primary subunit and loops D, E and F from the complimentary subunit.

```
Hco_UNC49_B    MRISDLFLFATTATFYHVSRAQEDDIIVDTSQLSTVLDRLTNKTIYDKRLRPRYGDKPVD  60
Hco_UNC49_C    MRISDLFLFATTATFYHVSRAQEDDIIVDTSQLSTVLDRLTNKTIYDKRLRPRYGDKPVD  60
               ************************************************************

                                    ■▲▲▲▲
Hco_UNC49_B    VGITIHVSSISAVSEVDMDFTLDFYMRQTWQDPRLAFGTLDLGIAKQITSLTVGVDYLDR  120
Hco_UNC49_C    VGITIHVSSISAVSEVDMDFTLDFYMRQTWQDPRLAFGTLDLGIAKQITSLTVGVDYLDR  120
               ************************************************************
                                    Loop D

                  ▲   ■       ■           ■
Hco_UNC49_B    LWKPDTFFPNEKKSFFHLATTHNSFLRIDSDGTVYTSQRLTVTATCPMKLQLFPMDSQRC  180
Hco_UNC49_C    LWKPDTFFPNEKKSFFHLATTHNSFLRIDSDGTVYTSQRLTVTATCPMKLQLFPMDSQRC  180
               ************************************************************
                        Loop A                  Loop E

                  ■    ▲  ▲▲▲                                          ▲■
Hco_UNC49_B    KLEIESYCYTMADIDYFWGRQRSDPRQSAVVFGNFMLPQFKQTCYHVNYTQATTSSGSYR  240
Hco_UNC49_C    KLEIESYGYSTAAIEYHWCGAANPNCETAVVADDVELPSYRFAKVCIDRTMATTASGSYS  240
               ******* *: * *:*.*     .   ::*** .:. **.:: :   :: * ***:****
                        Loop B                  Loop F                  Loop C
```

Figure 5: Partial protein alignment of *H. contortus* UNC-49B and UNC-49C with binding loops shown. ■ indicate residues shown to be important to GABA response through mutagenesis by (Foster et al. 2018). ▲ indicates residues shown to be influential to GABA response by (Accardi and Forrester 2011) through mutational analysis.

Aromatic residues are known to play a major role in GABA binding and the binding site is sometimes referred to as the aromatic box, which is a highly hydrophobic area of the receptors with additional residues involved in hydrogen bonding and pi-cationic interactions (Padgett et al. 2007). This has been demonstrated extensively through mutagenic studies both in nematode and mammalian GABA receptors. Molecular simulations can also assist in determining where the ligand sits within the binding pocket and can help predict which residues may be interacting with specific portions of the ligands. The distance required for pi-cationic binding between GABA and an aromatic residue in the binding pocket is around 6 Å, and the distance between residues for a hydrogen bond range from 2.7 – 3.3 Å. Together, molecular mutagenesis and molecular modelling on these receptors help identify the specific residues which are involved in binding site GABA interactions and can direct further research.

There have been many residues found in the various binding loops that have been shown to be important for GABA binding and receptor activation. For example, binding loop D in the UNC-49 receptor has been characterized through mutagenesis studies. An arginine residue in this loop was shown to be influential in GABA activation of the channel (Accardi and Forrester 2011; Yamamoto et al. 2012). In the same loop, a tyrosine residue (indicated by a triangle in Figure 5) when changed to a nonpolar leucine residue has also been shown to have significant impact on GABA sensitivity in both homomeric and heteromeric UNC-49 receptors (Accardi and Forrester 2011). Furthermore, changes to a phenylalanine and methionine residue, both from loop D in UNC-49B, were shown to increase GABA EC_{50} significantly by about 1.5-fold each. This mutagenic analysis reveals the role that several amino acid residues from loop D play in GABA binding.

Through mutagenic studies, analysis of loop C revealed additional amino acids shown to be important for GABA response. A threonine from this loop has been shown to be important for GABA binding, through hydrogen bonds with the carboxylic end of GABA, and if mutated GABA sensitivity is abolished (Yamamoto et al. 2012). In UNC-49B, the hydroxyl group of tyrosine in loop C influences the GABA response since substitution with a phenylalanine deceases GABA sensitivity (Accardi and Forrester 2011). Many of these analogous residues in vertebrate GABA receptors have also been shown to be influential for GABA binding as well (Padgett et al. 2007; Lummis 2009).

Investigation into loop E reveals several more amino acids that have been shown to be influential to GABA binding. Through substituted cysteine accessibility method (SCAM), both a serine and tyrosine in this loop were shown to be capable of forming hydrogen bonds with GABA in *H. contortus* (Kwaka et al. 2018). Additional studies demonstrate that replacing the arginine residue in loop E decreases GABA sensitivity significantly when changed to a cystine (Kwaka et al. 2018), alanine or a lysine residue (Foster et al. 2018).

In loop A, a tyrosine residue is shown to be influential to GABA binding through a pi-cationic interaction (Padgett et al. 2007). In nematodes, phenylalanine mutations in loop A of UNC-49B have shown to also decrease GABA sensitivity by approximately 20-fold in both the homomeric and heteromeric channels (Accardi and Forrester 2011). This demonstrates the role of the aromatic and polar groups in the sensitivity of the receptors to GABA.

Other key residues in loop B have been shown to be important in ligand binding. In UNC-49B, a tyrosine residue has a significant impact on GABA EC_{50} since changing it to

another aromatic group phenylalanine, increases EC_{50} significantly by about 10-fold in both heteromeric and homomeric GABA receptors. Both the aromatic and hydroxyl portion of tyrosine were shown to be important in this position for GABA sensitivity, since the same substitution with a serine, a residue which is much smaller, but contains a hydroxyl group was not able to recover GABA response (Accardi and Forrester 2011). These results could indicate that in loop B, the electrostatic interaction between both the aromatic ring and the hydroxyl group with GABA is required for GABA interaction in the binding pocket. Additionally, in the same loop, threonine was shown to be important for GABA function. In fact, substitution to a very similar amino acid, serine, which differs only in one methyl group, decreases GABA sensitivity by 30-fold and 18-fold in the homomeric and heteromeric channel respectively (Accardi and Forrester 2011). This indicated that the distance between GABA and this residue is influential to GABA response.

1.3.1.1 GABA receptor antagonists

Picrotoxin (or cocculin) is a potent poisonous compound derived from *Radix Cocculi Trilobi* (Xu et al. 2018) and is a non-competitive GABA receptor antagonist. Picrotoxin is known to cause paralysis and death to organisms such as frogs by decreasing cardiac action (Yuan et al. 1986). It has been known for many years that picrotoxin does not bind to the same site that the natural ligand (Newland and Cull-Candy 1992). Through sequence analysis and site directed mutagenesis in *Drosophila* RDL-GABA receptors it was discovered that TM2 was a region that was extremely important to picrotoxin binding (Ffrench-Constant et al. 1993). TM2 is the portion of the membrane that spans the channel pore and therefore interacts with the incoming ions through the protein. Point mutagenesis studies in this area demonstrated multiple more residues that when mutated, prevent

picrotoxin inhibition (Ffrench-Constant et al. 1993; Erkkila et al. 2008). In UNC-49 GABA receptors, picrotoxin sensitivity is conferred in some heteromeric receptors. Both the *C. elegans* and *H. contortus,* the UNC-49B/UNC-49C heteromeric channel is less sensitive to picrotoxin than the UNC-49B homomeric channel (Bamber et al. 2003; Siddiqui et al. 2010; Brown et al. 2012). Protein alignment of the UNC-49B and UNC-49C subunits from *C. elegans* reveals that a methionine residue present in the M2 region of UNC-49C subunits, but not UNC-49B subunits was critical for picrotoxin resistance (Zhang et al. 1995).

1.3.1.2 GABA receptors as targets for novel anthelmintics

The ligand gated ion channel family is extremely diverse in nematodes, and the family of receptors are much broader than in vertebrates. Since GABA receptors are found in many relevant neural areas in nematodes, targeting these receptors with an anthelmintic which act on GABA receptors may be an appropriate way to manage nematode infections. There is now mounting evidence that nematode GABA receptors are pharmacologically distinct from their mammalian counterparts (Kaji et al 2015; Holden-dye et al 1988). This means that there is potential to develop novel anthelmintics that would target nematode GABA receptors such as UNC-49 with minimal impact on host GABA receptors. This presents an opportunity for parasite population control, without having effects on vertebrate or the host organism.

1.3.2 Nematode inhibitory acetylcholine receptors

Another major neurotransmitter in nematodes is acetylcholine and levamisole. The ACC family of receptors are a unique group of inhibitory acetylcholine-gated chloride channels that are only found in invertebrates. In addition to this, they also express

They are similar in structure to other cystine-loop ligand gated ion channels and contain all the same domains, and many conserved residues (Figure 3, Figure 4). In *C. elegans,* it acts on the body wall, at neuromuscular junctions (Jones and Sattelle 2004b), and possibly in the pharynx (Callanan et al. 2018).. In *C. elegans,* this family consists of *acc-1, acc-2, acc-3, lgc-46, lgc-47, lgc-48,* and *lgc-49* (Figure 2) (Jones and Sattelle 2008), where 'acc' and 'lgc' stand for acetylcholine gated chloride channels and ligand-gated ion channels of the cys-loop superfamily respectively. These receptors mediate fast inhibitory neurotransmission in nematodes (Putrenko et al. 2005b) and as such, are promising anthelmintic targets for future studies or as targets for drug development. In *H. contortus,* immunolocalization studies revealed that ACC-1 localizes to pharyngeal muscle tissue (Callanan et al. 2018) however, in *C. elegans,* it localizes to ventral cord and extrapharyngeal neurons (Wever et al. 2015) indicating diverse localization when comparing free living and parasitic nematodes.

Phenotypic screening of *C. elegans* levamisole resistant strains reveled additional genes that were essential for the functional expression of acetylcholine receptors *ric-3.1, unc-74* and *unc-50* (Fleming et al. 1997a; Boulin et al. 2008). RIC-3 is a chaperone protein which promotes the folding of the receptors (Millar 2008) originally identified to be mutated in levamisole resistant strains of *C. elegans* (Nguyen et al. 1995). UNC-74 is predicted to encode a thioredoxin (James A Lewis et al. 1980), which could be involved in chaperoning the folding of the proteins through the facilitation of disulfide bond formation. UNC-50 is a transmembrane protein which is localized to the Golgi apparatus in the cell and facilitates the localization of the ACC receptors to the cell surface (Eimer et al. 2007). These genes are evolutionarily conserved and are present in *X. laevis* oocytes, however it

is postulated that the expression might not be at sufficient levels to facilitate the heterologous expression of ACC channels (Boulin et al. 2008; Boulin et al. 2011).

Similar to GABA receptors, the ligand binding site consists of a hydrophobic 'aromatic box' and has the same binding loops as shown in Figure 4. The binding occurs on the interface between two adjacent subunits, and they are activated by a wide variety of agonists. In *H. contortus,* the ACC-2 receptors can form homomeric channels and are activated by; acetylcholine, choline, urecholine, carbachol, levamisole and pyrantel (Habibi et al. 2018). The *H. contortus* ACC-1 receptor cannot form a functional channel on its own, but when expressed with ACC-2, the acetylcholine sensitivity is increased (Habibi et al. 2018). *C. elegans* ACC-1, on the other hand can form a functional channel on its own (Putrenko et al. 2005b). In *H. contortus* LGC-46 is able to form a homomeric channel or a heteromeric channel with ACC-1 that is acetylcholine sensitive, however it requires much higher concentrations of agonist to produce small currents (Habibi et al. 2020). Until recently, there has been little work done on the other acetylcholine receptors including *lgc-47*. Recently in *C. elegans*, LGC-47 was shown to assemble to form a form a functional heteromeric channel with ACC-1 which decreases sensitivity to acetylcholine significantly compared to ACC-1 (Hardege et al. 2023). While acetylcholine is the primary agonist for most of these receptors, several are also partially activated by the anthelmintic levamisole (Habibi et al. 2018; Habibi et al. 2020).

Levamisole is a known selective agonist for nematode acetylcholine receptors, but lacks therapeutic effect on these same receptors in vertebrates, making it an attractive drug target. Through screening levamisole resistant strains of *C. elegans,* a subtype of levamisole sensitive acetylcholine receptors was identified (J A Lewis et al. 1980). In *C.*

elegans five proteins have been confirmed to be essential for levamisole action*;* UNC-63 (Culetto et al. 2004), LEV-1, UNC-29, UNC-38 (Fleming et al. 1997b), and LEV-8 (Towers et al. 2005). These receptors can co-assemble in *X. laevis* oocytes to form an ion channel which is sensitive to acetylcholine and levamisole at similar levels, although currents of lower amplitude are produced with levamisole (Boulin et al. 2008). Orthologues to some but not all of these receptors have been found in *H. contortus,* however no orthologue to LEV-8 has been identified (Neveu et al. 2010). UNC-29, UNC-38, UNC-63 have been identified in *H. contortus* to be levamisole sensitive receptors along with ACR-8 (Boulin et al. 2011). ACR-8 is present in *C. elegans but* is not levamisole sensitive (Touroutine et al. 2005). Levamisole is also a known activator of acetylcholine receptors in nematodes and is a commonly used drug in nematode control. Levamisole cannot pass the blood brain barrier of most vertebrates, making it an effect drug choice poor the prevention of parasitic nematodes. Resistance, however, is developing, and the development of new synthetic drugs, which can activate nematode acetylcholine receptors at lower concentrations than currently used would be significantly relevant in drug development.

2. Rationale and Objectives

2.1 Rationale

D. immitis infection is becoming a global concern due to the increasing resistance to macrocyclic lactones, the sole prophylactic option (Bourguinat et al. 2011). For regions such as southern Canada, this challenge is compounded by global warming extending mosquito season, increasing the length of time *D. immitis* can be transmitted to dogs. The extended warm seasons result in greater transmission of the disease, ultimately resulting in the evolution of greater genetic diversity and drug resistant phenotypes. Clearly, new drug targets will be necessary.

In *H. contortus* and *C. elegans*, the ligand gated ion channel family of receptors have been well characterized and are associated with nervous system behaviors such as locomotion, mating, and feeding. Importantly, many ligand-gated ion channels found in nematodes are functionally distinct from vertebrates, both in function and in assembly. Their role in survival and reproduction therefore represents a promising avenue for the development of new drug targets. However, in *D. immitis*, many of these receptors have not yet been identified nor characterized. Evidently, this presents a knowledge gap for the development of new prophylactic drugs against heartworm.

Previous studies comparing the ACC and UNC-49 gene families between *H. contortus* and *C. elegans* show that subtle amino acid differences in these receptors, especially in the binding loop, leads to large changes in the response to a ligand. It is for these reasons that the *D. immitis* receptors and binding sites need to be characterized to identify their potentially unique structural and pharmacological properties. Although there is striking similarity between the receptors of *H. contortus* and *C. elegans* with *D. immitis,* these

nematodes belong to different clades (Clade V and Clade III) (Blaxter et al. 1998) indicating substantial distance in their evolutionary relationship. It has been previously shown that similar channels in evolutionarily close organisms produce channels with vastly different pharmacological properties. Therefore, characterizing the ligand-gated ion channels in *D. immitis* becomes imperative to better understand their functionality, localization, and potential divergences from counterparts in *H. contortus* and *C. elegans.* This study will bridge this knowledge gap by investigating and characterizing the ACC and UNC-49 receptors in *D. immitis,* elucidating distinguishing features of the ligand gated ion channel family between clades, as well as identifying residues in the *D. immitis* ligand gated ion channel binding pocket which may be involved in ligand binding. Drawing upon mutational studies conducted in *C. elegans* and *H. contortus*, we can discern the patterns of residues involved in ligand binding, which will serve as a guiding framework for future investigations into *D. immitis* drug development.

2.2 Objectives

1. **Identify and clone the *unc-49* and *acc-1* gene family of ligand gated ion channels in *D. immitis***

The UNC-49 and ACC-1 families of cystine-loop receptors have potential as novel anthelmintic targets (Kaji et al. 2015; Wever et al. 2015). However, these receptors have not been identified in *D. immitis*. This thesis aims to identify the *D. immitis unc-49b, unc-49c,* and *acc* genes (*acc-1*, *lgc-46* and *lgc-47*) with subsequent sequence analysis. As *D. immitis unc-49b* has already been cloned, *D. immitis unc-49c* and the *acc* family of genes will be identified and cloned from adult female worms. The protein and DNA sequences

will then be characterized and compared with other nematodes through BLAST and ClustalW alignments to identify any differences.

2. Investigate and compare the pharmacological properties of *D. immitis* UNC-49 and ACC receptors with co-expression of *H. contortus* receptors.

Once all receptors have been isolated from *D. immitis*, they will be pharmacologically characterized and compared to the same receptors from *H. contortus and C. elegans. H. contortus* UNC-49 subunits will also us used to further characterize the role of various UNC-49 subunits from *D. immitis*. This will be accomplished by co-expressing *D. immitis* UNC-49 subunits with those from *H. contortus*. The agonist (GABA) or antagonist (picrotoxin) responses of *D. immitis* or *H. contortus* UNC-49 channels will be measured via electrophysiology after expression in *X. laevis* oocytes. Lastly, all *D. immitis* ACC subunits will be similarly characterized by electrophysiology in *X. laevis* oocytes using acetylcholine, levamisole and various cholinergic agonists.

3. *In silico* modelling of cystine loop receptors

To identify and visualize residues within the predicted binding pocket, receptors will be modelled *in silico.* Any of the individually or co-expressed *D. immitis* receptors with a measurable agonist response, as identified in objective 3, will also have their ligand interaction characterized using *in silico* analysis.

4. Analysis of UNC-49 and ACC expression in male, female and larval *D. immitis*

To investigate the relative importance of the various receptors in *D. immitis* life stages, their expression in different sex and life stage will be analyzed. Gene expression of *unc-49b*, *unc-49c, lgc-46, lgc-47* and *acc-1* will be measured via RT-qPCR in adult male, adult female, and L3 stage *D. immitis.*

5. Screening of novel levamisole derivatives on *D. immitis* and *H. contortus* ACC receptors

To showcase the applicability of rational drug design against *D. immitis* ion channel receptors, novel levamisole derivatives will be evaluated as ligands for ACC receptors. Electrophysiology will be used to measure ion channel responses after functional expression of ACC receptors in *X. laevis* oocytes. These responses will be compared to acetylcholine and levamisole.

3. Methods

Both *unc-49* and *acc* genes were cloned from the adult female *D. immitis* transcriptome using gene specific primers and directional cloning methods. cRNA was synthesized encoding the genes of interest and microinjected into *Xenopus laevis* oocytes for electrophysiological testing using both agonists and antagonists for the receptor. Gene expression levels were subsequently analyzed in male, female and L3 stages to determine if genes were expressed at relevant levels in all life stages. Finally, additional synthetic levamisole derivates were tested on *H. contortus* ACC-2 receptors to determine if any of these novel molecules had enhanced activity compared to levamisole action.

3.1 Identification and cloning of *unc-49c*, *acc-1*, *lgc-46*, *lgc-47*

Frozen Adult Female *D. immitis* worms were obtained from BEI Resources (managed by ATCC). Samples were ground using a mortar and pestle with liquid nitrogen until a powder was collected and, RNA was extracted using Trizol RNA extraction (Invitrogen, USA). RNA purity was assessed on a 1% agarose gel and concentration and purity was assessed using a BioDrop DUO®, an ultraviolet–visible spectrophotometer cDNA was synthesized using the QuantiTect® reverse transcriptase kit (Qiagen, USA). A 3’ oligo-dT adapter sequence was used to synthesize cDNA, with V being any nucleotide except thymine and N is any standard nucleotide. (5'CCTCTGAAGGTTCACGGATCCACATCTAGATTTTTTTTTTTTTTTTVN3'). The *unc-49b* clone was previously cloned by N. Lamassiaude (INRAE) and sent to us for further analysis.

Gene fragments were identified from a comparative genomic screen of parasitic worms through bioinformatic analysis of the genome (International Helminth Genomes

Consortium 2019). From there, Basic Local Alignment Search Tool (BLAST) (Altschul et al. 1990) was used to compare sequences to known sequences from other nematodes. NCBI was used to obtain protein sequences for UNC-49B (GenBank: ACL14329.1) and UNC-49C (GenBank: ABW22635.1) from *H. contortus*, as well as *C. elegans* UNC-49B (GenBank: AAD42384.1) and UNC-49C (GenBank: AAD42386.1). These sequences were used in tBLASTn which uses protein sequence to search a translated nucleotide database in all six reading frames (Altschul et al. 1990; Gish and States 1993). The search was limited to whole genome shotgun (wgs) contigs since it is currently the only complete genetic database available for *D. immitis* (NCBI Accession: JAKNDB000000000.1). The wgs contigs predicted by tBLASTn to contain exons coding for a protein of interest were imported into SnapGene Viewer (v6.2.1) (https://www.snapgene.com/snapgene-viewer) and translated in all 6 reading frames to identify intronic regions of the wgs contig. Genes of interest were pieced together based on the sequences from *H. contortus, C. elegans*, ensuring the 5' and 3' ends of the genes were complete with a start and stop codon and through sequence alignments (described previously). The sequence was translated *in silico* using SnapGene Viewer to ensure the complete coding sequence was being captured.

To clone the complete coding sequence of the various genes, primers were designed to bind to both the 5' and 3' ends of the gene. PCR was performed using Taq DNA Polymerase (Thermo- Fisher, USA), and successful amplification was determined via electrophoresis on a 1% agarose gel. The sample was purified using Bio Basic PCR Cleanup kit, according to manufacturer's instructions (Bio Basic, Canada) and subsequently cloned into the pGEMT easy^{TM} (Promega, USA) sequencing vector through an overnight ligation at 4 ºC. The sample was transformed into SIG10 chemically

competent *E. coli* cells (Sigma-Aldrich, Canada) according to manufacturer's instructions, and plated onto LB agar (Sigma-Aldrich, Canada) plates supplemented with 100 μg/mL of Ampicillin (Sigma- Aldrich, Canada) and 20 μg/mL of X-Gal (Bio Basic, Canada). Plates were incubated at 37 ºC for 16 hours and eight white colonies (indicative of DNA insertion into the plasmid) were selected for growth in LB (Sigma-Aldrich, Canada) 4 mL liquid cultures. Plasmids were isolated and purified using a Plasmid DNA cleanup kit (Bio Basic, Canada) according to manufacturer's instructions. Vectors were sent for sequencing at Genome Quebec (Montreal, Canada) and compared to the DNA sequences of known genes from *H. contortus* and *C. elegans.*

Once it was confirmed that the complete sequence was cloned, primers were designed containing 5' restriction sites to facilitate directional cloning into pGEMHE, described in Table 2. pGEMHE contains an ampicillin resistance gene, a linearization site (PstI, NheI, SphI), directional cloning site, and the 3' and 5' UTR of the *X. laevis* β-globin gene for heterologous expression in *Xenopus laevis* oocytes (Krieg and Melton 1984; Liman et al. 1992). A high-fidelity polymerase, PFU DNA Polymerase (Agilent, California), was used to amplify genes from cDNA to ensure no polymorphisms were created due to enzymes. The genes were then subsequently restriction cloned into pGEMHE and transformed into SIG10 chemically competent *E. coli* cells (Sigma-Aldrich, Canada), as described previously. Eight colonies were selected, and plasmid extraction was performed according to manufacturer's instructions, as described previously. To identify which plasmids contained the target DNA, small samples of the plasmid were linearized and run on a 1% agarose gel to confirm the size of the full-length plasmid. All samples

containing an insertion were sent for sequencing to detect if there were any genetic polymorphisms. Sequencing was performed at Genome Quebec (Montreal, Canada).

Table 2: Gene specific primers used for cloning into expression vectors.

Gene	Forward Primer	Reverse Primer	Restriction enzymes for cloning
unc-49c	GCAGTCCCGGGATGCATCTTATC TCATTC	ATGTCGGATCCTTAACAGGCTCTTT GTTC	XbaI, XmaI
acc-1	TCGATCCCGGGATGCGTCATCCT GGATGGATGATG	TGACTTCTAGATTAGCTCATAGTAG GTTCTTCAGATGATGAAAGAC	XbaI, XmaI
lgc-46	TAGCTCCCGGGATGCACTACCTC AATCGTC	GCTAGTCTAGATCAATCCTTGAGGT AATGATACC	Xmai, Xbai
lgc-47	ACTGAGGATCCATGCTCCAGAG AACAATCGTAAGC	GCTGAAAGCTTCTAGTGATTCTGTA GAAGTAGTCCATTC	HindIII, BamHI

3.2 Sequence analysis and phylogenetic analysis

NCBI was used to obtain protein sequences for UNC-49B and UNC-49C from *H. contortus* (Clade III), *C. elegans* (Clade III)*, Brugia malayi* (Clade V)*,* and *Pristionchus pacificus* (Clade III) as described in section 3. Clustal W (Madeira et al. 2022) was used to align the protein sequences for visual analysis. BLASTp (Altschul et al. 1990) was used to determine the percentage of identical amino acids (identities) and the percentage of similar amino acids (positives) that exist between any of the sequences analyzed and other known parasites.

To determine the presence of signal peptides, the web program SignalP6.0 was used (https://services.healthtech.dtu.dk/services/SignalP-6.0/), which predicts the presence of signal peptides in a protein sequence (Teufel et al. 2022). The SignalP search was limited to eukaryotes. Transmembrane domains were identified using DeepTMHMM 2.0 (https://services.healthtech.dtu.dk/services/TMHMM-2.0/) (Sonnhammer et al. 1998; Krogh et al. 2001), and confirmed through alignment with known transmembrane domains of both *C. elegans* and *H. contortus.*

For phylogenetic tree construction, complete protein sequences were obtained from our lab, NCBI as described previously or through UniProt, a protein sequence database (https://www.uniprot.org/) (The UniProt Consortium 2023). An online tool, phylogeny.fr (http://www.phylogeny.fr/simple_phylogeny.cgi) (Dereeper et al. 2008; Dereeper et al. 2010) was used to construct phylogenetic trees showing the relationship between sequences and which proteins clustered together, showing the most sequence similarity. Additional proteins from the cystine loop ligand gated ion channel family *D. immitis,* GLC-4, AVR-14 and LGC-49, which are currently unpublished were obtained through similar methods as described previously in our lab by J. Nichols (2023) as a part of her Master's thesis to be included in the phylogenetic analysis.

3.3 Homology modelling and docking of ligands

The SWISS-MODEL Repository (Bienert et al. 2017; Waterhouse et al. 2018) was used to search the databases of existing three-dimensional protein models against genes of interest from this study. Homology modeling for all receptors was done using *C. elegans* glutamate-gated chloride channel 3RIF as a template, as determined by SWISS-MODEL. As discussed previously, a great deal of structural conservation exists between cysteine loop ion channels, which makes 3RIF an excellent model for structural alignment. Using MODELLER 10.4 (Šali and Blundell 1993), protein sequences of interest were aligned to 3RIF in a three- dimensional conformation, which proved to be the most energetically favorable. These protein sequences were then arranged as a homodimer through MODELLER 10.4. From there, ligands were docked into the hypothetical binding pocket using AutoDockTools 1.5.7 (Trott and Olson 2010). The ligand dock with the most energetically favorable score was selected for further analysis. The visualization of the

interaction of the ligand with the receptors was done using Chimera 1.16 (Pettersen et al. 2004), which also allows for putative distance calculations to be performed, and the residues in the predicted *in silico* binding pocket to be identified.

3.4 Heterologous expression of channels in *Xenopus laevis* oocytes

All animal procedures followed the University of Ontario Institute of Technology Animal Care Committee and the Canadian Council on Animal Care guidelines. Female frogs were supplied by NASCO (Dexter, Michigan) and housed in a temperature-controlled room with 12-hour light-dark cycling. The frogs were anesthetized with 0.15 % 3-aminobenzoic acid ethyl ester methanesulphonate salt (MS-222) (Sigma-Aldrich, Canada), and pH adjusted to 7 with sodium bicarbonate. Surgical extraction of ovaries was performed, and the eggs were defolliculated with 2mg/ml of collagenase-II (Sigma-Aldrich, Canada) in calcium-free oocyte Ringer's solution (82 mM NaCl, 2 mM KCl, 1 mM MgCl2, 5 mM HEPES pH 7.5 (Sigma-Aldrich, Canada)). The eggs were placed on a rocker and left to defolliculate at room temperature for 1 hour. The eggs were rinsed with ND96 solution (1.8 mM $CaCl_2$, 96 mM NaCl, 2 mM KCl, 1 mM $MgCl_2$, 5 mM HEPES, pH 7.5), and stored in ND96 supplemented with 50 µg/mL gentamycin and 275 µg/mL of pyruvic acid (ND96-Supp) and stored at 18ºC for use.

H. contortus unc-49b and *unc-49c,* cloned previously in our lab into the pT7Ts *X. laevis* expression vector, were also used for analysis. The six plasmids containing. *H. contortus unc-49b* and *unc-49c* as well as *D. immitis unc-49c, acc-1, lgc-46* and *lgc-47* were linearized using restriction enzymes either NheI or PstI for genes in pGEMHE and BamHI or XbaI (New England Biolabs, USA) for those in pT7TS. The *D. immitis unc-49b*

was cloned into the vector pTB-207 and was linearized using XbaI. The reactions were incubated for an hour in a 37 ºC dry bath, since incubating for recommended protocol time (5 -15 minutes) did not yield fully linear plasmid. For each gene, cRNA was synthesized using the T7 mMessage mMachine kit, (Ambion, Texas, USA) 1 µg of the linear plasmid was added to each reaction and incubated according to kit instructions. cRNA concentration and purity were assessed using a BioDrop DUO®, an ultraviolet–visible spectrophotometer. Samples were diluted to 400 ng/µL with Water for Molecular Biology (Sigma-Aldrich, Canada). Glass Capillaries (1.2 OD x 0.69 ID x 100 L mm) (Harvard Apparatus, Massachusetts) were pulled into needles for injection on a P-97 Micropipette Puller (Sutter Instrument Co., California, USA). The needles were backfilled with mineral oil and loaded onto a Nanoject II microinjector (Drummond Scientific, USA) and the required cRNA was loaded into the needle. For all receptor combinations tested (Table 3), *X. laevis* oocytes we injected with 50 nL (20 ng) of RNA, and oocytes were incubated at 18ºC in ND96-Supp for 48 to 90 hours. In addition to the acetylcholine receptor combination to be studied, *H. contortus unc-50, unc-74,* and *ric-3* were also injected into the same eggs to facilitate expression (Boulin et al. 2008; Boulin et al. 2011), which were supplied by Dr. Cédric Neveu (INRAE) as previously done in our lab (Habibi et al 2018).

Table 3: Receptor combinations investigated, and ligands tested. Receptor names in green indicate receptors from *H. contortus* not cloned as part of this study but utilized for various experiments.

Receptor combinations analyzed in this study	Required co injection with *H. contortus* accessory proteins	Ligands tested
Hco-UNC-49B	NO	GABA, picrotoxin
Hco-UNC-49B+ Hco-UNC-49C	NO	GABA, picrotoxin
Hco-UNC-49B + Dim-UNC-49C	NO	GABA, picrotoxin
Dim-UNC-49B	NO	GABA, picrotoxin, R-GABOB, S-GABOB, DAVA, IMA
Dim-UNC-49B + Dim-UNC-49C	NO	GABA, picrotoxin, R-GABOB, S-GABOB, DAVA, IMA
Dim-UNC-49B + Hco-UNC-49C	NO	GABA, picrotoxin
Dim-UNC-49C	NO	GABA, picrotoxin
Dim-ACC-1	YES	Acetylcholine
Dim-ACC-1 + Dim-LGC-46	YES	Acetylcholine
Dim-LGC-47	YES	Acetylcholine
Hco-ACC-2	YES	Acetylcholine, levamisole, levamisole derivatives

3.5 Two-electrode voltage clamp electrophysiology

Glass electrodes (1.5OD x 0.86 ID x 100 L mm) (Harvard Apparatus, Massachusetts) were pulled using the P-97 Micropipette Puller (Sutter Instrument Co., California, USA). The electrodes were backfilled with 2M KCL, silver wires were inserted into the back, and the electrodes were mounted on the electrode holder. Stocks of 100mM GABA (Sigma Aldrich, Canada) or 20 mM picrotoxin (Sigma-Aldrich, Canada), or 100 mM acetylcholine were dissolved in ND96. Serial dilutions of GABA were made for various concentrations between 30 mM and 10 µM. Axoclamp 900A (Molecular Devices, USA) was used to perform two-electrode voltage clamp electrophysiology (TEVC) on oocytes. The oocyte was placed in the RC-1Z perfusion chamber (Warner Instruments, USA) and agonist dose response curves were generated by washing increasing concentrations of agonists over the oocyte. Data was collected by washing various ligands over the oocyte and measuring the current generated. Data was analyzed using Clampex Software v10.2 (Molecular Devices, USA). The concentrations which produced 50% of the maximal response (EC_{50} values)

were generated using the data from the dose response curves using GraphPad Prism Software 8.0.2 for Windows 10 (GraphPad Software, USA).

For picrotoxin experiments, the GABA (Figure 6 A) EC_{50} concentration for each receptor were first determined and then dissolved in ND96 with increasing concentrations of picrotoxin from 1 μM to 250 μM. For these experiments the oocytes were washed with EC_{50} GABA concentration, followed up with a solution containing both GABA and one of the picrotoxin experimental concentrations. This technique was repeated on a new egg each time, with an increasing concentration of picrotoxin, each time until maximum inhibition was reached. The GABA with picrotoxin (Figure 6 B) response was compared to the GABA only response for each picrotoxin concentration tested. Inhibition response curves were generated with Graphpad Prism Software 6 (California, USA).

Other known GABA receptor agonists used (Figure 6) were imidazole-4-acetic acid (IMA), (R)-(-)− 4-Amino-3-hydroxybutyric acid (R-GABOB), (S)-(+)− 4-Amino-3-hydroxybutyric acid (S-GABOB), and 5-aminovaleric acid (DAVA), all obtained from Sigma-Aldrich (Canada). 20 mM stocks were made with ND96 as described previously and diluted into 5 mM and 10 mM working concentrations based on previous GABA EC_{50} and maximum calculations.

At least 5 oocytes, and at most 18 oocytes from a minimum of 2 different frogs were used to generate each data point. Data was analyzed using students t-test in Graphpad Prism Software 6. Significance was determined if $p \leq 0.05$.

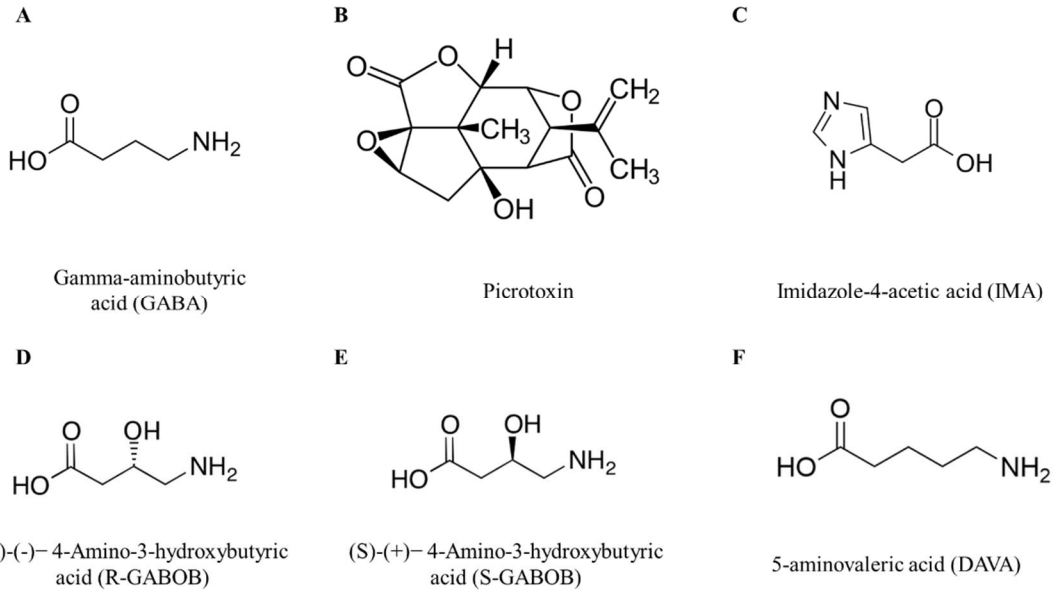

Figure 6: Structure of (A) Gamma-aminobutyric acid (GABA), and (B) picrotoxin, (C) Imidazole-4-acetic acid (IMA), (D) (R)-(-)− 4-Amino-3-hydroxybutyric acid (R-GABOB), (E) (S)-(+)− 4-Amino-3-hydroxybutyric acid (S-GABOB), and (F) 5-aminovaleric acid (DAVA).

3.6 Quantitative-real time PCR analysis of *unc-49b, unc-49c, acc-1, lgc-46* and, *lgc-47*

Adult female RNA extracted previously as identified in section 3, as well as male and L3 total RNA obtained through BEI Resources (managed by ATCC) were used in quantitative-real-time-PCR analysis (q-PCR) analysis. A total of two biological replicates were able to be obtained for each life stage. The L3 is a pooled sample of one isolate. iScript™ reverse transcriptase (Bio-Rad, California) was used for cDNA synthesis reactions, and 200 nM of RNA was used per reaction. Reverse transcriptase was not added for no-reverse transcriptase controls. cDNA was diluted to a concentration of 6.5 ng/µL for further analysis. Primers were designed using primerBLAST (NCBI) and limited to amplicons of 90-180 base pairs long, and exon spanning. netPrimer (NCBI), was used to ensure the primers had melting temperatures in the optimal range for our experiment (60-63 ºC), with no secondary structures and cross or self-complementarity between primer sets. Primers were sourced through Integrated DNA Technologies (Iowa, USA) (Table 4). All q-PCR reactions used SsoAdvanced™ Universal SYBR® Green Supermix (Bio-Rad, California) using the CFX96 Connect Real-Time PCR System (Bio-Rad, California) thermocycler in 96-well plates (Bio-Rad, California). To evaluate the efficiency of the primers, 5 serial dilutions were performed using a 1:4 dilution factor to generate a standard curve. All concentrations were evaluated through qPCR analysis, using the optimal temperature determined from the primer validation (55 ºC). CFX manager (Bio-Rad, California) was used to evaluate standard curves to ensure a sufficient linear dynamic range and efficiency (95-105%) for all genes. Conditions were as follows: (98 °C for 3:00; 40 cycles of 95 °C for 0:10 and 47-60 °C for 0:30) and melt curve analysis (65 °C to 95 °C, 0.5 °C increment per 0:05). An annealing temperature of 55 ºC was chosen for all genes

tested including the control genes: *gapdh* (encoding glyceraldehyde 3-phosphate dehydrogenase; Accession: JQ780095.1) and *ditpn* (encoding *D. immitis* tumor suppressor protein, a growth factor; Accession: JX469415.1). *gapdh* was chosen to be the control gene for the experiment. qPCR analysis was done in triplicate, and analyzed using CFX manager (Bio-Rad, California) and Graphpad Prism Software 6 (California, USA).

Table 4: Primer sets used for qPCR analysis. Genes in bold are control genes.

Gene	Forward Primer	Reverse Primer
unc-49b	TACTACTGTACTAACGATGACCACACTTAT	CGGTATTCCTTGCTCAACCTGTT
unc-49c	TCCACCTGTTTCCTATATTAAGGCT	GCGACAGTAGCAAATTCAATAAGT
acc-1	TTTGGGAAGACCCAGCACTT	AGCAGCATTTTTCGAATTGATGA
lgc-46	CGGAGTTGGCACACGAAAAG	TGTGTTGCTCGTTCCCTTTG
lgc-47	AAGTACGGATGAAATGGAACGAAC	CTGCCGCATACTCAGCTTC
gapdh	GGGAAACTGTGGCGAGATGG	CGGAGTTGGCACACGAAAAG
ditpn	AAGGTCGACAAGTGGTGAGAA	GTAGCCATATCTTCGTAACAGTTC

3.7 Levamisole derivative screening

Eight novel levamisole derivative compounds, synthesized by Autumn Collins (Ontario Tech University) as a part of her MSc project. *Hco-acc-2* linear plasmid was obtained from stocks in our lab, cRNA was synthesized as described in 3.4, standardized and injected into *X. laevis* oocytes along with the cRNA encoding *H. contortus* accessory proteins *unc-50*, *unc-74* and *ric-3.1*, and incubated as described in section 3.4. Levamisole (Sigma-Aldrich, Canada) (Figure 7 A) and acetylcholine (Sigma-Aldrich, Canada) (Figure 7 B) were made into stock solutions with ND96 for use. Levamisole derivatives (Figure 7 C) were dissolved first in dimethylsulfoxide (DMSO), and then diluted into ND96 for testing. Between runs, oocytes were washed ND96 supplemented with 0.1% DMSO to account for the DMSO in the testing solutions. For each oocyte, a concentration of 500 μM was used for all conditions to achieve a maximal response from the ligands. For compound 13, a dose response curve was created from various concentrations from 5 μM to 500 μM. Data was analyzed, and students t-test was done to determine significance ($p \leq 0.05$) using Graphpad Prism 6 (California, USA). A minimum of five and a maximum of fifteen eggs were used from a minimum of 2 different frogs for each experiment.

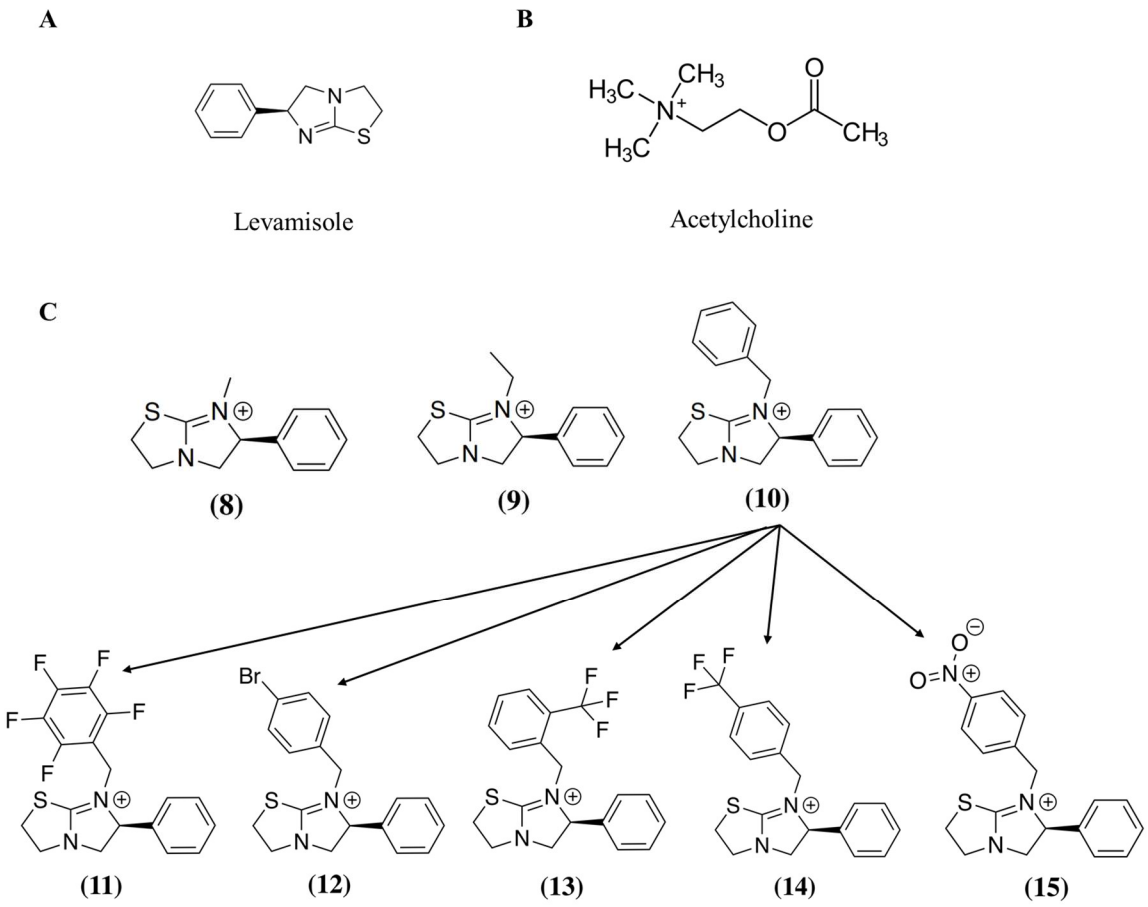

Figure 7: Structure of (A) levamisole, (B) acetylcholine and (C) novel levamisole derivative compounds created by (Collins 2022) used for testing on Hco-ACC-2 receptors. Compounds 8-10 were first preliminarily tested for activation in comparison to levamisole itself. Compound 10 elicited a higher response than levamisole based on electrophysiology results. For further analysis, compounds 11-15 were subsequently synthesized using compound 10 as the backbone, with varying substitutions on the phenyl group attached to the amine nitrogen.

4. Results

4.1 Bioinformatic analysis of *unc-49b* from *D. immitis*

dim-unc-49b was kindly sent to us by our collaborators for bioinformatic analysis and for functional analysis. The cDNA transcript of *dim-unc-49b* encodes a 1455 base pair gene (Appendix) and encodes a 485 long amino acid sequence. The protein sequence was aligned to both *H. contortus* and *C. elegans* (Figure 8). Dim-UNC-49B had 72% identical amino acids and was 82% like Hco-UNC-49B. Dim-UNC-49B had 69% of amino acids identical and 80% similar to Cel-UNC-49B. There is an amino acid variation in *D. immitis* loop D compared to *H. contortus* (Figure 8, first star) which has been shown to have a small impact in the GABA response in *H. contortus* (Accardi and Forrester 2011).

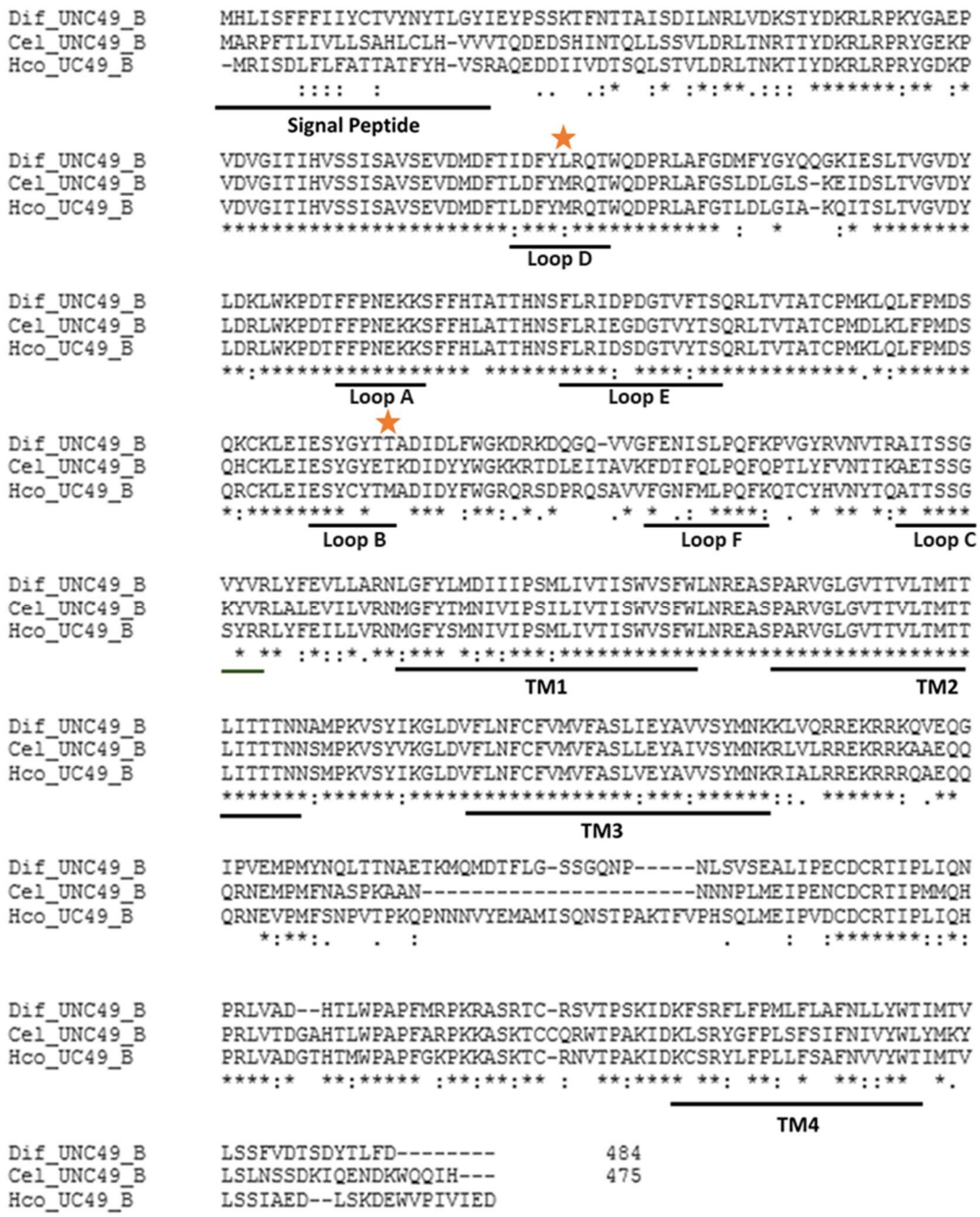

Figure 8: Protein sequence alignment of *D. immitis* UNC-49B with *C. elegans* UNC-49B, and *H. contortus* UNC-49B. Asterisks (*) indicate identical amino acids and (:) represents similar amino acids. The binding loops, and transmembrane domains (TM) are displayed. Orange stars indicate residues where there are variations from the *H. contortus* receptor, which have been shown previously to be important for GABA sensitivity (Accardi and Forrester 2011).

4.2 Cloning of *unc-49c* from *D. immitis*

To obtain the rest of the members of the *unc-49* gene family, the cloning of *unc-49c* was required. The full-length *dim-unc-49c* was determined to be 1341 base pairs long (Appendix). As observed in other nematode species, the 5' and of *dim-unc-49c* is identical to the 5' end of *dim-unc-49b* (Figure 9 A), and the gene only differs in its 3' end though differential splicing (Figure 9 B). Binding loop D, A, E and a portion of Loop B are encoded for by the identical 5' region in 5 exons, the remainder of the protein is encoded for by the 3' portion which differs between the two gene (ie. Mature mRNA) variants. Exons six to 11 encode the UNC-49B receptor and exons 12 through 16 encode the UNC-49C receptor. The exons which encode UNC-49C are much closer together than UNC-49B. The protein sequence encoded by *dim-unc-49c* is 446 amino acids and contains a predicted signal peptide sequence (Figure 10). Alignments were performed to both *H. contortus* and *C. elegans.* According to a BLAST inquiry on the amino acid composition, Dim-UNC-49C is 66% identical and 80% similar to Hco-UNC-49C, the parasitic species. Dim-UNC-49C is 62% identical and 77% similar to Hco-UNC-49C, the free-living species. There is a single amino acid variation in transmembrane domain 2 (TM2) (Leucine instead of Methionine) in *D. immitis* in comparison to *C. elegans* and *H. contortus* (Figure 10, star), which is associated with picrotoxin resistance.

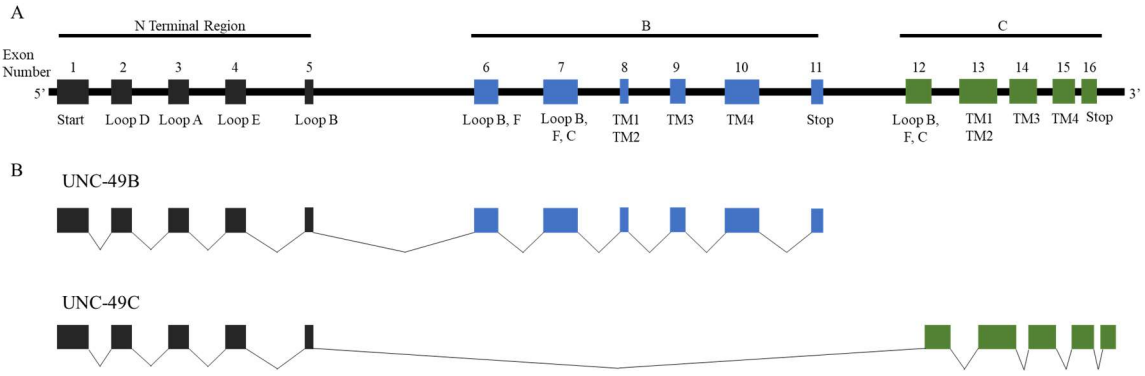

Figure 9: (A) Genomic organization of the *unc-49* receptors in *D. immitis* (NCBI Accession: JAKNDB000000000.1). Black indicates exons shared between both UNC-49B and UNC-49C, providing the characteristic identical 5' regions. Blue indicates UNC49-B exons, green indicates UNC49-C exons. Binding loops are labelled, and transmembrane domains are labelled TM1-TM4 (B) Splicing pattern of the *unc-49B* and *unc-49C* genes. Black lines indicate the introns that are spliced out of the gene.

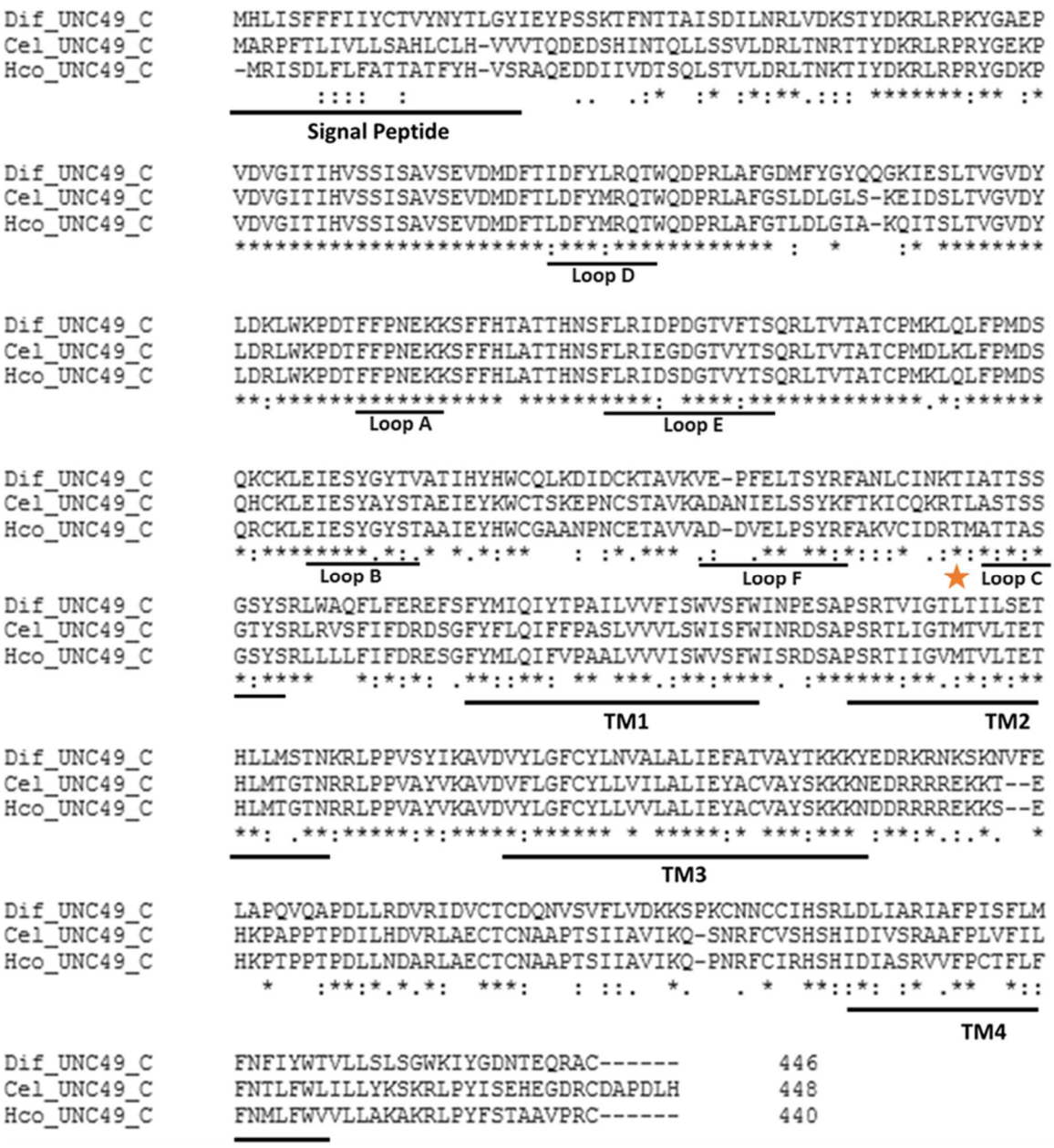

Figure 10: Protein sequence alignment of *D. immitis* UNC-49C with *C. elegans* UNC-49C, and *H. contortus* UNC-49C. Asterisks (*) indicate identical amino acids and (:) represents similar amino acids. The binding loops, and transmembrane domains (TM) are displayed. Orange star are above TM2 is where there are variations associated with picrotoxin resistance (Zhang et al. 1995).

4.3 Cloning of *lgc-46*, *lgc-47* and *acc-1* from *D. immitis* and identification of *acc-2*

The putative members of the *acc* gene family were identified through a bioinformatic screen of the genome. Putative full-length gene sequences were cloned for *dim-acc-1, dim-lgc-46,* and *dim-lgc-47;* and are 1338, 1614, and 1197 base pairs respectively (Appendix). A putative gene sequence of *dim-acc-2,* which encoded a full-length protein was noted in the genome but was not able to be cloned in this study (Appendix). The Dim-LGC-46 protein sequence is 539 amino acids long and is 66% identical and 75% similar to *H. contortus* as well as 64% identical and 73% similar to *C. elegans* (Figure 11). The Dim-LGC-47 protein sequence is 400 amino acids in length and is 66% identical and 75% similar to *H. contortus;* and 64% identical and 73% similar to *C. elegans* (Figure 12). The putative Dim-ACC-1 amino acid sequence is 447 amino acids long and is 68% identical and 76% similar to *H. contortus;* and 68% identical and 77% similar to *C. elegans (*Figure 13). All proteins contained predicted transmembrane domains and binding loops; however, only Dim-ACC-1 and Dim-LGC-47 have a predicted N-terminal signal peptide sequence (Figure 14 A, B, C). In Dim-ACC-1, the signal peptide is predicted with 0.53 likelihood, with a cleavage site between positions 23 and 24. In Dim-LGC-47, the sequence is predicted with a probability of 0.957 with the cleavage site between amino acids 31 and 32. However, Dim-LGC-46, was predicted to not contain a signal peptide sequence as seen by the green consensus line (Figure 14 A). Although a putative sequence for *dim-acc-2* was identified (Appendix), the gene was unable to be cloned using the same methods described for the other *acc* genes.

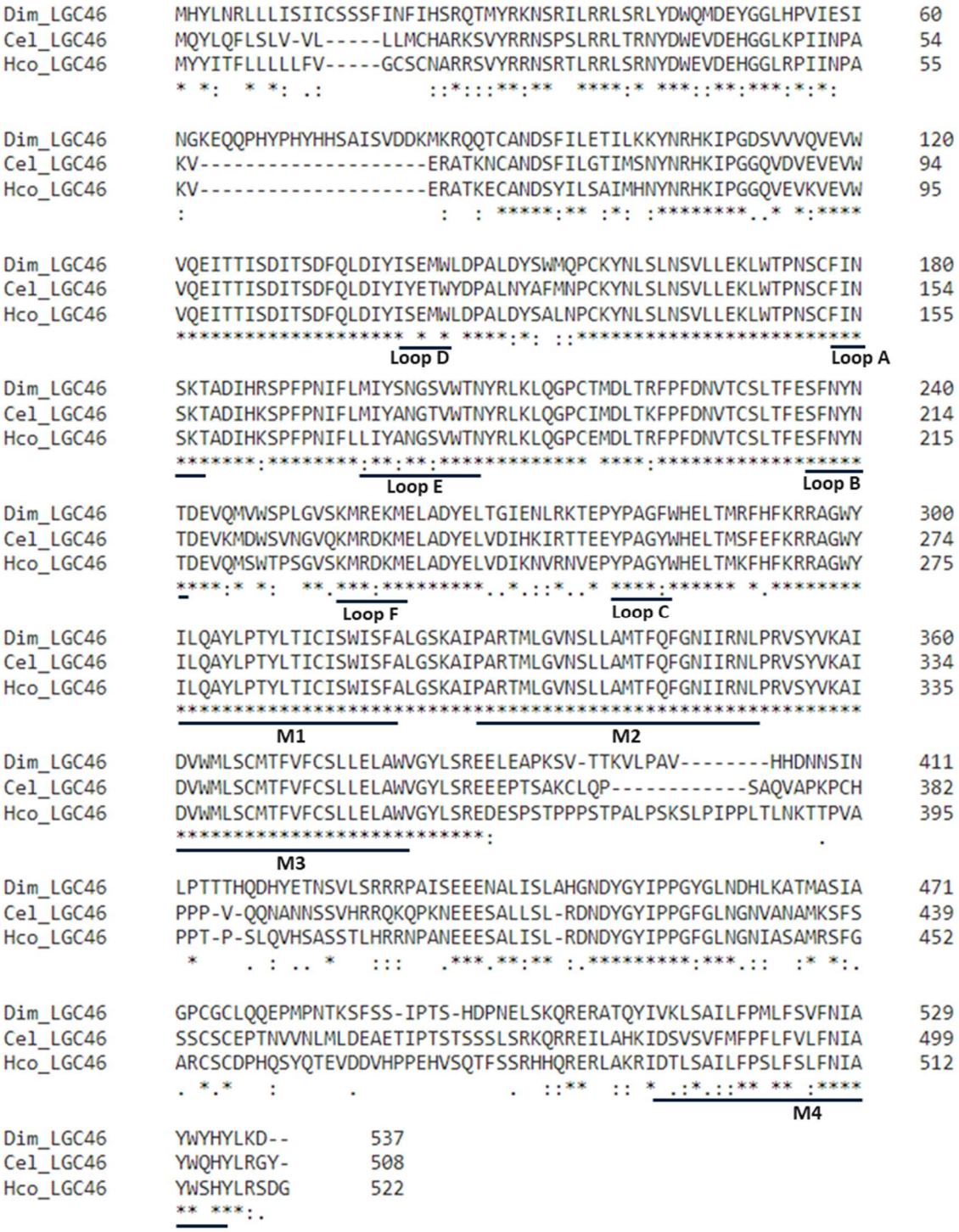

Figure 11: Protein sequence alignment of *D. immitis* LGC-46 with *C. elegans* LGC-46, and *H. contortus* LGC-46. Asterisks (*) indicate identical amino acids and (:) represents similar amino acids. The binding loops, and transmembrane domains (TM) are displayed. There is no predicted signal peptide sequence for this protein.

Figure 12: Protein sequence alignment of *D. immitis* LGC-47 with *C. elegans* LGC-47, and *H. contortus* LGC-47. Asterisks (*) indicate identical amino acids and (:) represents similar amino acids. The binding loops, and transmembrane domains (TM) are displayed.

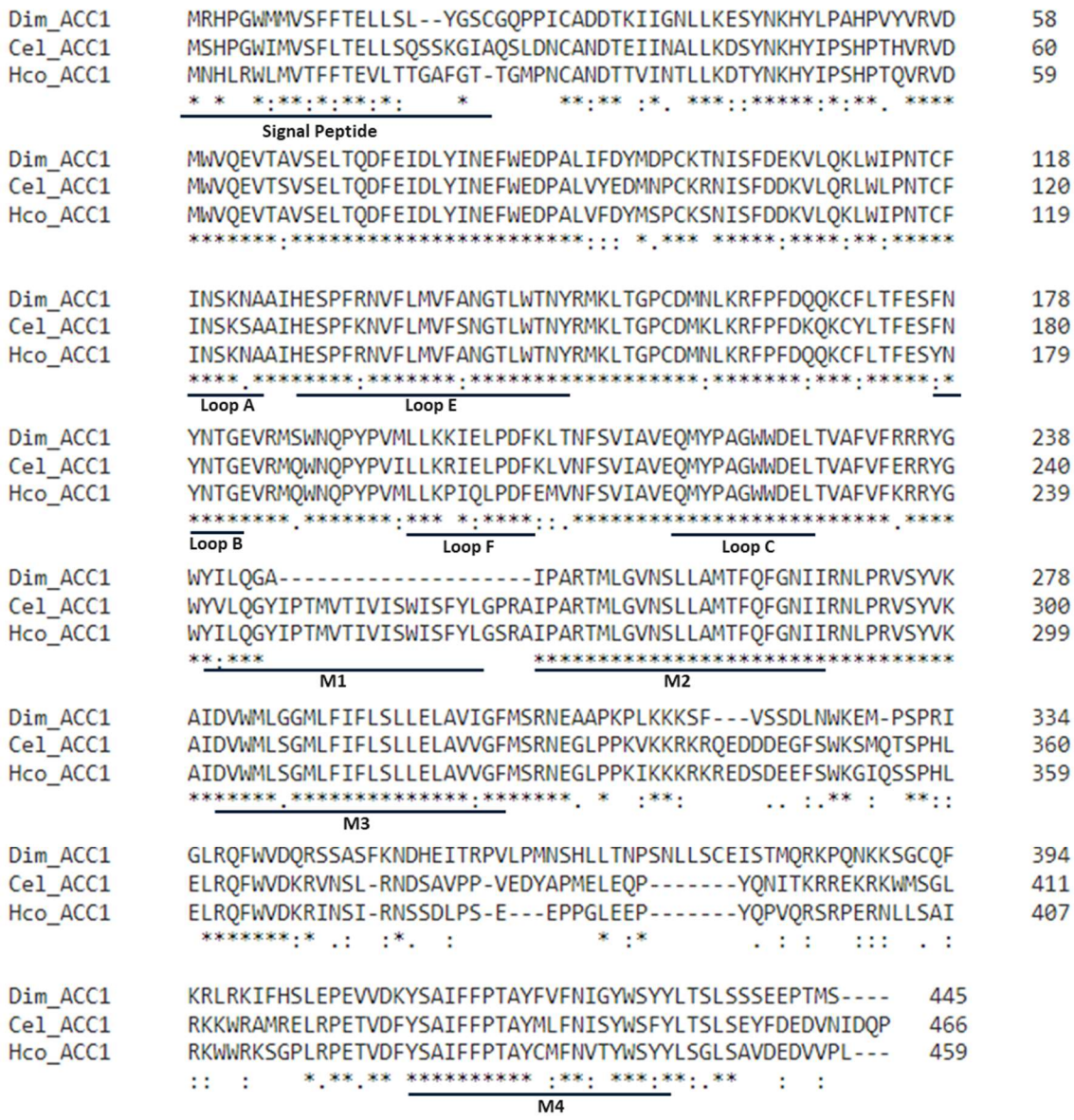

Figure 13: Protein sequence alignment of *D. immitis* ACC-1 with *C. elegans* ACC-1, and *H. contortus* ACC-1. Asterisks (*) indicate identical amino acids and (:) represents similar amino acids. The binding loops, signal peptide sequence, and transmembrane domains (TM) are displayed.

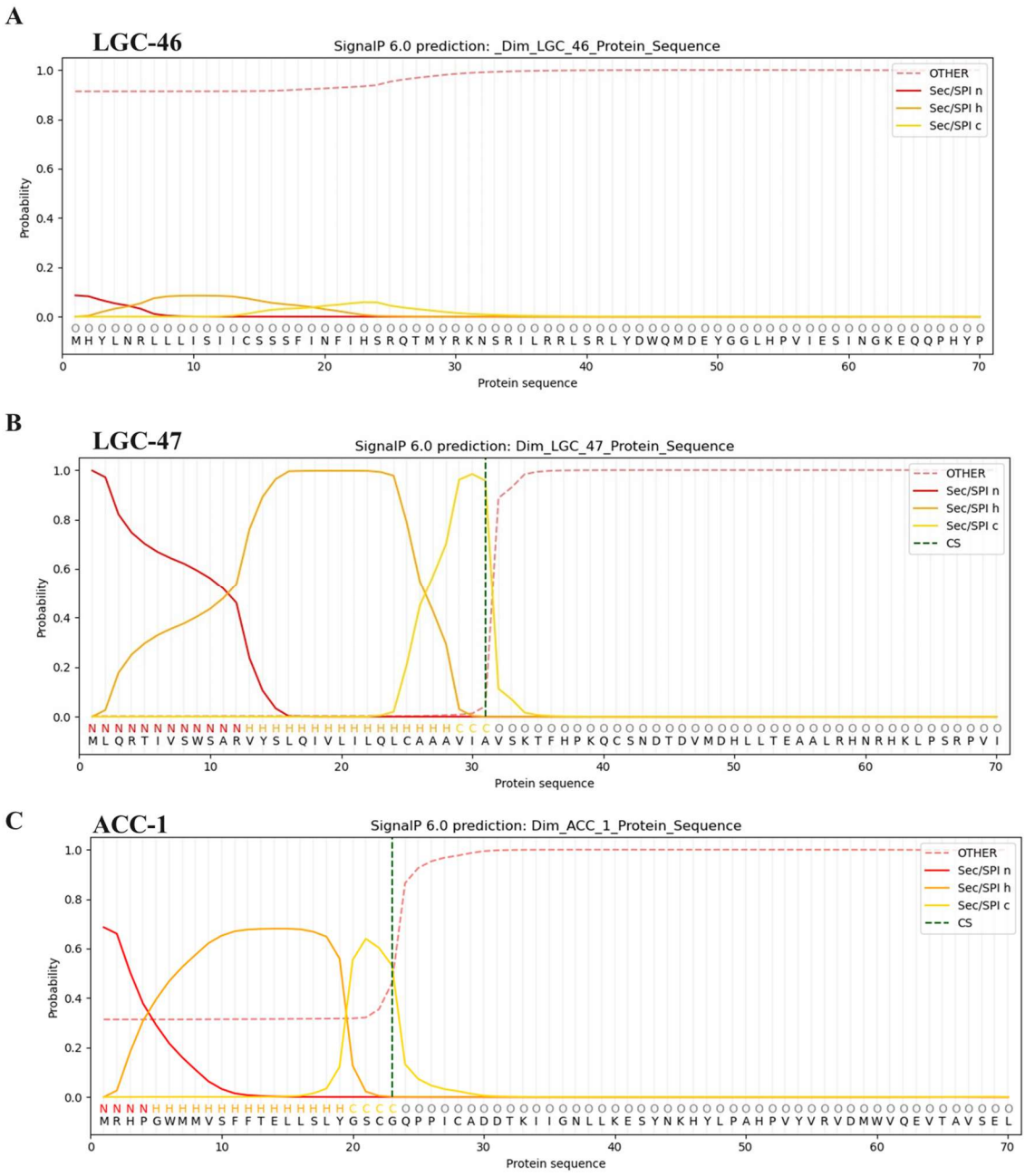

Figure 14: Signal protein prediction done by SignalP6.0 (Teufel et al. 2022) of (A) LGC-46, (B) LGC-47 and (C) ACC-1. The red, orange and yellow line correspond to the N-terminal region, the hydrophobic internal region and the C-terminal region of the signal peptide sequence respectively. The dotted green line is the predicted cleavage site for the protein. Both ACC-1 and LGC-47 are predicted to have a signal peptide sequence, while LGC-46 is not predicted to have one.

4.4 Heterologous expression in *Xenopus laevis* oocytes

4.4.1 UNC-49 family of receptors

4.4.1.1 GABA and agonist response

The *dim-unc-49b* and *dim-unc-49c* sequences were reverse transcribed into cRNA through *in vitro* transcription for analysis through heterologous expression. UNC-49 receptor combinations from Table 3 were injected into *X. laevis* oocytes. We first confirmed whether Dim-UNC49C was unresponsive to GABA. As recognized for Hco-UNC-49C and Cel-UNC-49C, expression of Dim-UNC49C alone did not form a channel that could respond to GABA (data not shown). Dim-UNC-49B produced a homomeric channel which was sensitive to GABA with an EC_{50} of 5.11 ± 0.23 mM (n=10). Heteromeric channels formed via co-expression with either Dim-UNC-49C or Hco-UNC-49C provided EC_{50} values of 9.60 ± 0.50 mM (n=14) and 904.2 ± 33 µM (n=7), respectively. Compared to the GABA response of the Dim-UNC-49B homomer, the Dim-UNC-49B/Dim-UNC-49C heteromer is 1.9 times less sensitive, and the Dim-UNC-49B/Hco-UNC-49C heteromer is 2.5-fold more sensitive. There is no significant differences between the hill slopes of these receptors (Figure 16). When expressed alone, Hco-UNC-49B has an EC_{50} of 136.7 ± 7.0 µM (n=5), and a hill slope of 4.421 ± 0.445. When co-expressed with Hco-UNC-49C the EC_{50} decreased to 84.87 ± 4.0 µM (trend similar to Siddiqui et al. 2010), and when co-expressed with Dim-UNC-49C, EC_{50} values increase to 252.2 ± 8.0 µM. The Hco-UNC-49B/Dim-UNC-49C heteromer is 1.9-fold less sensitive and the Hco-UNC-49B/Hco-UNC-49C heteromer is 1.6-fold more sensitive to GABA than the Hco-UNC-49B homomeric channel.

Dim-UNC-49B (5.11 ± 0.23 mM) is 37 times less sensitive to GABA than Hco-UNC-49B (136.7 ± 7.0 μM) (Figure 16, Figure 15). The hill slopes for Hco-UNC-49B, Hco-UNC-49B/Hco-UNC-49C, and Hco-UNC-49B/Dim-UNC-49C receptors are 4.421 ± 0.445, 3.551 ± 0.341, 5.131 ± 0.364 respectively. The hill slopes are not significantly different between any of the Dim-UNC-49B homomeric or heteromeric channels regardless of the species used for co-expression. Conversely, the Hco-UNC-49B containing receptor hill slopes are statistically different from one another and statistically different than all the Dim-UNC-49B receptor combinations. All receptors tested had EC_{50} values that were statistically different than one another (Figure 16). We also analyzed current amplitudes between receptors that were measured on the same day. Interestingly, co-expression of Dim-UNC-49B with Dim-UNC-49C resulted in receptors which had lower currents than that of the homomeric Dim-UNC-49B receptor (Figure 15 A, Figure 17 A). Conversely, when Dim-UNC-49B was co-expressed with Hco-UNC-49C, the amplitude of expression was higher compared to the Dim-UNC-49B homomeric channel on two out of the three days analyzed (Figure 17 B). The Dim-UNC-49 homomeric and heteromeric channels were also tested using 5 mM, 10 mM and 20 mM of classical GABA receptor agonists, IMA, S-GABOB, R-GABOB and DAVA. However, results were variable and not consistent and thus were not further pursued (Data not shown).

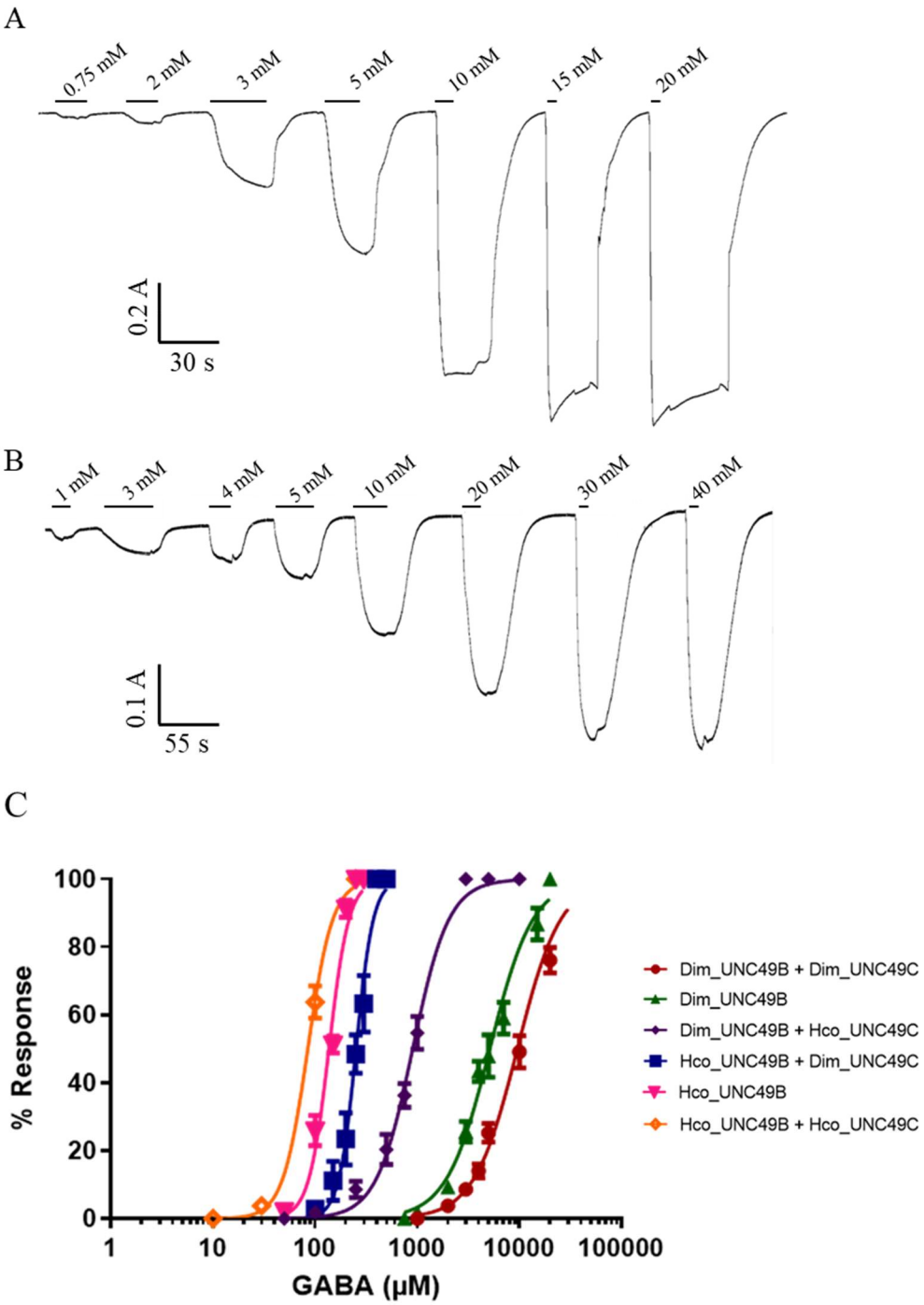

Figure 15: Shown are representative traces of a dose response for the novel (A) Dim-UNC-49B homomer and (B) Dim-UNC-49B/Dim-UNC-49C heteromer. The heteromeric channel is less sensitive to GABA than the homomeric channel. (C) GABA dose response curve of all tested receptor combinations.

A

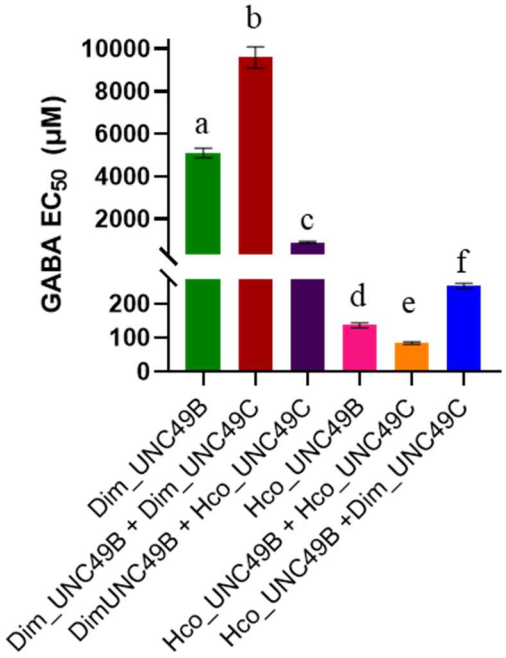

B

Receptor	EC_{50} GABA	HillSlope	N
Dim_UNC49B + Dim_UNC49C	9600 ± 500 µM	2.046 ± 0.0835	14
Dim_UNC49B	5110 ± 230 µM	2.056 ± 0.0970	10
Dim_UNC49B + Hco_UNC49C	904.2 ± 33 µM	2.049 ± 0.102	7
Hco_UNC49B + Dim_UNC49C	252.2 ± 8.0 µM	5.131 ± 0.364	7
Hco_UNC49B	136.7 ± 7.0 µM	4.421 ± 0.445	5
Hco_UNC49B + Hco_UNC49C	84.87 ± 4.0 µM	3.551 ± 0.341	5

Figure 16: (A) GABA EC_{50} values for all receptor combinations tested along with the (B) statistical analysis. No significant difference ($p \leq 0.05$) between receptors identified by the same letter. Dim-UNC-49B receptors combinations have significantly higher EC_{50} when compared to Hco-UNC-49B receptors. In addition, Dim-UNC-49C significantly increases the EC_{50}, whereas Hco-UNC-49C significantly decreases it in all receptor combinations tested.

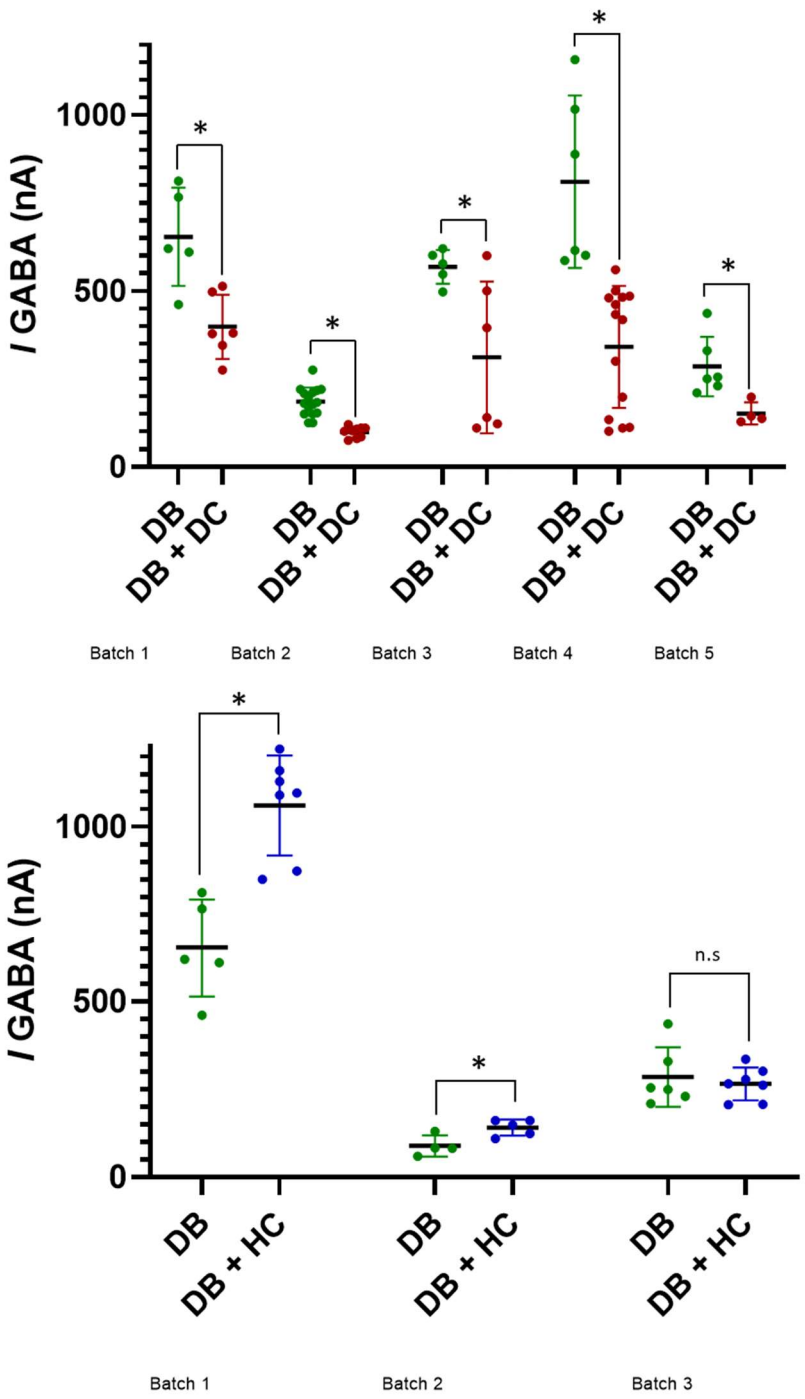

Figure 17: Comparison of the response amplitude (using the maximum current achieved from EC_{50} GABA concentration in nA) between (A) Dim- UNC-49B (DB) homomer and Dim-UNC-49B + Dim-UNC-49C (DB + DC) heteromer, and (B), Dim-UNC-49B (DB) homomer and the Dim-UNC-49B + Hco-UNC-49C (DB + HC) heteromer. Batches indicate the receptors were tested on the same day. Different batches represent oocytes from different frogs. Significance ($p \leq 0.05$) was determined through students t-test and displayed as asterisks. n.s indicates no significant difference ($p > 0.05$) between conditions. The Dim-UNC-49B + Dim-UNC-49C heteromeric channel exhibited significantly lower amplitudes in comparison with the homomeric Dim-UNC-49B channels on all days analyzed. The Dim-UNC-49B + Hco-UNC-49C heteromeric channel had significantly higher amplitude than the Dim-UNC-49B homomeric channel on two of the three days analyzed.

4.4.1.2 Picrotoxin Response

As described previously, receptor combinations from Table 3 were injected into *X. laevis* oocytes and the antagonistic response for picrotoxin was measured by the relative decrease in the EC_{50} observed with GABA. We first tested the picrotoxin effect using a high concentration (250 uM) of picrotoxin. Here it was found that unlike previous studies with *C. elegans* and *H. contortus* UNC-49 receptors, the Dim-UNC-49C subunit does not confer resistance to picrotoxin. However, consistent with previous studies, Hco-UNC-49C subunit does confer picrotoxin resistance (Figure 18). To further investigate this phenomena picrotoxin dose response analysis was performed on all receptor combinations (Figure 19). The Dim-UNC-49B homomeric channel has an IC_{50} of 5.03 ± 0.23 μM and the Dim-UNC-49B/Dim-UNC-49C heteromeric channel has an IC_{50} of 4.15 ± 0.50 μM, and according to a student's t-test, there is no significant difference in the IC_{50} values of these receptors (Figure 19, B). Interestingly, this is lower than the IC_{50} values of Hco-UNC-49B homomeric channel (IC_{50} of 21.4 ± 5.82 μM) and the Hco-UNC-49B/Dim-UNC-49C heteromeric channel (IC_{50} of 16.75 ± 3.15 μM) (Figure 19 C). Unlike observations with Hco-UNC-49C, there was no significant change in picrotoxin sensitivity when Dim-UNC-49C assembles in a heteromeric channel. Hco-UNC-49B/Hco-UNC-49C is picrotoxin insensitive, and when Hco-UNC-49C is expressed with Dim-UNC-49B, it increased the IC_{50} by 80-fold compared to Dim-UNC-49B alone.

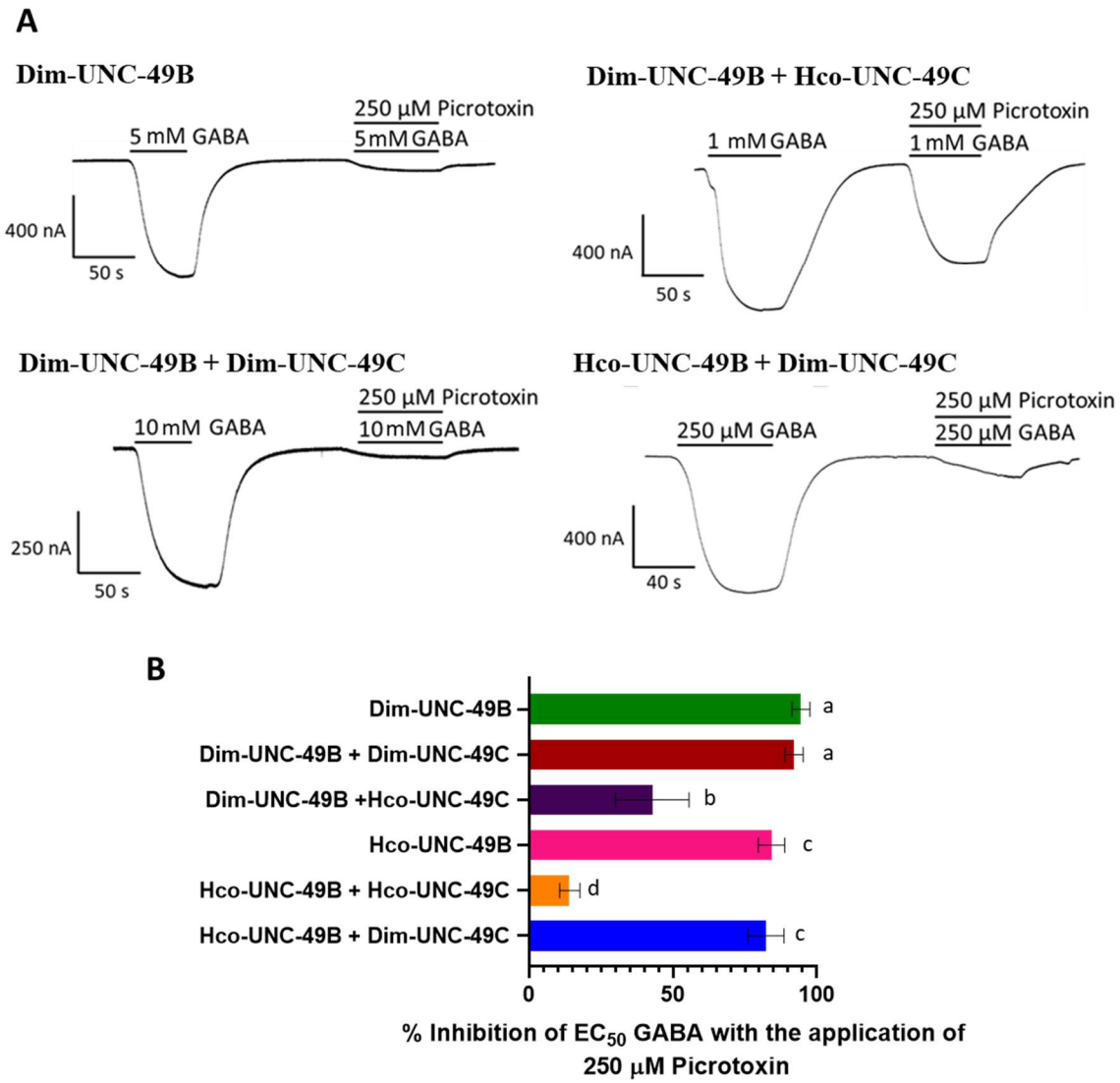

Figure 18: (A) Representative electrophysiological traces showing the effect maximal picrotoxin concentration (250 µM) on EC50 GABA. Single line represents EC50 GABA application, double line represents EC50 GABA with 250 µM of Picrotoxin. (B) Maximum EC50 GABA inhibition, with statistical analysis done by students t-test. Groups with the same letter are not significantly different ($p > 0.05$) and groups with different letters are significantly different ($p < 0.05$).

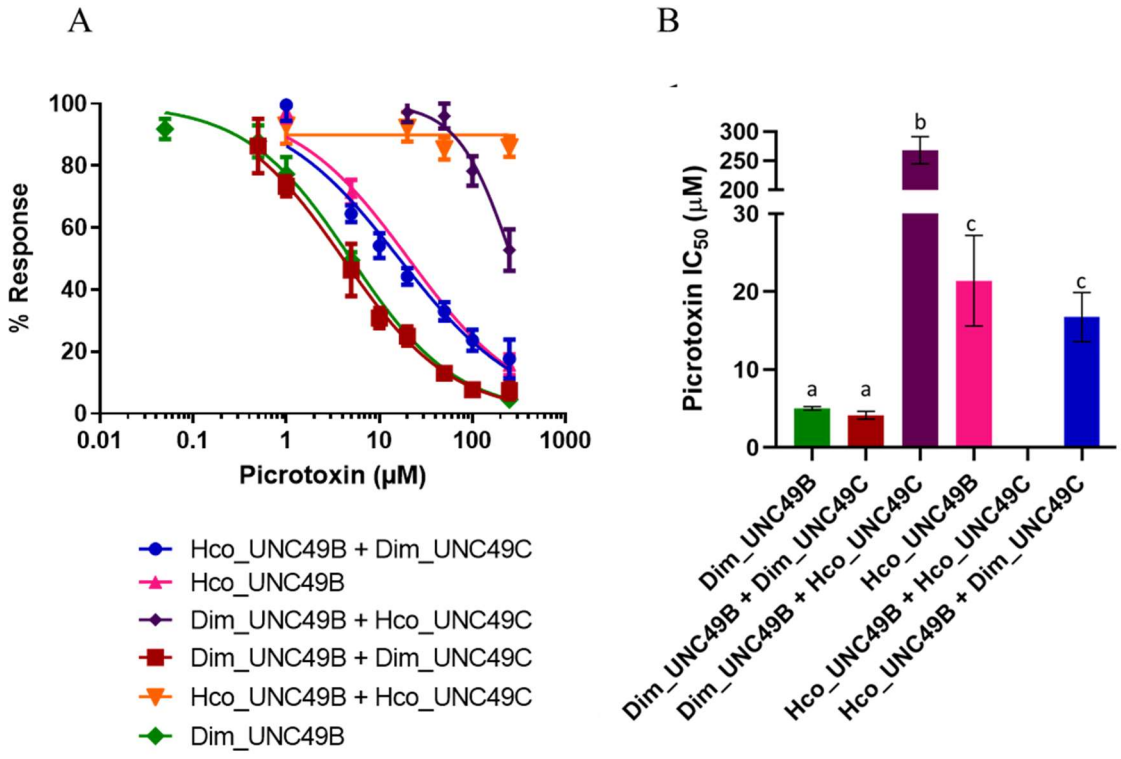

C

Receptor	IC_{50} Picrotoxin	Hill Slope	N
Dim_UNC49B + Dim_UNC49C	4.15 ± 0.500 μM	0.030	5
Dim_UNC49B	5.03 ± 0.23 μM	0.038	6
Dim_UNC49B + Hco_UNC49C	268 ± 23 μM	0.16	5
Hco_UNC49B + Dim_UNC49C	16.74 ± 3.15 μM	0.045	6
Hco_UNC49B	21.4 ± 5.82 μM	0.049	5
Hco_UNC49B + Hco_UNC49C	N/A	N/A	5

Figure 19: (A) Picrotoxin inhibition of GABA EC_{50} response for all receptor combinations tested. (B) IC_{50} picrotoxin concentrations calculated EC_{50} concentration of GABA with increasing concentrations of picrotoxin. No significant difference ($p \leq 0.05$) between receptors identified by the same letter. (C) Summary of the IC_{50} data, the hill slope and number of replicates (N). Hco-UNC-49C increased picrotoxin resistance, but Dim-UNC-49C did not have the same effect. Dim_UNC-49 receptors are more sensitive to picrotoxin than Hco_UNC-49 receptors.

4.5 Phylogenetic analysis of ACC, and UNC-49 receptors in nematodes

Phylogenetic analysis reveals that the ACC proteins from *D. immitis* cluster with the *H. contortus* and *C. elegans* proteins and appears to be more closely related phylogenetically to *H. contortus* than the UNC-49 family of proteins are (in-group, instead of an out-group) (Figure 20). Branch lengths show that the UNC-49 group is more closely related to the AVR-14 group genes (*glc-2, glc-4, avr-14* and *avr-15*) as shown previously by (Jones and Sattelle 2008) (Figure 2). *D. immitis* (Clade III) subunits appear to be more closely related to *B. malayi* (Clade III) than to *C. elegans* or *H. contortus* (both Clade V).

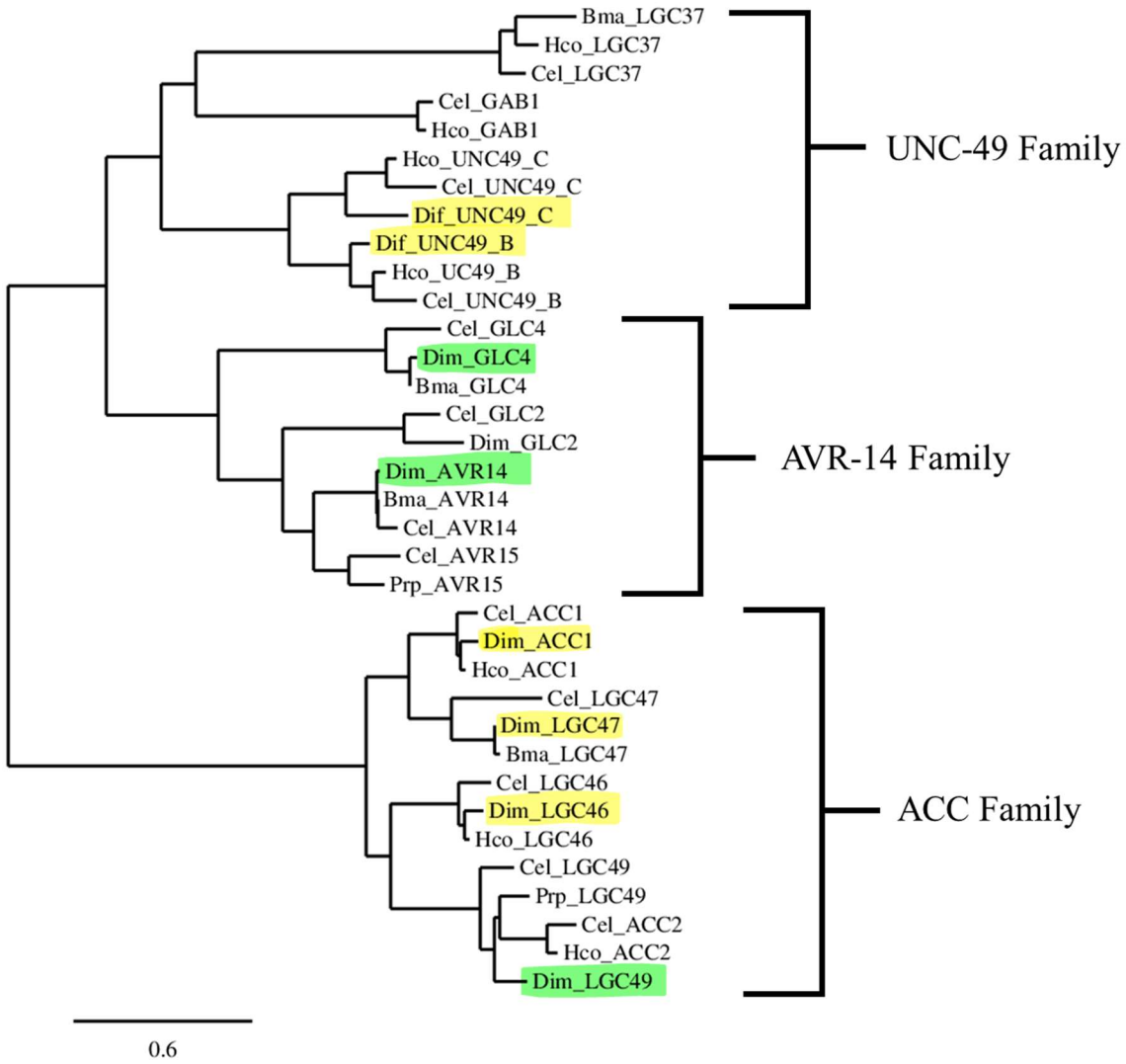

Figure 20: Phylogram of nematode cystine loop ligand gated ion channels, including those cloned, and currently unpublished, from our lab. The genes highlighted in yellow were cloned in this study. The genes highlighted in green were cloned by my colleague J. Nichols (2023). Legend displays the percent of amino acid variation as a decimal.

4.6 Homology modelling and ligand docking of GABA in *D. immitis* UNC-49B and UNC-49C

4.6.1 *D. immitis* GABA Receptors

Since GABA was confirmed to be an agonist of the UNC-49 receptors in *D. immitis,* homology models were created to visualize the interaction between GABA and the binding pocket as well as the relevant residues which may be able to interact with GABA. The criteria for resides to be chosen was that they were within approximately 5 Å of the ligand. GABA models were only generated for the Dim-UNC-49B homomer since we know that binding occurs on the interface of two UNC-49B subunits (Figure 21 A). The amine group of GABA is oriented towards Y190 (from loop B) and is a predicted distance of 3.6 Å from the hydroxyl group of the tyrosine. The OH group from serine S238 (loop C) is also predicted to be positioned 5 Å away from the amine group. T236 (loop C) is located a predicted 2.4 Å from the oxygen on the carboxylic acid group. On the complimentary subunit, Y87 (loop D) is a predicted 2.5 Å away from the amine group and R162 is predicted to be 5.1 Å from the binding pocket.

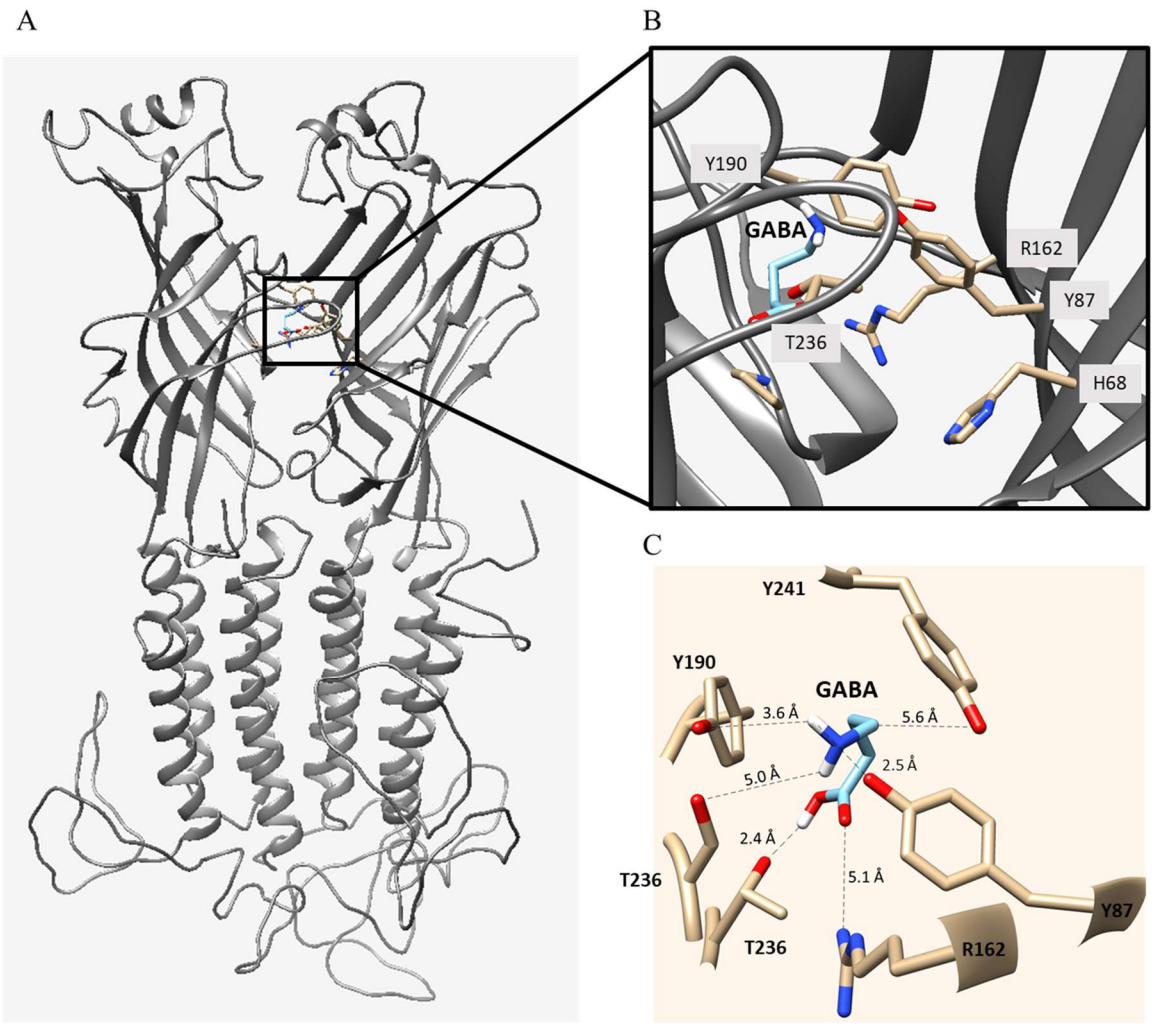

Figure 21: (A) Homology model of Dim-UNC-49B with GABA docked. (B) View of the binding pocket with relevant residues exposed. (C) View of the binding pocket with all non-relevant residues and amino acids removed. Residues are displayed and distances are displayed in Angstroms.

4.7 Quantitative-real-time PCR analysis

Quantitative real time PCR (qPCR) was performed to assay the relative amount of each gene cloned in female, male and L3 samples. qPCR results revealed there was significant amount of variation in gene expression in the female and L3 life-stages, and the males had the least variation. Overall, *lgc-46* is expressed more than *unc-49c* in all stages, and *acc-1* is expressed less than most genes in all stages tested (Figure 22). In both the female and the male, *unc-49c* was expressed in lower quantities than in L3. Overall, all genes tested were present in all life stages in varying amounts. Sequencing revealed that *unc-49b, unc-49c, lgc-47* fragments aligned to the predicted areas in the protein (Data not shown). *lgc-46* and *acc-1* have not been sequenced yet.

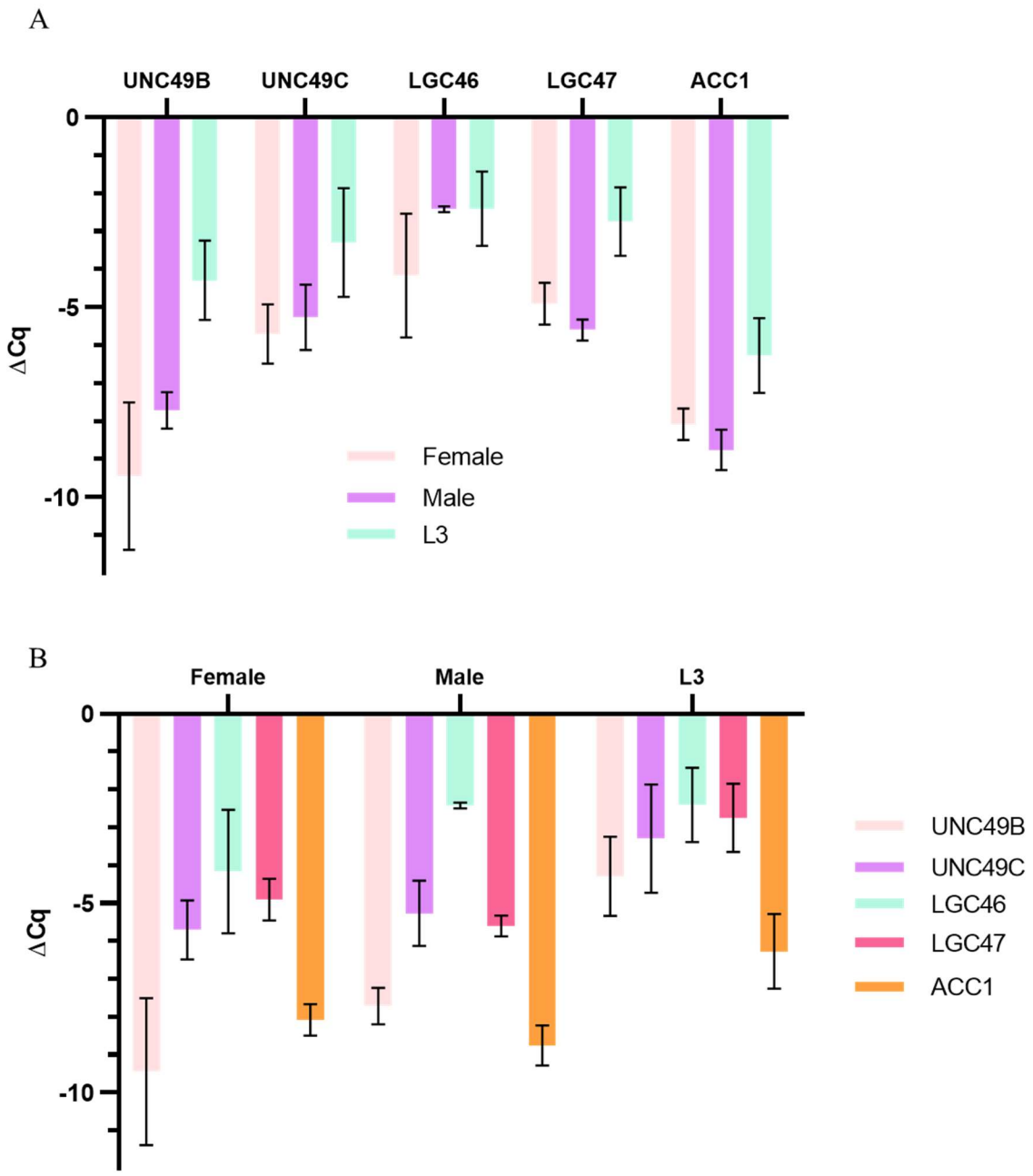

Figure 22: Quantitative-real-time PCR analysis of *unc-49c, unc-49c, acc-1 lgc-46, lgc-47* across female, male and L3 larvae displayed grouped as (A) organism and (B) genes. Error bars represent the standard error of the mean. Higher ΔCq values relates to higher expression.

4.8 Characterization of *D. immitis* ACC receptors and levamisole derivative screening

None of the *D. immitis* ACC family of acetylcholine receptors combinations injected into oocytes formed functional channels, despite successful cRNA synthesis, and the use of *H. contortus* accessory proteins. Receptor combinations used in this study were ACC-1/LGC-46, LGC-46 and LGC-47. Since no expression was achieved, the ACC family from *D. immitis* was not able to be characterized. However, to pursue objective 5 we utilized instead Hco-ACC-2 to screen levamisole derivatives. Levamisole is an anthelmintic that normally activates acetylcholine-gated cation channels in nematodes (Fleming et al. 1997b). In addition, levamisole was shown to be a partial agonist at ACC-2 receptors from *H. contortus* (Habibi et al. 2018). The aim was to generate novel derivatives of levamisole that exhibited higher efficacy at ACC receptors. Three novel levamisole substitutions (Compounds 8-10, Figure 7) on the amine group were synthesized by MSc student A. (Collins 2022a). Heterologous expression of *H. contortus* ACC-2 was performed as described in section 3.5. Synthesized compounds were screened for their relative response compared to acetylcholine, and levamisole (Figure 23 A). Compound 10 (Figure 7, Figure 23), with the phenyl- group added to the free amine group on the nitrogen, produced a higher response (on average) on the receptor compared to levamisole (Figure 23 B). That compound was selected for further modification resulting in six additional compounds that are derivatives of compound 10 (Figure 7, Figure 24 A) (Collins 2022b). Five novel substitutions on the aromatic group of compound 10 were generated (compounds 11-15) and tested on Hco-ACC-2 receptors (Figure 7) (Collins 2022). These derivatives were screened through electrophysiological analysis, and compound 13, a compound with 3 fluorine substituted on the phenyl group, on average exhibited an

increased the response compared to levamisole (Figure 7, Figure 24). However, none of the compounds produced currents as large in amplitude as acetylcholine (Figure 24). Dose response analysis (Figure 24 B, D) of compound 13 revealed that it has the same EC_{50} that compared to acetylcholine (20 μM) and was more sensitive than levamisole (Figure 24 D, E), but did not produce amplitudes as high as acetylcholine (Figure 25 C, D). Data for acetylcholine and levamisole EC_{50} was obtained from (Habibi et al. 2018).

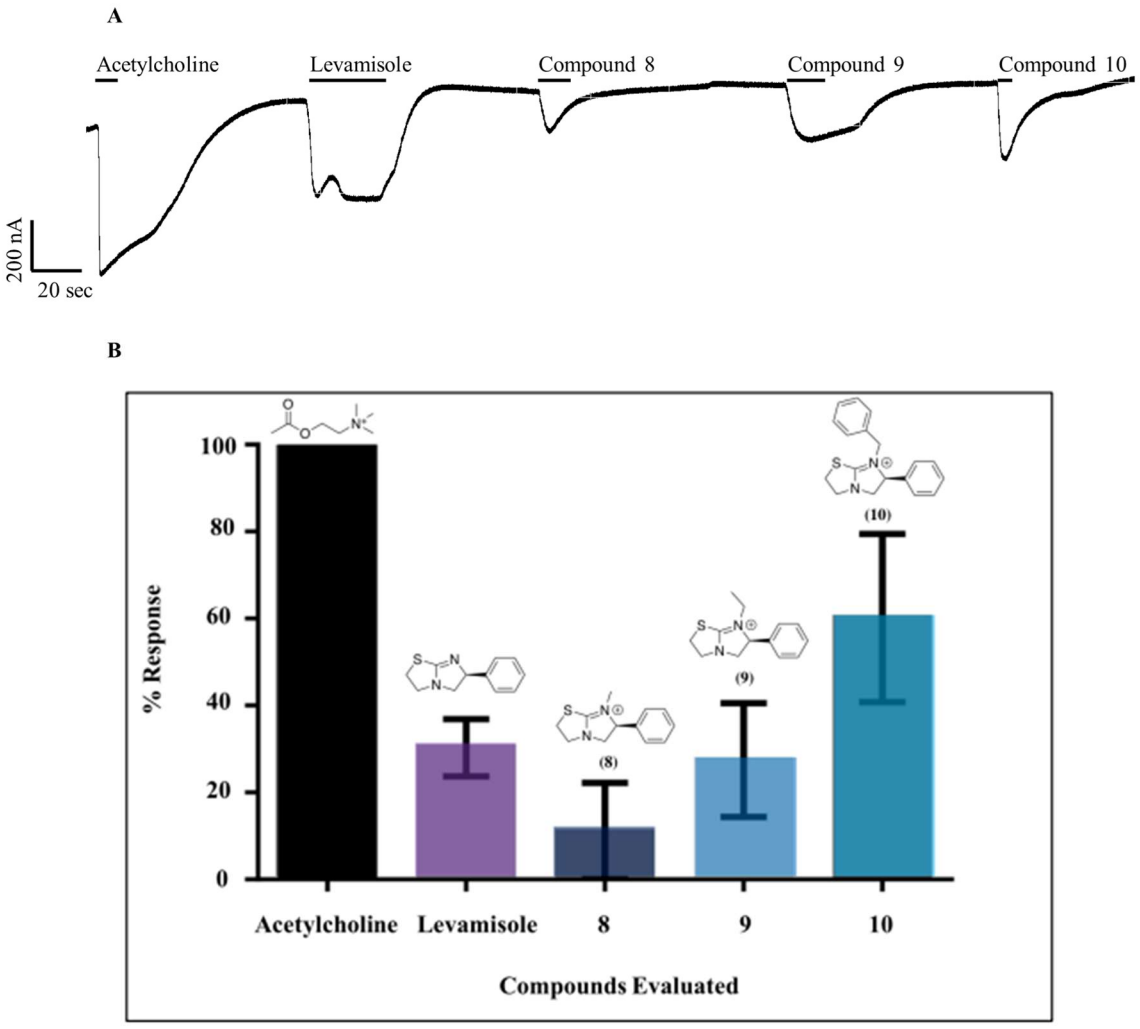

Figure 23: Percent response of Hco-ACC-2 receptors to 500 μM of the following ligands: acetylcholine, levamisole and 3 levamisole derivatives (compounds 8, 9 and 10). Compound 10 had higher sensitivity to the receptor compared to levamisole. Compound 10 was chosen for further analysis.

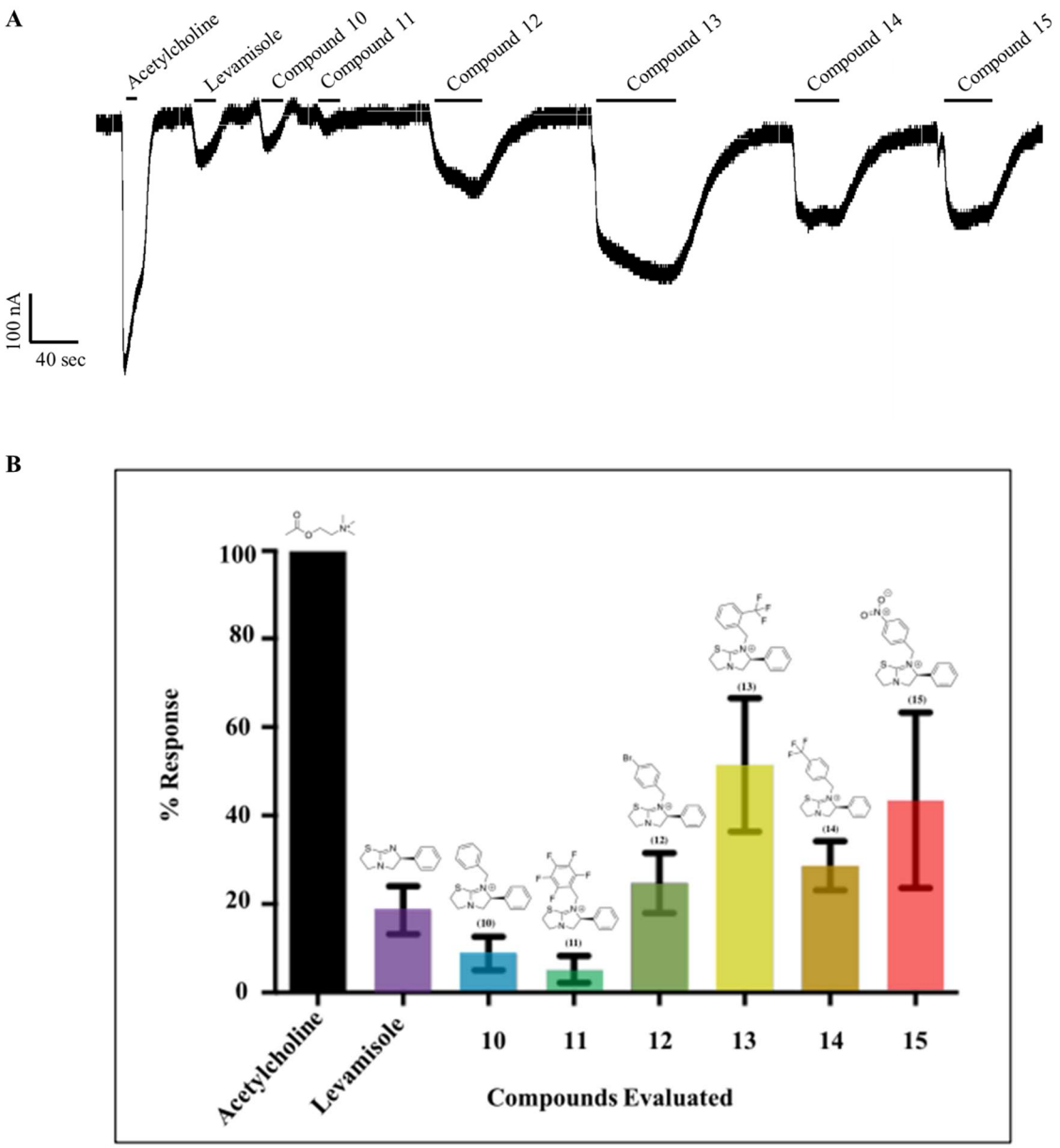

Figure 24: (A) Representative trace of the percent response in comparison to acetylcholine with 500 µM of all compounds tested (acetylcholine, levamisole, and derivatives 10-15). (B) Percent response of Hco-ACC-2 receptors to 500 µM acetylcholine, levamisole as well as compound 10-15, created by A. Collins (2022).

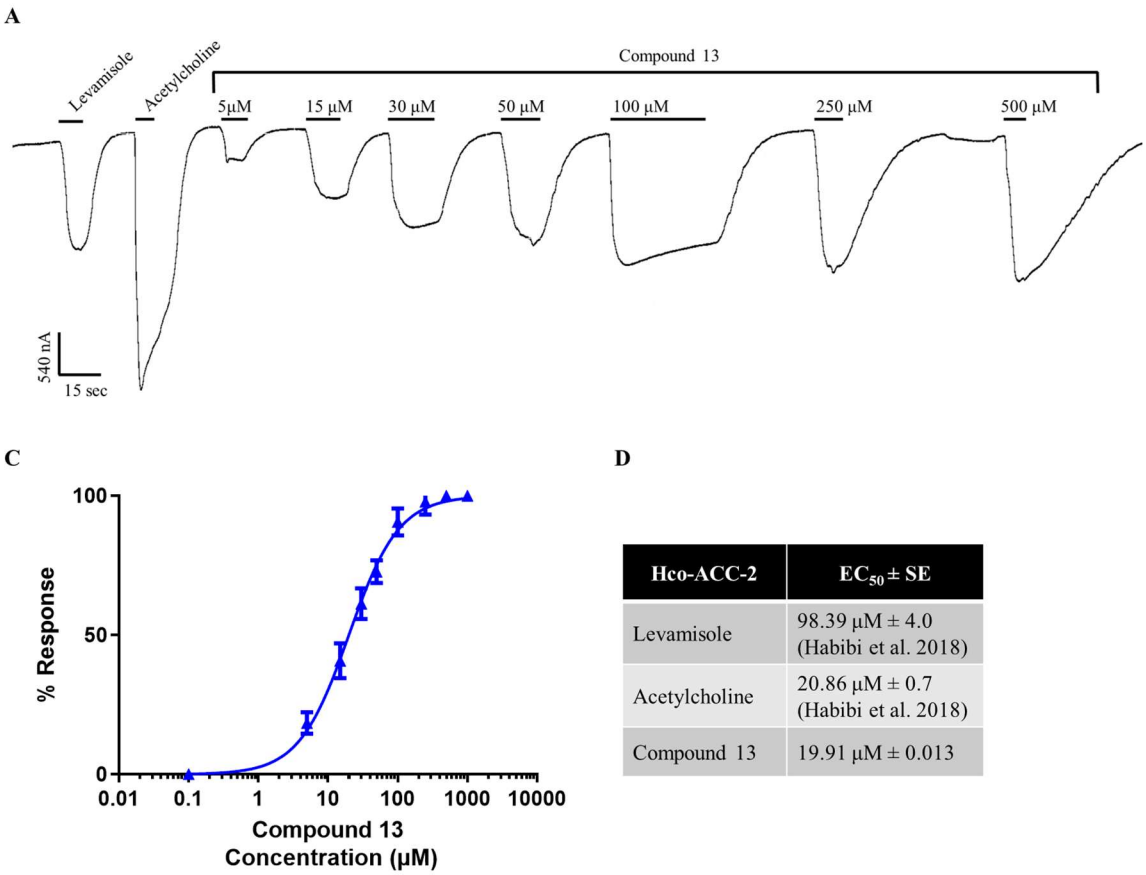

Hco-ACC-2	EC_{50} ± SE
Levamisole	98.39 µM ± 4.0 (Habibi et al. 2018)
Acetylcholine	20.86 µM ± 0.7 (Habibi et al. 2018)
Compound 13	19.91 µM ± 0.013

Figure 25: (A) Representative trace of the dose response curve analysis for compound 13. Concentrations of levamisole and acetylcholine used were 500 µM (B) Dose response curve of compound 13 on Hco-ACC-2 receptors. (C) EC_{50} ± standard error for the response of Hco-ACC-2 to acetylcholine and levamisole, and compound 13. Data for EC_{50} acetylcholine and levamisole were obtained from (Habibi et al. 2018).

5. Discussion and Future Directions

5.1 Characterization of UNC-49B and UNC-49C from *D. immitis*

This study describes the identification of two subunits from the UNC-49 family (UNC-49B and UNC-49C) from *D. immitis*. Interestingly, like in *C. elegans* the genes that encode both UNC-49 B and C arose through alternative splicing of the *unc-49* gene. The slicing patterns are similar where both *unc-49b* and *unc-49c* genes contain the same 5' (N-terminal) end but different 3' ends. In addition, analysis of genomic organization (Figure 9) revealed that the same five exons in *D. immitis* encode for the N terminal end of UNC-49B and UNC-49C as in *C. elegans* (Bamber et al. 1999; Nomura et al. 2021). It is interesting that these two evolutionally different nematodes retain the same mechanism for generating UNC-49B and UNC-49C subunits.

This study was also able to identify and characterize the pharmacological responses of both Dim-UNC-49B and Dim-UNC-49C to GABA and picrotoxin. Our results revealed some fascinating key functional insights of these *D. immitis* homologues. Dim-UNC-49B can form a GABA-sensitive, functional homomeric channel with an EC_{50} of 5.11 ± 0.23 mM, while Dim-UNC-49B assembles with Dim-UNC-49C, forming a channel with an EC_{50} of almost twice that of the homomeric channel (9.60 ± 0.5 mM). These receptors can form functionally distinct ligand gated ion channels, each with their own different pharmacological properties. We found that the EC_{50} for the Dim-UNC-49B homomeric channel is significantly higher than for Hco-UNC-49B. Notably, the EC_{50} of Hco-UNC-49B was originally reported to be 64.0 ± 4.4 μM, and the Hco-UNC-49B/Hco-UNC-49C heteromer to be 39.9 ± 5.7 (Siddiqui et al. 2010). However, in this study, we report higher EC_{50} values around 137 μM for the homomeric and 85 μM heteromeric channels (Figure

16 B). Despite this discrepancy, both studies demonstrated the same trend: that co-expression of Hco-UNC-49B with Hco-UNC-49C enhances the GABA response by about 1.6-fold in comparison to the Hco-UNC-49B homomer. The variation in the EC_{50} values could be attributed to the experimental setup, the amount of RNA injected or oocyte health at the time of the extraction. Indeed, variations in EC_{50} values have been observed previously in our lab and, other labs that have investigated UNC-49 receptors from both *H. contortus* and *C. elegans* (Bamber et al. 2003; Siddiqui et al. 2010). We have also found that the Dim-UNC-49B homomeric channel's EC_{50} is 37-fold higher than that of Hco-UNC-49B, and the *D. immitis* heteromeric channel's EC_{50} is 270-fold times higher than *H. contortus.* Interestingly, analysis of the UNC-49B receptor from *Meloidogyne incognita* a clade I parasitic nematode, had an EC_{50} GABA of 592 ± 56 μM (Nomura et al. 2021), which is also significantly higher than the EC_{50} of the *C. elegans* and the *H. contortus* UNC-49B homomer. This furthers evidence that the ligand gated ion channels of nematodes from the same clade are pharmacologically more similar to each other than those of differing clades (Figure 20).

Cross-species co-expression has been previously done using *H. contortus* and *C. elegans* to form pharmacologically distinct channels (Siddiqui et al. 2010), whereas this study explored co-expression of channels from *H. contortus* and *D. immitis.* Expression of Cel-UNC-49B with Hco-UNC-49C produced channels more sensitive to GABA than Cel-UNC-49B alone, and expression of Hco-UNC-49B with Cel-UNC-49C significantly decreased GABA sensitivity compared to the homomer (Siddiqui et al. 2010). This aligns with the data collected in this study, where the expression of Hco-UNC-49B with Dim-UNC-49C decreases GABA sensitivity compared to the Hco-UNC-49B homomeric

channel and the expression of Dim-UNC-49B with Hco-UNC-49C increases GABA sensitivity compared to the Hco-UNC-49B homomeric channel (Figure 15). We hypothesize that the co-assembly of Dim-UNC-49B/Hco-UNC-49C creates a GABA binding site which is more energetically favorable and, facilitates GABA binding better compared to the Dim-UNC-49B/Dim-UNC-49C channel.

In the past, researchers have interpreted that a hill slope greater than one suggests that there are more potential binding sites for GABA; however, this considers the assumption that GABA does not exhibit cooperative binding (Weiss 1997). Although this assumption has been made in the past with vertebrate GABA receptors (Lema and Auerbach 2006) as well as nematode GABA receptors (Bamber et al. 1999), recent research demonstrates that the number of binding sites cannot be estimated by the hill coefficient number alone (Prinz 2010; Cattoni et al. 2015). Despite this, hill slopes are a good approximation of how responsive a receptor is when ligand concentration is increased. Typically, the greater the hill slope value, the more sensitive the channel is to small changes in ligand concentration. All receptor combinations tested with Dim-UNC-49B have hill slopes of around 2, and all receptor combinations tested with Hco-UNC-49B have higher hill slopes of between 3.5-5 (Figure 16). Although this is a poor indicator for the number of ligands bound to each receptor, as postulated by (Prinz 2010), it still reveals valuable information about the sensitivity of the receptor to the ligand. The high hill slope value of Hco-UNC-49B receptors indicates that receptors containing Hco-UNC-49B subunits are much more sensitive to small changes in GABA concentrations compared to those containing Dim-UNC-49B subunits.

In both *C. elegans* and *D. immitis*, the heteromeric UNC-49B/UNC-49C channel is less sensitive to GABA than the homomeric UNC-49B channel. In comparison, in *H. contortus,* the heteromeric channel is more sensitive compared to the homomeric channel. This phenomenon of increased GABA sensitivity in *H. contortus* heteromeric UNC-49 channels has been postulated to be linked to the presence of a methionine residue in loop B of the Hco-UNC-49B subunit (second orange star in Figure 8) (Accardi and Forrester 2011). However, in both *C. elegans* and *D. immitis* this residue is a threonine (Figure 8). In subsequent analysis in *H. contortus* through mutagenesis, when this methionine is mutated to a threonine, the sensitivity to GABA decreases significantly compared to the homomer during co-expression with Hco-UNC-49C (Accardi and Forrester 2011). This same phenomena was observed in vertebrate GABA receptors, where the substitution of the conserved analogous threonine residue to an alanine decreased GABA sensitivity significantly (Amin and Weiss 1993) indicating the likely evolutionary significance of this residue in GABA response. In *H. contortus,* this threonine residue was predicted to be in the binding pocket, but was not close enough to the ligand for meaningful interactions (Cochrane 2017) (Figure 21). Further investigation through alanine substitution of this threonine in Dim-UNC-49B loop B (Figure 8) would be valuable to confirm this hypothesis and elucidate the importance of this residue in GABA binding.

The ‘aromatic box’ of cystine-loop GABA receptors plays an important role in the binding pocket for GABA. Through *in silico* analysis we can also describe these relevant amino acids in the Dim-UNC-49B receptor. Y87 from loop D is predicted to play an important role due to its distance from the amine group of GABA (2.5 Å). In Human GABA receptors, a tyrosine residue is in a similar position and was shown to be in the binding

pocket (Padgett et al. 2007). Mutational analysis also revealed that this residue is important for GABA sensitivity in human receptors (Padgett et al. 2007). In *H. contortus,* mutagenesis of this analogous tyrosine residue in Hco-UNC-49B to leucine, decreased the sensitivity of the homomeric UNC-49B receptor by approximately 200-fold (Accardi and Forrester 2011). Repetition of a similar experiment in *D. immitis* may reveal insights into the structural similarity of the binding pocket between *H. contortus* and *D. immitis.*

Additionally, a tyrosine residue in loop B has been shown to be potentially involved in pi-cationic interactions with the amine group in both mammalian and nematode receptors due to the proximity to the ligand in simulations (Padgett et al. 2007; Accardi and Forrester 2011). Our result support this, since Y190 (analogous to Y166 from *H. contortus*), from loop B is oriented towards the amine group and is close enough (5.6 Å) to form a possible interaction. This aromatic box is known to be conserved through ion channels and relevant to ligand binding and receptor function, so these similarities are not surprising. Another residue shown to be relevant in this study is R162 from loop E, which orients closer to the carboxylic acid portion of GABA and has previously been predicted to be involved in the binding and release of GABA (Wagner et al. 2004; Padgett et al. 2007). It was proposed that the arginine creates a positively charged environment suitable for the binding of the carboxyl group of GABA in the binding pocket, which helps stabilize binding (Wagner et al. 2004). The molecular model of Dim-UNC-49B also revealed that a threonine in loop C (T236) orients towards the oxygen of the carboxylic acid of GABA at 2.4 Å (Figure 21) indicating a possible role in interaction with GABA. Additionally, a serine in loop C (S237) is predicted to be 5.0 Å away from the amine group of GABA (Figure 21 C). When the analogous residue in *H. contortus* UNC-49B loop C (S215), was

mutated to either threonine or lysine, no significant changes in GABA EC_{50} were observed (Accardi and Forrester 2011). This residue, although close to the binding pocket in *D. immitis* may therefore not be involved with GABA binding.

In addition to the analysis of *D. immitis* UNC-49 receptors with GABA, the antagonist picrotoxin was used to further characterize these receptors. Picrotoxin is known to have a potent effect on UNC-49 receptors in nematodes, blocking the channel from responding to GABA. There are many studies which have investigated the mechanism in which picrotoxin acts on these receptors (Zhang et al. 1995; Dibas et al. 2002). It is known that the Hco-UNC-49B/Hco-UNC-49C heteromeric channel is significantly less sensitive to picrotoxin than the Hco-UNC-49B homomer (Brown et al. 2012). The same phenomenon is observed in *C. elegans,* where the Cel-UNC-49B/Cel-UNC-49C heteromer is also significantly less sensitive to picrotoxin than the Cel-UNC-49B homomeric channel (Bamber et al. 2003). This contrasts what was found in this study with *D. immitis*, where the Dim-UNC-49B/Dim-UNC-49C heteromeric channel is just as sensitive to picrotoxin inhibition as the Dim-UNC-49B homomeric channel (Figure 19). Dim-UNC-49C was unable to confer resistance to picrotoxin in any of the receptor combinations tested. Moreover, Dim-UNC-49 receptors have lower picrotoxin IC_{50} values than *H. contortus* receptors. However, when Dim-UNC-49B is co-expressed with Hco-UNC-49C, picrotoxin resistance is conferred confirming that the influence on picrotoxin resistance in Hco-UNC-49 receptors indeed lies in the UNC-49C receptor as previously suggested (Bamber et al. 2003; Siddiqui et al. 2010).

Receptor analysis has revealed that a methionine needs to exist at a particular portion of the TM2 region of UNC-49C (starred in Figure 10) for it to be capable of

conferring picrotoxin resistance (Bamber et al. 2003). Interestingly, Dim-UNC-49C has a leucine at this position, while both the *C. elegans* and *H. contortus* UNC-49C receptors have a methionine in that position (Figure 10). This leucine amino acid substitution could be the reason Dim-UNC-49C confers no picrotoxin resistance to any UNC-49B receptor tested. Further studies doing mutational analysis of the TM2 region of Dim-UNC-49B would be valuable to determine if a leucine to methionine mutation in the TM2 region of Dim-UNC-49C would restore the picrotoxin resistance as seen in other organisms. The TM2 is the part of the receptor which lines the channel pore and has been noted to be important for various channel properties as mentioned previously. Notably, the TM2 section of UNC-49B in *H. contortus, C. elegans,* and *D. immitis* display 100% sequence similarity (Figure 8). However, the same level of similarity is not shared among UNC-49C sequences (Figure 10). This could indicate a conserved function of the pore lining region of the UNC-49B homomer which requires sequence conservation across nematode species. Phylogenetic analysis reveals that both UNC-49 subunits from *H. contortus* and *C. elegans,* (both from clade III) share more evolutionary history and conservation with each other than they do with *D. immitis* (clade V) (Figure 20). This suggests that the shared characteristics in the GABA responses of Cel-UNC-49C and Dim-UNC-49C likely arose independently through convergent evolution, rather than being the result of an inherited mutation.

Overall, both Dim-UNC-49B and Dim-UNC-49C are expressed in all life stages, which makes them good potential drug targets to broadly treat *D. immitis* infections. The variations observed in female samples are likely due to the presence of the transcriptome of their eggs in the body, expressing genes also relevant to the egg stage. The variations in the data with the L3 samples may be due to the sample being a pooled sample which may

capture other life stages in addition to L3. Although the co-assembly of UNC-49B and UNC-49C has been confirmed at nematode neuromuscular junctions, the contribution of UNC-49 to GABA neurotransmission has not been explored in live *D. immitis*. In fact, there is a notable absence of studies analyzing larval response to GABA in *D. immitis,* despite the importance of GABA receptors as potential drug targets. Future studies investigating the response of live *D. immitis* larvae to known UNC-49 receptor agonists and antagonists would be valuable to determine the phenotype of these larvae in response to these compounds. Future experiments may also involve silencing *unc-49* gene expression in various life stages using short interfering RNA (siRNA) to knockdown one or both *unc-49* subunits in *D. immitis.* This would provide information on the role of these receptors in the biology of the parasite throughout its life cycle. It's important to note that there are other members of UNC-49 family such as GAB-1, and LGC-37 which may also be present in *D. immitis*. Investigations into the role that other subunits play in would also be required to fully elucidate the role of GABA neurotransmission in *D. immitis.*

Overall, this study uncovered the potentially unique role that the UNC-49C subunit from *D. immitis* is playing in the function of these receptors. This thesis provides evidence that Dim-UNC-49C when assembled with Dim-UNC-49B produces a receptor that has a lower sensitivity to GABA, produces lower currents and does not confer resistance to picrotoxin. The findings from this study contribute to the growing knowledge surrounding GABA receptor diversity and function across different nematode species, specifically identifying key differences between the UNC-49 receptors of *D. immitis, H. contortus* and *C. elegans*.

5.2 Identification of *lgc-46*, *lgc-47* and *acc-1* in *D. immitis*

Three genes belonging to the *acc* family were identified in *D. immitis: lgc-46*, *lgc-47* and *acc-1.* However, only *lgc-47* and *acc-1* contain a signal peptide sequence, possibly explaining why LGC-46 is incapable of forming functional channels in oocytes. Additionally, despite the presence of a signal peptide, ACC-1 is not capable of assembling a channel on its own. Drawing on comparisons from *H. contortus*, it likely requires Dim-ACC-2 for functional expression (Callanan et al. 2018). Conversely, ACC-1 from *C. elegans* is capable of forming a functional homomeric channel on its own (Putrenko et al. 2005b). To determine which subunits are required for *D. immitis* ACC channel expression *X. laevis*, we have identified a putative gene sequence for *dim-acc-2* (Appendix); however, attempts to clone the gene using methods described previously have not been successful.

From gene transcript abundance, *lgc-46* appeared to be expressed at high levels in all life stages and was expressed higher than any of the genes analyzed in this study. This might mean *lgc-46* plays an important role in the *D immitis* nervous system, despite our inability functionally express LGC-46 in *X. laevis* oocytes in this study. Further analysis of the gene sequence and a second attempt at cloning the gene using other techniques such as 5' RACE would be valuable to ensure that the entire 5' region of the gene was captured. Despite the lack of signal peptide sequence, the LGC-46 putative protein sequence aligns well to LGC-46 from other nematode species. Phylogenetic analysis revealed that the ACC proteins cluster together with the ACC proteins from other nematodes, and clustered closer to *H. contortus* compared to UNC-49 genes which may indicate that they share sequence similarity, and shared ancestry. This, combined with the high levels of expression of *lgc-46* give promising evidence that this gene is involved in the *D. immitis* neurochemical

pathway. Overall, this project was able to clone three members of the *acc* family, *acc-1, lgc-46,* and *lgc-47* and identify a putative fourth gene sequence in *D. immitis* so there may be many future avenues to explore.

It is known that the ACC family of receptors require the accessory proteins *unc-50, unc-74,* and *ric-3.1* for functional expression (Boulin et al. 2008). In this study, the *H. contortus* accessory proteins were used for co-injection, however it is possible that the native homologues for the accessory proteins in *D. immitis* may be required for functional expression in *X. laevis* oocyes. The identification and the cloning of these genes may be a valuable next step in the endeavor to functionally characterize these proteins in *D. immitis*. Genome screening using the *H. contortus* proteins as a template would be a valuable way of identifying if these homologues exist in the *D. immitis* transcriptome.

Further studies to sequence the 5' region to identify missing gene fragments should be the first step in determining why LGC-46 is not capable of forming a functional channel through heterologous expression. This will indicate if LGC-46 is a nonfunctional protein, or if we have an incomplete clone. ACC-1 was predicted to have a signal peptide sequence, however may not capable of assembling a functional homomeric channel on its own in *D. immitis*, which would be opposite of the *C. elegans* ACC-1 protein which does form a functional homomeric channel (Putrenko et al. 2005b). Other experiments such as cross species expression of Dim-ACC-1 with Hco-ACC-2, may reveal if Dim-ACC-1 can assemble into a functional heteromeric channel *in vivo*. Subsequently, the cloning on the putative *D. immitis acc-2* gene will further clarify the role of ACC-1 in *D. immitis.*

5.3 Levamisole derivative testing on Hco-ACC-2

Levamisole, acetylcholine, and levamisole derivatives were tested on *H. contortus* ACC-2 receptors, since the *D. immitis* ACC receptors were not able to be functionally expressed in *X. laevis* oocytes. When compound 10, with the phenyl substitution on the amine nitrogen (Figure 7) was tested, it activated the Hco-ACC-2 channels significantly more than levamisole and several of the other novel levamisole derivatives (Figure 23). From there, five substitutions were added to compound 10 to generate compounds 11-15. Work in our lab done by A. Collins (Collins 2022a) suggested that the novel levamisole derivatives are larger in size, and may have additional amino acid interactions in the binding pocket in comparison to levamisole. The three aromatic fluorine atoms bound to the levamisole nitrogen had the most impact on enhancing levamisole action in Hco-ACC-2 (Figure 24). Interestingly, a more recently developed anthelmintic, monepantel, also contains fluorine atoms on its aromatic ring in triplicate. The further development of levamisole derivatives may aid in further characterizing the binding pocket of other members of the ACC family. In addition, these results demonstrate that levamisole is a viable scaffold for the development of potent, novel receptor ligands.

6. Conclusions

Overall, this study identified five new members of the cystine-loop ligand gated ion channel family in *D. immitis*: UNC-49B, UNC-49C, ACC-1, LGC-46 and LGC-47. All of these receptors have high sequence similarity with the same receptors in *H. contortus* and *C. elegans.* Dim-UNC-49B can form a functional homomeric channel which responds to GABA but is much less sensitive to GABA than the UNC-49B homomer from both *H. contortus* and *C. elegans* despite the high sequence conservation. The Dim-UNC-49B/Dim-UNC-49C heteromeric channel is less sensitive to GABA than the Dim-UNC-49B homomeric channel which is a similar trend as seen with the *C. elegans* UNC-49 heteromeric channel. In addition, Dim-UNC-49B can form a functional heteromeric channel with Hco-UNC-49C which is much more sensitive to GABA than the homomeric channel. Both *unc-49b* and *unc-49c* are expressed in all life stages tested in this study indicating the likely importance of the UNC-49 receptors in GABA neurotransmission, and their suitability as a drug target versatile for use in many life stages.

D. immitis LGC-46, LGC-47 and ACC-1 were unable to be functionally expressed in *X. laevis* oocytes, however qPCR analysis revealed that these genes are still expressed in all life stages indicating some possible relevance in neurotransmission. *lgc-46* was expressed at high levels in all life stages, so follow up analysis to determine if LGC-46 can form a functional channel with Hco-ACC-1 will assist in identifying the role it plays in *D. immitis,* and whether it has the potential to be a good drug target.

The testing of novel levamisole derivatives on Hco-ACC-2 receptors activation in comparison to levamisole and acetylcholine were assayed. A fluorine substituted levamisole was able to activate the Hco-ACC-2 receptor and produce EC_{50} values

significantly higher than levamisole itself. This opens avenues for the development of new synthetic drugs which may be more effective than traditional treatment options at lower doses. This has also validated the use of levamisole as a compound with potential for synthetic modifications as a method of drug development. This allows the possibility of enhancing the activity of drugs which have already been validated to bind to these receptors.

7. References

Accardi M V, Forrester SG. 2011. The *Haemonchus contortus* UNC-49B subunit possesses the residues required for GABA sensitivity in homomeric and heteromeric channels. Mol Biochem Parasitol. 178(1–2):15–22.

Agyekum TP, Botwe PK, Arko-Mensah J, Issah I, Acquah AA, Hogarh JN, Dwomoh D, Robins TG, Fobil JN. 2021. A systematic review of the effects of temperature on *Anopheles* mosquito development and survival: implications for malaria control in a future warmer climate. Int J Environ Res Public Health. 18(14):7255.

Altschul SF, Gish W, Miller W, Myers EW, Lipman DJ. 1990. Basic local alignment search tool. J Mol Biol. 215(3):403–410.

American Heartworm Society, Nelson TC, McCall JW, Jones S, Moorhead A. 2018. Current Canine Guidelines for the Prevention, Diagnosis, and Management of Heartworm (*Dirofilaria immitis*) Infection in Dogs.

Amin J, Weiss DS. 1993. GABAA receptor needs two homologous domains of the & beta;-subunit for activation by GABA but not by pentobarbital. Nature. 366(6455):565–569.

Anvari D, Narouei E, Daryani A, Sarvi S, Moosazadeh M, Hezarjaribi HZ, Narouei MR, Gholami S. 2020. The global status of *Dirofilaria immitis* in dogs: a systematic review and meta-analysis based on published articles. Res Vet Sci. 131:104–116.

Atkins CE. 2003. Comparison of results of three commercial heartworm antigen test kits in dogs with low heartworm burdens. J Am Vet Med Assoc. 222(9):1221–1223.

Atkins CE, Murray MJ, Olavessen LJ, Burton KW, Marshall JW, Brooks CC. 2014. Heartworm 'lack of effectiveness' claims in the Mississippi delta: Computerized analysis of owner compliance–2004–2011. Vet Parasitol. 206(1–2):106–113.

Baldrighi E, Zeppilli D, Appolloni L, Donnarumma L, Chianese E, Russo GF, Sandulli R. 2020. Meiofaunal communities and nematode diversity characterizing the Secca delle Fumose shallow vent area (Gulf of Naples, Italy). PeerJ. 8:e9058.

Bamber BA, Beg AA, Twyman RE, Jorgensen EM. 1999. The *Caenorhabditis elegans unc-49* locus encodes multiple subunits of a heteromultimeric GABA receptor. Journal of Neuroscience. 19(13):5348–5359.

Bamber BA, Twyman RE, Jorgensen EM. 2003. Pharmacological characterization of the homomeric and heteromeric UNC-49 GABA receptors in *C. elegans*. Br J Pharmacol. 138(5):883–893.

Bargmann CI. 1998. Neurobiology of the *Caenorhabditis elegans* genome. Science (1979). 282(5396):2028–2033.

Barnette C, Ruotsalo K, Tant MS. Testing for Heartworm Disease in Dogs. VCA Animal Hospital. https://vcacanada.com/know-your-pet/testing-for-heartworm-disease-in-dogs.

Beg AA, Jorgensen EM. 2003. EXP-1 is an excitatory GABA-gated cation channel. Nat Neurosci. 6(11):1145–1152.

Bellec L, Cambon-Bonavita M-A, Cueff-Gauchard V, Durand L, Gayet N, Zeppilli D. 2018. A nematode of the Mid-Atlantic Ridge hydrothermal vents harbors a possible symbiotic relationship. Front Microbiol. 9:2246.

Bienert S, Waterhouse A, De Beer TAP, Tauriello G, Studer G, Bordoli L, Schwede T. 2017. The SWISS-MODEL Repository—new features and functionality. Nucleic Acids Res. 45(D1):D313–D319.

Blanchard RAÉ, Laveran A. 1895. Les hématozoaires de l'homme et des animaux. Paris: Rueff.

Blaxter ML, De Ley P, Garey JR, Liu LX, Scheldeman P, Vierstraete A, Vanfleteren JR, Mackey LY, Dorris M, Frisse LM. 1998. A molecular evolutionary framework for the phylum Nematoda. Nature. 392(6671):71–75.

Boulin T, Fauvin A, Charvet CL, Cortet J, Cabaret J, Bessereau J, Neveu C. 2011. Functional reconstitution of *Haemonchus contortus* acetylcholine receptors in *Xenopus oocytes* provides mechanistic insights into levamisole resistance. Br J Pharmacol. 164(5):1421–1432.

Boulin T, Gielen M, Richmond JE, Williams DC, Paoletti P, Bessereau J-L. 2008. Eight genes are required for functional reconstitution of the *Caenorhabditis elegans* levamisole-sensitive acetylcholine receptor. Proceedings of the National Academy of Sciences. 105(47):18590–18595.

Bourguinat C, Keller K, Bhan A, Peregrine A, Geary T, Prichard R. 2011. Macrocyclic lactone resistance in *Dirofilaria immitis*. Vet Parasitol. 181(2–4):388–392.

Bowman DD, Mannella C. 2011. Macrocyclic lactones and *Dirofilaria immitis* microfilariae. Top Companion Anim Med. 26(4):160–172.

Brejc K, Van Dijk WJ, Klaassen R V, Schuurmans M, Van Der Oost J, Smit AB, Sixma TK. 2001. Crystal structure of an ACh-binding protein reveals the ligand-binding domain of nicotinic receptors. Nature. 411(6835):269–276.

Brenner S. 1974. The genetics of *Caenorhabditis elegans*. Genetics. 77(1):71–94.

Brown DDR, Siddiqui SZ, Kaji MD, Forrester SG. 2012. Pharmacological characterization of the *Haemonchus contortus* GABA-gated chloride channel, Hco-UNC-49: modulation by macrocyclic lactone anthelmintics and a receptor for piperazine. Vet Parasitol. 185(2–4):201–209.

Browne LE, Carter TD, Levy JK, Snyder PS, Johnson CM. 2005. Pulmonary arterial disease in cats seropositive for *Dirofilaria immitis* but lacking adult heartworms in the heart and lungs. Am J Vet Res. 66(9):1544–1549.

Brust RA. 1967. Weight and development time of different stadia of mosquitoes reared at various constant temperatures. Can Entomol. 99(9):986–993.

Bürglin TR, Lobos E, Blaxter ML. 1998. *Caenorhabditis elegans* as a model for parasitic nematodes. Int J Parasitol. 28(3):395–411.

Callanan MK, Habibi SA, Law WJ, Nazareth K, Komuniecki RL, Forrester SG. 2018. Investigating the function and possible biological role of an acetylcholine-gated chloride channel subunit (ACC-1) from the parasitic nematode *Haemonchus contortus*. Int J Parasitol Drugs Drug Resist. 8(3):526–533.

Del Castillo J, De Mello WC, Morales T. 1963. The physiological role of acetylcholine in the neuromuscular system of *Ascaris lumbricoides*. Arch Int Physiol Biochim. 71(5):741–757.

Del Castillo J, De Mello WC, Morales T. 1964. Inhibitory action of γ-aminobutyric acid (GABA) on *Ascaris muscle*. Experientia. 20(3):141–143.

Cattoni DI, Chara O, Kaufman SB, González Flecha FL. 2015. Cooperativity in binding processes: new insights from phenomenological modeling. PLoS One. 10(12):e0146043.

Cochrane E. 2017. An examination of interacting residues in the GABA-gated ion channel UNC-49 within the parasitic nematode *Haemonchus contortus*. Ontario Tech University.

Collins AM. 2022. Investigation into potential *Dirofilaria immitis* drug targets through rational anthelmintic synthesis and design [Dissertation]. Ontario Tech University.

Culetto E, Baylis HA, Richmond JE, Jones AK, Fleming JT, Squire MD, Lewis JA, Sattelle DB. 2004. The *Caenorhabditis elegans* unc-63 gene encodes a levamisole-sensitive nicotinic acetylcholine receptor α subunit. Journal of Biological Chemistry. 279(41):42476–42483.

Cully DF, Vassilatis DK, Liu KK, Paress PS, Van Der Ploeg LHT, Schaeffer JM, Arena JP. 1994. Cloning of an avermectin-sensitive glutamate-gated chloride channel from *C. elegans* . Nature. 371(6499):707–711.

Dent JA. 2006. Evidence for a diverse Cys-loop ligand-gated ion channel superfamily in early bilateria. J Mol Evol. 62:523–535.

Dent JA. 2010. The evolution of pentameric ligand-gated ion channels. IJournal of insect nicotinic acetylcholine receptors.:11–23.

Dereeper A, Audic S, Claverie J-M, Blanc G. 2010. BLAST-EXPLORER helps you building datasets for phylogenetic analysis. BMC Evol Biol. 10(1):8.

Dereeper A, Guignon V, Blanc G, Audic S, Buffet S, Chevenet F, Dufayard J-F, Guindon S, Lefort V, Lescot M. 2008. Phylogeny. fr: robust phylogenetic analysis for the non-specialist. Nucleic Acids Res. 36(suppl 2):W465–W469.

Dibas MI, Gonzales EB, Das P, Bell-Horner CL, Dillon GH. 2002. Identification of a novel residue within the second transmembrane domain that confers use-facilitated block by picrotoxin in glycine α1 receptors. Journal of Biological Chemistry. 277(11):9112–9117.

Dorris M, De Ley P, Blaxter ML. 1999. Molecular analysis of nematode diversity and the evolution of parasitism. Parasitology today. 15(5):188–193.

Eimer S, Gottschalk A, Hengartner M, Horvitz HR, Richmond J, Schafer WR, Bessereau J. 2007. Regulation of nicotinic receptor trafficking by the transmembrane Golgi protein UNC-50. EMBO J. 26(20):4313–4323.

Erickson AB. 1944. Helminths of Minnesota Canidae in relation to food habits, and a host list and key to the species reported from North America. Am Midl Nat. 32(2):358–372.

Erkkila BE, Sedelnikova A V, Weiss DS. 2008. Stoichiometric pore mutations of the GABAAR reveal a pattern of hydrogen bonding with picrotoxin. Biophys J. 94(11):4299–4306.

Faust EC, Thomas EP, Jones J. 1941. Discovery of human heartworm infection in New Orleans. J Parasitol. 27(2):115–122.

Ffrench-Constant R, Rocheleau TA, Steichen JC, Chalmers AE. 1993. A point mutation in a *Drosophila* GABA receptor confers insecticide resistance. Nature. 363(6428):449–451.

Filippova N, Sedelnikova A, Zong Y, Fortinberry H, Weiss DS. 2000. Regulation of recombinant γ-aminobutyric acid (GABA) A and GABAC receptors by protein kinase C. Mol Pharmacol. 57(5):847–856.

Fleming JT, Squire MD, Barnes TM, Tornoe C, Matsuda K, Ahnn J, Fire A, Sulston JE, Barnard EA, Sattelle DB. 1997. Caenorhabditis elegans levamisole resistance geneslev-1, unc-29, and unc-38 encode functional nicotinic acetylcholine receptor subunits. Journal of Neuroscience. 17(15):5843–5857.

Fortin JF, Slocombe JOD. 1981. Temperature requirements for the development of *Dirofilaria immitis* in *Aedes triseriatus* and *Ae. vexans*. Mosq News. 41(4):625–633.

Foster J, Cochrane E, Khatami MH, Habibi SA, de Haan H, Forrester SG. 2018. A mutational and molecular dynamics study of the cys-loop GABA receptor Hco-UNC-49 from *Haemonchus contortus*: agonist recognition in the nematode GABA receptor family. Int J Parasitol Drugs Drug Resist. 8(3):534–539.

Frank JR, Nutter FB, Kyles AE, Atkins CE, Sellon RK. 1997. Systemic arterial dirofilariasis in five dogs. J Vet Intern Med. 11(3):189–194.

Freckman DW. 1988. Bacterivorous nematodes and organic-matter decomposition. Agric Ecosyst Environ. 24(1–3):195–217.

Genchi C, Rinaldi L, Mortarino M, Genchi M, Cringoli G. 2009. Climate and Dirofilaria infection in Europe. Vet Parasitol. 163(4):286–292.

Gilleard JS. 2013. *Haemonchus contortus* as a paradigm and model to study anthelmintic drug resistance. Parasitology. 140(12):1506–1522.

Gish W, States DJ. 1993. Identification of protein coding regions by database similarity search. Nat Genet. 3(3):266–272.

Goble FC. 1942. Dog heartworm in the muskrat in New York. J Mammal. 23(3).

Green WN, Wanamaker CP. 1997. The role of the cystine loop in acetylcholine receptor assembly. Journal of Biological Chemistry. 272(33):20945–20953.

Grutter T, de Carvalho LP, Dufresne V, Taly A, Edelstein SJ, Changeux J-P. 2005. Molecular tuning of fast gating in pentameric ligand-gated ion channels. Proceedings of the National Academy of Sciences. 102(50):18207–18212.

Gubanov NM. 1951. A giant nematode from the placenta of cetaceans *Placenttnema gigantissima ngn sp.* Dokl Akad Nauk SSSR. 77(6):1123–1125.

Habibi SA, Blazie SM, Jin Y, Forrester SG. 2020. Isolation and characterization of a novel member of the ACC ligand-gated chloride channel family, Hco-LCG-46, from the parasitic nematode *Haemonchus contortus*. Mol Biochem Parasitol. 237:111276.

Habibi SA, Callanan M, Forrester SG. 2018. Molecular and pharmacological characterization of an acetylcholine-gated chloride channel (ACC-2) from the parasitic nematode *Haemonchus contortus*. Int J Parasitol Drugs Drug Resist. 8(3):518–525.

Hailu FA, Hailu YA. 2020. Agro-ecological importance of nematodes (round worms). Acta Sci Agric. 4(1):156–162.

Hampshire VA. 2005. Evaluation of efficacy of heartworm preventive products at the FDA. Vet Parasitol. 133(2–3):191–195.

Hardege I, Morud J, Courtney A, Schafer WR. 2023. A novel and functionally diverse class of acetylcholine-gated ion channels. Journal of Neuroscience. 43(7):1111–1124.

Holden-Dye L, Krogsgaard-Larsen P, Nielsen L, Walker RJ. 1989. GABA receptors on the somatic muscle cells of the parasitic nematode, *Ascaris suum*: stereoselectivity indicates similarity to a GABAA-type agonist recognition site. Br J Pharmacol. 98(3):841.

International Helminth Genomes Consortium. 2019. Comparative genomics of the major parasitic worms. Nat Genet. 51(1):163–174.

Jones AK, Sattelle DB. 2004. Functional genomics of the nicotinic acetylcholine receptor gene family of the nematode, *Caenorhabditis elegans*. Bioessays. 26(1):39–49.

Jones AK, Sattelle DB. 2008. The cys-loop ligand-gated ion channel gene superfamily of the nematode, *Caenorhabditis elegans*. Invertebrate Neuroscience. 8(1):41–47.

Kaji MD, Kwaka A, Callanan MK, Nusrat H, Desaulniers J-P, Forrester SG. 2015. A molecular characterization of the agonist binding site of a nematode cys-loop GABA receptor. Br J Pharmacol. 172(15):3737–3747. doi:10.1111/bph.13158.

Kaminsky R, Ducray P, Jung M, Clover R, Rufener L, Bouvier J, Weber SS, Wenger A, Wieland-Berghausen S, Goebel T. 2008. A new class of anthelmintics effective against drug-resistant nematodes. Nature. 452(7184):176–180.

Kaplan RM. 2004. Drug resistance in nematodes of veterinary importance: a status report. Trends Parasitol. 20(10):477–481.

Kashyap P, Afzal S, Rizvi AN, Ahmad W, Uniyal VP, Banerjee D. 2022. Nematode community structure along elevation gradient in high altitude vegetation cover of Gangotri National Park (Uttarakhand), India. Sci Rep. 12(1):1–13.

Kiontke K, Fitch DHA. 2013. Nematodes. Current Biology. 23(19):R862–R864.

Kneussel M, Betz H. 2000. Receptors, gephyrin and gephyrin-associated proteins: novel insights into the assembly of inhibitory postsynaptic membrane specializations. J Physiol. 525(1):1–9.

Knott J. 1939. A method for making microfilarial surveys on day blood. Trans R Soc Trop Med Hyg. 33(2).

Koppenhöfer AM. 2000. Nematodes. In: Field manual of techniques in invertebrate pathology. Springer. p. 283–301.

Krieg PA, Melton DA. 1984. Functional messenger RNAs are produced by SP6 in vitro transcription of cloned cDNAs. Nucleic Acids Res. 12(18):7057–7070.

Krogh A, Larsson B, Von Heijne G, Sonnhammer ELL. 2001. Predicting transmembrane protein topology with a hidden Markov model: application to complete genomes. J Mol Biol. 305(3):567–580.

Kume S, Itagaki S. 1955. On the life-cycle of *Dirofilaria immtis* in the dog as the final host. British Veterinary Journal. 111(1):16–24.

Kwaka A, Khatami MH, Foster J, Cochrane E, Habibi SA, de Haan HW, Forrester SG. 2018. Molecular characterization of binding loop E in the nematode cys-loop GABA receptor. Mol Pharmacol. 94(5):1289–1297.

Laing R, Kikuchi T, Martinelli A, Tsai IJ, Beech RN, Redman E, Holroyd N, Bartley DJ, Beasley H, Britton C. 2013. The genome and transcriptome of *Haemonchus contortus*, a key model parasite for drug and vaccine discovery. Genome Biol. 14:1–16.

Ledesma N, Harrington L. 2015. Fine-scale temperature fluctuation and modulation of Dirofilaria immitis larval development in *Aedes aegypti*. Vet Parasitol. 209(1–2):93–100.

Lema GMC, Auerbach A. 2006. Modes and models of GABAA receptor gating. J Physiol. 572(1):183–200.

Levitan IB. 1994. Modulation of ion channels by protein phosphorylation and dephosphorylation. Annu Rev Physiol. 56(1):193–212.

Lewis James A, Wu CH, Berg H, Levine JH. 1980. The genetics of levamisole resistance in the nematode Caenorhabditis elegans. Genetics. 95(4):905–928.

Lewis J A, Wu C-H, Levine JH, Berg H. 1980. Levamisole-resitant mutants of the nematode *Caenorhabditis elegans* appear to lack pharmacological acetylcholine receptors. Neuroscience. 5(6):967–989.

Li X-Y, Cowles RS, Cowles EA, Gaugler R, Cox-Foster DL. 2007. Relationship between the successful infection by entomopathogenic nematodes and the host immune response. Int J Parasitol. 37(3–4):365–374.

Liman ER, Tytgat J, Hess P. 1992. Subunit stoichiometry of a mammalian K+ channel determined by construction of multimeric cDNAs. Neuron. 9(5):861–871.

Ludlam KW, Jachowski LA, Otto GF. 1970. Potential vectors of Dirofilaria immitis. J Am Vet Med Assoc. 157:1354–1359.

Lummis SCR. 2009. Locating GABA in GABA receptor binding sites. Biochem Soc Trans. 37(6):1343–1346.

Lynagh T, Lynch J. 2012. Molecular mechanisms of Cys-loop ion channel receptor modulation by ivermectin. Front Mol Neurosci. 5:60.

Madeira F, Pearce M, Tivey ARN, Basutkar P, Lee J, Edbali O, Madhusoodanan N, Kolesnikov A, Lopez R. 2022. Search and sequence analysis tools services from EMBL-EBI in 2022. Nucleic Acids Res. 50(W1):W276–W279.

Majdi N, Traunspurger W. 2015. Free-living nematodes in the freshwater food web: a review. J Nematol. 47(1):28.

Mann PH, Fratta I. 1953. Transplantation of adult heartworms, *Dirofilaria immitis*, into dogs and cats. J Parasitol. 39(2):139–144.

Martin RJ, Sitamze J-M, Duittoz AH, Wermuth CG. 1995. Novel arylaminopyridazine-GABA receptor antagonists examined electrophysiologically in *Ascaris suum*. Eur J Pharmacol. 276(1–2):9–19.

McGill E, Berke O, Peregrine AS, Weese JS. 2019. Epidemiology of canine heartworm (Dirofilaria immitis) infection in domestic dogs in Ontario, Canada: geographic distribution, risk factors and effects of climate. Geospat Health. 14(1).

Millar NS. 2008. RIC-3: a nicotinic acetylcholine receptor chaperone. Br J Pharmacol. 153(S1):S177–S183.

Miller TW, Chaiet L, Cole DJ, Cole LJ, Flor JE, Goegelman RT, Gullo VP, Joshua H, Kempf AJ, Krellwitz WR. 1979. Avermectins, new family of potent anthelmintic agents: isolation and chromatographic properties. Antimicrob Agents Chemother. 15(3):368–371.

Morchón R, Carretón E, González-Miguel J, Mellado-Hernández I. 2012. Heartworm disease (*Dirofilaria immitis*) and their vectors in Europe–new distribution trends. Front Physiol. 3:196.

Morchón R, Montoya-Alonso JA, Rodríguez-Escolar I, Carretón E. 2022. What has happened to heartworm disease in Europe in the last 10 years? Pathogens. 11(9):1042.

Nelson CT, McCall JW, Rubin SB, Buzhardt LF, Dorion DW, Graham W, Longhofer SL, Guerrero J, Robertson-Plouch C, Paul A. 2005. 2005 Guidelines for the diagnosis, prevention and management of heartworm (*Dirofilaria immitis*) infection in dogs. Vet Parasitol. 133:255–266.

Nelson TC. 2012. Canine heartworm disease. Greene CE Infectious Diseases of the Dog and Cat 4th ed Oxford: Elsevier.:865–873.

Neveu C, Charvet CL, Fauvin A, Cortet J, Beech RN, Cabaret J. 2010. Genetic diversity of levamisole receptor subunits in parasitic nematode species and abbreviated transcripts associated with resistance. Pharmacogenet Genomics. 20(7):414–425.

Newland CF, Cull-Candy SG. 1992. On the mechanism of action of picrotoxin on GABA receptor channels in dissociated sympathetic neurones of the rat. J Physiol. 447(1):191–213.

Newton WL, Wright WH. 1956. The occurrence of a dog filariid other than *Dirofilaria immitis* in the United States. J Parasitol. 42(3):246–258.

Nguyen M, Alfonso A, Johnson CD, Rand JB. 1995. Caenorhabditis elegans mutants resistant to inhibitors of acetylcholinesterase. Genetics. 140(2):527–535.

Nomura K, Yoshizumi S, Ozoe F, Ozoe Y. 2021. Molecular cloning and pharmacology of Min-UNC-49B, a GABA receptor from the southern root-knot nematode Meloidogyne incognita. Pest Manag Sci. 77(8):3763–3776.

Padgett CL, Hanek AP, Lester HA, Dougherty DA, Lummis SCR. 2007. Unnatural amino acid mutagenesis of the GABAA receptor binding site residues reveals a novel cation–π interaction between GABA and β2Tyr97. Journal of Neuroscience. 27(4):886–892.

Perozo E, Marien D, Cortes, Cuello LG. 1999. Structural rearrangements underlying K+-channel activation gating. Science (1979). 285(5424):73–78.

Pettersen EF, Goddard TD, Huang CC, Couch GS, Greenblatt DM, Meng EC, Ferrin TE. 2004. UCSF Chimera—a visualization system for exploratory research and analysis. J Comput Chem. 25(13):1605–1612.

Platt H. 1994. The phylogenetic systematics of free living nematodes. Ray society.

Prichard RK. 2021. Macrocyclic lactone resistance in *Dirofilaria immitis*: risks for prevention of heartworm disease. Int J Parasitol. 51(13–14):1121–1132.

Prinz H. 2010. Hill coefficients, dose–response curves and allosteric mechanisms. J Chem Biol. 3:37–44.

Pulaski CN, Malone JB, Bourguinat C, Prichard R, Geary T, Ward D, Klei TR, Guidry T, Delcambre B, Bova J. 2014. Establishment of macrocyclic lactone resistant *Dirofilaria immitis* isolates in experimentally infected laboratory dogs. Parasit Vectors. 7(1):494.

Putrenko I, Zakikhani M, Dent JA. 2005. A family of acetylcholine-gated chloride channel subunits in *Caenorhabditis elegans*. Journal of Biological Chemistry. 280(8):6392–6398.

Ranganathan R, Cannon SC, Horvitz HR. 2000. MOD-1 is a serotonin-gated chloride channel that modulates locomotory behaviour in *C. elegans*. Nature. 408(6811):470–475.

Ringstad N, Abe N, Horvitz HR. 2009. Ligand-gated chloride channels are receptors for biogenic amines in *C. elegans*. Science (1979). 325(5936):96–100.

Robertson AP, Buxton SK, Puttachary S, Williamson SM, Wolstenholme AJ, Neveu C, Cabaret J, Charvet CL, Martin RJ. 2012. Antinematodal drugs–modes of action and resistance: and worms will not come to thee (Shakespeare: Cymbeline: IV, ii). Parasitic Helminths: Targets, Screens, Drugs and Vaccines.:233–249.

Roux B. 2017. Ion channels and ion selectivity. Essays Biochem. 61(2):201–209.

Šali A, Blundell TL. 1993. Comparative protein modelling by satisfaction of spatial restraints. J Mol Biol. 234(3):779–815.

Shen X-M, Ohno K, Tsujino A, Brengman JM, Gingold M, Sine SM, Engel AG. 2003. Mutation causing severe myasthenia reveals functional asymmetry of AChR signature cystine loops in agonist binding and gating. J Clin Invest. 111(4):497–505.

Shi M, Neville P, Nicholson J, Eden J-S, Imrie A, Holmes EC. 2017. High-resolution metatranscriptomics reveals the ecological dynamics of mosquito-associated RNA viruses in Western Australia. J Virol. 91(17):10–1128.

Siddiqui SZ, Brown DDR, Rao VTS, Forrester SG. 2010. An UNC-49 GABA receptor subunit from the parasitic nematode *Haemonchus contortus* is associated with enhanced GABA sensitivity in nematode heteromeric channels. J Neurochem. 113(5):1113–1122.

Simmons JM, Nicholson WS, Hill EP, Briggs DB. 1980. Occurrence of (*Dirofilaria immitis*) in gray fox (*Urocyon cinereoargenteus*) in Alabama and Georgia. J Wildl Dis. 16(2):225–228.

Sine SM. 2002. The nicotinic receptor ligand binding domain. J Neurobiol. 53(4):431–446.

Skinner TM, Bascal ZA, Holden-Dye L, Lunt GG, Wolstenholme AJ. 1998. Immunocytochemical localization of a putative inhibitory amino acid receptor subunit in the parasitic nematodes *Haemonchus contortus* and *Ascaris suum*. Parasitology. 117(1):89–96.

Sonnhammer ELL, Von Heijne G, Krogh A. 1998. A hidden Markov model for predicting transmembrane helices in protein sequences. In: Ismb. Vol. 6. p. 175–182.

Teufel F, Almagro Armenteros JJ, Johansen AR, Gíslason MH, Pihl SI, Tsirigos KD, Winther O, Brunak S, von Heijne G, Nielsen H. 2022. SignalP 6.0 predicts all five types of signal peptides using protein language models. Nat Biotechnol. 40(7):1023–1025.

The UniProt Consortium. 2023. UniProt: the universal protein knowledgebase in 2023. Nucleic Acids Res. 51(D1):D523–D531.

Thompson AJ, Lester HA, Lummis SCR. 2010. The structural basis of function in Cys-loop receptors. Q Rev Biophys. 43(4):449–499.

Touroutine D, Fox RM, Von Stetina SE, Burdina A, Miller DM, Richmond JE. 2005. *acr-16* encodes an essential subunit of the levamisole-resistant nicotinic receptor at the *Caenorhabditis elegans* neuromuscular junction. Journal of Biological Chemistry. 280(29):27013–27021.

Towers PR, Edwards B, Richmond JE, Sattelle DB. 2005. The *Caenorhabditis elegans lev-8* gene encodes a novel type of nicotinic acetylcholine receptor α subunit. J Neurochem. 93(1):1–9.

Trott O, Olson AJ. 2010. AutoDock Vina: improving the speed and accuracy of docking with a new scoring function, efficient optimization, and multithreading. J Comput Chem. 31(2):455–461.

Velasquez L, Blagburn BL, Duncan-Decoq R, Johnson EM, Allen KE, Meinkoth J, Gruntmeir J, Little SE. 2014. Increased prevalence of *Dirofilaria immitis* antigen in canine samples after heat treatment. Vet Parasitol. 206(1–2):67–70.

Wagner DA, Czajkowski C, Jones M V. 2004. An arginine involved in GABA binding and unbinding but not gating of the GABAA receptor. Journal of Neuroscience. 24(11):2733–2741.

Waterhouse A, Bertoni M, Bienert S, Studer G, Tauriello G, Gumienny R, Heer FT, de Beer TAP, Rempfer C, Bordoli L. 2018. SWISS-MODEL: homology modelling of protein structures and complexes. Nucleic Acids Res. 46(W1):W296–W303.

Wecker L, Guo X, Rycerz AM, Edwards SC. 2001. Cyclic AMP-dependent protein kinase (PKA) and protein kinase C phosphorylate sites in the amino acid sequence corresponding to the M3/M4 cytoplasmic domain of α4 neuronal nicotinic receptor subunits. J Neurochem. 76(3):711–720.

Weiss JN. 1997. The Hill equation revisited: uses and misuses. The FASEB Journal. 11(11):835–841.

Wever CM, Farrington D, Dent JA. 2015. The validation of nematode-specific acetylcholine-gated chloride channels as potential anthelmintic drug targets. PLoS One. 10(9):e0138804.

Wolstenholme AJ, Evans CC, Jimenez PD, Moorhead AR. 2015. The emergence of macrocyclic lactone resistance in the canine heartworm, *Dirofilaria immitis*. Parasitology. 142(10):1249–1259.

Wolstenholme AJ, Rogers AT. 2005. Glutamate-gated chloride channels and the mode of action of the avermectin/milbemycin anthelmintics. Parasitology. 131(S1):S85–S95.

Xu H-L, Du L-D, Du G-H. 2018. Picrotoxin. In: Natural Small Molecule Drugs from Plants. Springer. p. 303–307.

Yamamoto I, Absalom N, Carland JE, Doddareddy MR, Gavande N, Johnston GAR, Hanrahan JR, Chebib M. 2012. Differentiating enantioselective actions of GABOB: A possible role for threonine 244 in the binding site of GABAC ρ1 receptors. ACS Chem Neurosci. 3(9):665–673.

Yuan X, XU J, Shi H, Bai X, HU X, LI R, Wang Y, Zhou Q, Zhang W, BI X. 1986. Effects of Picrotoxin on the Rate, Contractility and Action Potential of Isolated Frog Heart. Journal of Third Military Medical University.

Zhang D, Pan Z-H, Zhang X, Brideau AD, Lipton SA. 1995. Cloning of a gamma-aminobutyric acid type C receptor subunit in rat retina with a methionine residue critical for picrotoxinin channel block. Proceedings of the National Academy of Sciences. 92(25):11756–11760.

8. Appendix

8.1 Gene and Protein Sequences

>Dim-UNC49_B
ATGCATCTTATCTCATTCTTTTTCATCATTTATTGCACCGTTTACAACTACACACTCGGTTATATAGAATAT
CCGAGTAGTAAAACTTTCAATACAACAGCAATTTCTGATATCTTAAATCGTCTTGTCGATAAATCAACAT
ATGATAAAAGATTAAGGCCGAAATATGGTGCTGAACCTGTTGATGTAGGTATAACTATTCATGTATCCAG
TATCAGTGCTGTTTCCGAAGTCGATATGGATTTTACAATTGATTTTTATTTACGACAAACTTGGCAAGATC
CACGTTTAGCATTTGGTGATATGTTTTATGGTTATCAACAGGGAAAGATTGAATCATTGACGGTTGGTGTT
GATTATTTGGATAAACTTTGGAAACCGGATACATTTTTTCCGAATGAAAAAAAATCATTCTTTCATACCGC
AACAACACATAATTCCTTTTTAAGAATCGATCCTGATGGCACTGTTTTCACTTCTCAAAGGTTAACGGTAA
CAGCAACATGTCCAATGAAATTACAACTTTTTCCAATGGATTCACAAAAATGCAAACTTGAAATCGAAAG
TTATGGTTATACAACTGCTGATATCGATTTATTTTGGGGTAAAGATCGTAAAGATCAGGGTCAAGTTGTC
GGGTTCGAGAATATTTCGCTGCCACAATTTAAGCCGGTTGGTTATCGGGTAAATGTTACCCGAGCAATCA
CTTCTTCAGGTGTATATGTTCGATTATATTTTGAAGTATTGTTGGCTCGTAACCTCGGTTTCTACCTCATGG
ATATCATCATTCCTTCCATGCTTATTGTTACCATTTCTTGGGTATCATTTTGGCTTAATCGTGAAGCATCAC
CAGCACGAGTTGGTCTTGGTGTTACTACTGTACTAACGATGACCACACTTATCACTACTACTAATAATGCA
ATGCCAAAaGTTAGTTATATCAAAGGACTTGATGTTTTCTTAAaTTTTTGTTtTGTGATGGTATTTGCAAGCC
TAATTGAATATGCGGTAGTTAGTTATATGAATAAAAAATTAGTACAAAGACGGGAAAAAAGACGAAAAC
AGGTTGAGCAAGGAATACCGGTCGAAATGCCTATGTATAATCAACTTACAACTAATGCTGAAACAAAAA
TGCAAATGGATACGTTCCTTGGTAGTTCAGGACAAAATCCTAATTTAAGTGTATCAGAAGCGTTAATACC
AGAATGTGATTGTCGTACGATACCGTTGATACAGAATCCACGATTGGTAGCAGATCATACATTATGGCCT
GCACCATTTATGAGGCCAAAACGTGCATCACGTACGTGTCGAAGTGTAACACCATCAAAAATTGATAAAT
TTTCACGCTTCCTATTTCCTATGCTATTTTTGGCTTTTAATTTACTTTATTGGACAATAATGACGGTGCTCA
GTTCATTCGTTGATACCAGTGACTATACATTATTTGATTAA

>Dim_UNC_49_C
ATGCATCTTATCTCATTCTTTTTCATCATTTATTGCACCGTTTACAACTACACACTCGGTTATATAGAATAT
CCGAGTAGTAAAACTTTCAATACAACAGCAATTTCTGATATCTTAAATCGTCTTGTCGATAAATCAACAT
ATGATAAAAGATTAAGGCCGAAATATGGTGCTGAACCTGTTGATGTAGGTATAACTATTCATGTATCCAG
TATCAGTGCTGTTTCCGAAGTTGATATGGATTTTACAATTGATTTTTATTTACGACAAACTTGGCAAGATC
CACGTTTAGCATTTGGTGATATGTTTTATGGTTATCAACAGGGAAAGATTGAATCATTGACGGTTGGTGTT
GATTATTTGGATAAACTTTGGAAACCGGATACATTTTTTCCGAATGAAAAAAAATCATTCTTTCATACCGC
AACAACACATAATTCCTTTTTAAGAATCGATCCTGATGGCACTGTTTTCACTTCTCAAAGGTTAACGGTAA
CAGCAACATGTCCAATGAAATTACAACTTTTTCCAATGGATTCACAAAAATGCAAACTTGAAATCGAAAG
TTATGGTTATACTGTCGCAACAATACATTATCATTGGTGTCAATTAAAAGATATCGATTGCAAGACAGCG
GTCAAAGTTGAACCATTTGAATTGACCAGTTATCGATTTGCTAATTTATGCATTAATAAAACTATTGCAAC
AACTTCGTCCGGTTCTTATTCACGATTATGGGCGCAATTTTTATTCGAGAGAGAATTTAGCTTTTATATGA
TTCAAATTTATACACCTGCAATACTTGTCGTCTTCATTAGTTGGGTATCATTTTGGATCAATCCAGAATCA
GCTCCATCTCGTACAGTTATTGGAACATTAACTATATTAAGTGAAACTCATCTATTAATGAGTACCAATAA
ACGACTTCCACCTGTTTCCTATATTAAGGCTGTGGATGTTTACCTTGGATTTTGTTACTTAAATGTAGCATT
AGCACTTATTGAATTTGCTACTGTCGCATATACAAAAAAGAAATATGAAGATAGGAAGAGAAATAAAAG
TAAAAATGTTTTCGAACTTGTGCCACAGGTACAGGCACCTGATTTACTTCGAGATGTTCGTATAGATGTAT
GCACTTGTGATCAAAATGTTTCGGTATTTTTGGTAGATAAAAAATCACCAAAATGTAATAATTGCTGTAT
ACATAGTCGATTAGACCTCATCGCTCGAATTGCATTTCCTATTTCGTTTCTTATGTTCAACTTCATTTATTG
GACAGTGCTTCTCTCCTTATCAGGTTGGAAAATATATGGAGATAATACGGAACAAAGAGCCTGTTAA

>Dim_LGC_46
ATGCACTACCTCAATCGTCTGCTTCTTATTAGTATAATCTGCTCTTCTTCCTTCATCAATTTCATCCACTCA
AGACAAACAATGTATAGAAAGAATTCACGAATTCTTCGAAGGTTGAGCAGATTATATGATTGGCAAATG
GATGAGTATGGTGGCTTACATCCAGTGATTGAATCAATTAACGGAAAGGAACAGCAGCCACACTATCCCC
ATTATCATCATTCAGCAATCTCAGTGGATGATAAAATGAAACGCCAACAAACTTGTGCCAATGATTCATT
CATTCTGGAAACTATCCTCAAAAAATATAATCGCCATAAAATTCCAGGAGATTCAGTGGTTGTTCAGGTT
GAGGTTTGGGTACAAGAAATTACGACAATTAGCGATATTACCTCCGACTTTCAACTCGATATTTACATAA
GTGAAATGTGGTTGGATCCAGCTTTAGATTATTCTTGGATGCAACCCTGTAAATATAATTTGTCACTGAAT
AGCGTTTTGCTGGAAAAGCTTTGGACTCCTAATTCATGTTTTATCAATTCGAAAACTGCTGATATACATCG
AAGTCCATTTCCAAACATTTTTTTAATGATTTATTCCAATGGATCAGTATGGACTAATTATAGGCTCAAAT
TGCAAGGACCATGCATTATGGATTTAACAAGATTTCCATTCGACAATGTTACATGCTCGCTCACTTTCGAA
AGCTTCAATTATAATACTGATGAAGTTCAAATGGTTTGGTCGCCACTTGGTGTTTCAAAAATGCGTGAAA
AAATGGAACTAGCTGATTATGAGCTTACCGGTATAGAGAACCTCAGGAAGACAGAGCCTTATCCCGCTG

GTTTTTGGCATGAATTAACAATGAGATTTCATTTTAAAAGACGCGCAGGATGGTATATTCTGCAAGCTTAT
CTTCCAACTTATCTTACTATTTGTATATCATGGATTTCGTTTGCTCTTGGTTCCAAAGCAATACCAGCACG
AACAATGTTAGGGGTTAATTCACTTCTTGCAATGACTTTTCAGTTTGGCAATATTATAAGAAATTTACCGC
GAGTTAGCTATGTCAAGGCAATAGATGTTTGGATGCTAAGTTGTATGACTTTCGTATTCTGTTCATTGTTG
GAGCTTGCGTGGGTCGGATACTTGAGCAGGGAAGAACTCGAAGCACCTAAATCCGTAACAACAAAGGTA
TTACCAGCAGTGCATCATGATAATAACAGTATCAACTTACCAACAACAACGCATCAAGACCATTATGAAA
CGAATTCTGTACTTTCCAGACGGAGACCAGCAATTTCTGAGGAAGAAAATGCATTGATAAGTCTTGCACA
TGGTAATGATTACGGTTACATACCGCCAGGTTACGGTCTCAACGATCATTTGAAAGCAACTATGGCTTCC
ATAGCTGGACCTTGCGGTTGCTTGCAGCAAGAGCCAATGCCTAATACAAAATCCTTTTCATCCATTCCAA
CATCACACGATCCTAACGAACTCTCCAAACAAAGGGAACGAGCAACACAGTATATTGATAAGTTATCAG
CAATACTATTCCCGATGTTATTCAGTGTGTTTAATATTGCTTATTGGTATCATTACCTCAAGGATTGA

> Dim_LGC_46_Protein_Sequence
MHYLNRLLLISIICSSSFINFIHSRQTMYRKNSRILRRLSRLYDWQMDEYGGLHPVIESINGKEQQPHYPHYHHS
AISVDDKMKRQQTCANDSFILETILKKYNRHKIPGDSVVVQVEVWVQEITTISDITSDFQLDIYISEMWLDPAL
DYSWMQPCKYNLSLNSVLLEKLWTPNSCFINSKTADIHRSPFPNIFLMIYSNGSVWTNYRLKLQGPCIMDLTRF
PFDNVTCSLTFESFNYNTDEVQMVWSPLGVSKMREKMELADYELTGIENLRKTEPYPAGFWHELTMRFHFKR
RAGWYILQAYLPTYLTICISWISFALGSKAIPARTMLGVNSLLAMTFQFGNIIRNLPRVSYVKAIDVWMLSCMT
FVFCSLLELAWVGYLSREELEAPKSVTTKVLPAVHHDNNSINLPTTTHQDHYETNSVLSRRRPAISEEENALISL
AHGNDYGYIPPGYGLNDHLKATMASIAGPCGCLQQEPMPNTKSF

>Dim_LGC_47
ATGCTCCAGAGAACAATCGTAAGCTGGTCTGCCCGGGTCTACTCTCTGCAAATAGTACTAATACTGCAAT
TATGCGCAGCTGCGGTAATAGCTGTGTCAAAAACTTTCCATCCGAAACAGTGTTCTAACGATACTGATGT
AATGGATCACCTTTTAACCGAGGCTGCACTTCGCCATAATCGCCATAAATTACCGTCTAGACCAGTCATT
GTACGAATTGAAATGTGGATTCAAGAAGTAACTTACGTTTCTGAACTCACTCAGGATTTTGAAATTGATTT
ATATGTGAATGAATTTTGGGAAGATCCAGCGCTAAATTATGAAGTACTTCTACCATGTAATGGCAATTTA
AGTTTTGATCACAGCATCCAGGAAAGTATTTGGATTCCTAATACTTGCTTTATCAACTCAAAAAAGGCAC
TCATACACAGCTCACCATTTCGAAATGTTTTTCTTATGGTCTTTCCAAATGGCTCAATATGGTCATGTTGG
CGTATTAAGAGCACTGGTCCGTGTCATATGGACCTGACTAATTTTCCAATGGATTCTATTTCGTGTATGCT
AACGTTTGAATCTTATAATTACAACATCCAGGAAGTACGGATGAAATGGAACGAACCTCATGCTGTCTTA
ATGTTTAAGGATATCGAACTACCAGATTTCACTTTGGTCAACTACACAACTTCTGTCATTGAAGCTGAGTA
TGCGGCAGGTTTATGGGACGAACTTACTGTTTCGTTCACATTCAAAAGAAGATATGGATGGTACATTTTG
CAAGGATATATTCCAACGTATCTAACTATATTTATCTCATGGATACCATTTTATATGAGTCCACGTGCAAT
GCCAGCTCGAACTATGATTGGTGTCAATTCACTGCTTGCAATGACATTCCAATTCGGAAACATTATACGG
AATCTTCCACGAGTATCTTACATAAAGGCGATCGATATTTGGGTTCTAAGTGGGATGACTTTCATATTCGC
GTCGTTGATCGAGCTTGCAATTGTTGGTTTTATGAATCGGCACGAAGGCCGAGCAGATACCAAATTGAAT
CATATGCACAAAAAAAGAAAATCATCCATTCTGGATAGTGAGAAACTAGACTTATATTCAAGGACTAGTT
TTCCTCTGGTATATGCAATGTTCAACATGATATATTGGGGTTATTATATGAATGGACTACTTCTACAGTAA

>Dim_LGC_47_Protei_Sequence
MLQRTIVSWSARVYSLQIVLILQLCAAAVIAVSKTFHPKQCSNDTDVMDHLLTEAALRHNRHKLPSRPVIVRIE
MWIQEVTYVSELTQDFEIDLYVNEFWEDPALNYEVLLPCNGNLSFDHSIQESIWIPNTCFINSKKALIHSSPFRN
VFLMVFPNGSIWSCWRIKSTGPCHMDLTNFPMDSISCMLTFESYNYNIQEVRMKWNEPHAVLMFKDIELPDFT
LVNYTTSVIEAEYAAGLWDELTVSFTFKRRYGWYILQGYIPTYLTIFISWIPFYMSPRAMPARTMIGVNSLLAM
TFQFGNIIRNLPRVSYIKAIDIWVLSGMTFIFASLIELAIVGFMNRHEGRADTKLNHMHKKRKSSILDSEKLDLY
SRTSFPLVYAMFNMIYWGYYMNGLLLQ

>Dim_ACC_1
ATGCGTCATCCTGGATGGATGATGGTATCATTTTTTACTGAACTTTTAAGTTTGTATGGTAGCTGTGGACA
ACCGCCAATTTGTGCTGATGATACAAAAATTATTGGCAACCTTTTGAAGGAATCGTATAATAAGCATTAT
CTACCAGCTCATCCCGTTTATGTTCGTGTCGATATGTGGGTACAGGAAGTTACCGCTGTTTCTGAATTAAC
TCAGGATTTTGAAATTGATTTATATATAAATGAATTTTGGGAAGACCCAGCACTTATATTTGATTATATGG
ATCCATGCAAAACTAACATTTCCTTTGATGAAAAAGTGTTACAAAAACTTTGGATTCCAAATACTTGTTTC
ATCAATTCGAAAAATGCTGCTATACATGAATCACCATTCAGGAATGTTTTTCTAATGGTTTTTGCTAACGG
AACATTGTGGACCAATTATAGAATGAAATTAACTGGGCCATGTGATATGAATTTGAAACGATTCCCATTC
GATCAACAAAAATGCTTCCTTACTTTCGAGTCATTTAATTATAATACTGGTGAAGTACGTATGTCCTGGAA
TCAGCCTTATCCGGTAATGCTACTCAAGAAGATTGAACTACCTGATTTCAAATTGACAAATTTTAGCGTA
ATTGCAGTAGAGCAGATGTATCCGGCAGGTTGGTGGGATGAGTTAACTGTAGCATTTGTCTTCAGAAGGC
GATATGGTTGGTATATCCTTCAAGGAGCGATTCCAGCACGAACAATGTTGGGTGTCAACTCATTATTAGC
TATGACATTTCAATTTGGTAATATCATCCGGAACTTGCCTCGTGTATCATATGTTAAAGCGATCGATGTTT
GGATGCTGGGCGGTATGCTGTTTATCTTTTTATCTTTGCTGGAATTAGCGGTAATTGGTTTTATGTCACGA

AATGAAGCTGCTCCAAAACCATTGAAAAAGAAAAGTTTTGTTTCCAGTGATTTAAATTGGAAAGAGATGC
CTAGTCCCAGGATAGGTTTACGACAGTTTTGGGTCGACCAGCGATCTTCAGCATCGTTCAAAAATGATCA
TGAGATAACTAGGCCAGTATTACCGATGAATTCTCATTTACTAACTAATCCATCCAATCTTCTATCATGTG
AAATATCAACTATGCAAAGGAAGCCACAGAACAAGAAATCCGGATGTCAGTTTAAGAGATTGCGAAAGA
TATTCCATTCATTAGAACCTGAAGTCGTCGACAAATATAGCGCAATATTTTTTCCTACGGCATATTTCGTA
TTTAACATCGGTTACTGGAGCTACTATCTCACAAGTCTTTCATCATCTGAAGAACCTACTATGAGCTAA
>Dim_ACC_1_Protein_Sequence
MRHPGWMMVSFFTELLSLYGSCGQPPICADDTKIIGNLLKESYNKHYLPAHPVYVRVDMWVQEVTAVSELT
QDFEIDLYINEFWEDPALIFDYMDPCKTNISFDEKVLQKLWIPNTCFINSKNAAIHESPFRNVFLMVFANGTLW
TNYRMKLTGPCDMNLKRFPFDQQKCFLTFESFNYNTGEVRMSWNQPYPVMLLKKIELPDFKLTNFSVIAVEQ
MYPAGWWDELTVAFVFRRRYGWYILQGAIPARTMLGVNSLLAMTFQFGNIIRNLPRVSYVKAIDVWMLGGM
LFIFLSLLELAVIGFMSRNEAAPKPLKKKSFVSSDLNWKEMPSPRIGLRQFWVDQRSSASFKNDHEITRPVLPM
NSHLLTNPSNLLSCEISTMQRKPQNKKSGCQFKRLRKIFHSLEPEVVDKYSAIFFPTAYFVFNIGYWSYYLTSLS
SSEEPTMS-

Putative Dim_ACC-2 DNA Sequence
>Dim_ACC-2_DNA
ATGAACTTTTTTTTAAAATATAATCCAAGAAAACAGTATAGTATAAATTATAACCGATCTTATCATTTCTT
TTATAAACAACGAATTTTTTCAATATTCAAATTTGCAAAAATATATTTTGCAGTAGAAACTGGGGTCGAT
GTCGCTGTCGAGTTTTGGATACAGTCAATTACATCGATCAATGAAATCACCAATGATTTTGAGGTAATGG
AAATTTACATCAATGAAATGTGGCTTGATCCTGCTTTAAATTTCGAACATCTTACTCCATGCAAAGATAAC
TTATCATTGAATCATCAGGTTCTAGATCGACTCTGGACTCCGAATAGCTGTTTTATTAACAGTAAAATTGC
TGAGATTCACGAATCTCCTTTCAGGAATTTTAGAAACATATTCCTGATGCTTTATCCAAATGGTACTGTTT
GGGTCAATTATAGAGTTCGAGTAAAAGGGCCATGTATCATGGATTTGTCAAATTTTCCGATGGATGTACA
AACTTGCCATTTAATTTATGAAAGGTTAAATAGCTTTAATTACAATAACCAAGAGGTAAGAATGCGTTGG
AATACAATTAATCCAAGTCCAGTTTATGTCGTCAGTGAAATATTGCTACCCGATTTTATTTTAATTAATAT
TTCATCGACTCTTAGGATAGAATATCCAGCCGGTATGTGGGATGAATTACATGTGAATTTAACATTCGAA
AGGCGCTGCATATGGTATTTCATGCAAGCCTATGTTCCTACCTATCTTACTATTTTCATTTTTTTCAGCTGG
GTATCATTTTCATTAGGACCACGAGCAATACCAGCCCGTACAATGCTTGGTGTTAATGCTCTCTTGGCAAT
GATATTCCAATTTGGCAATATTATGCGAAATTTGCCTAGAGTATCCTATATCAAAGCTATTGGTATAGATG
TATGGATGTTAGTTTCAATGACTTTCATATTTTCATCATTAATTGAACTAGCAATAATCGGTTCGAAAGTA
AAAAATATGGAGAGCGGTCAACGACCAAGGAAGGAATCAAGTCCGAAAGGTCTTTGCGAATTCGAGAAA
AGATTTATGCTTCCGGTGGAAGGATTTGAGTTGAAATGGTGTCGATCACGTTGGAAATCTTCTTCTTGGAC
ACCAGATCGTATAGATCGTTTGTCAAGCATCATATTTCCCGCATTTTTTGCATGCTTCAATGCAAGCTTTC
GAAATAATTTGTTGATTTGA

Putative Dim_ACC-2 Protein Sequence
> Dim_ACC-2_Protein Sequence
MNFFLKYNPRKQYSINYNRSYHFFYKQRIFSIFKFAKIYFAVETGVDVAVEFWIQSITSINEITNDFEVMEIYINE
MWLDPALNFEHLTPCKDNLSLNHQVLDRLWTPNSCFINSKIAEIHESPFRNFRNIFLMLYPNGTVWVNYRVRV
KGPCIMDLSNFPMDVQTCHLIYERLNSFNYNNQEVRMRWNTINPSPVYVVSEILLPDFILINISSTLRIEYPAGM
WDELHVNLTFERRCIWYFMQAYVPTYLTIFIFFSWVSFSLGPRAIPARTMLGVNALLAMIFQFGNIMRNLPRVS
YIKAIGIDVWMLVSMTFIFSSLIELAIIGSKVKNMESGQRPRKESSPKGLCEFEKRFMLPVEGFELKWCRSRWK
SSSWTPDRIDRLSSIIFPAFFACFNASFRNNLLI